

CONTRACT REPORT S-69-3

AD687365  
EFFECT OF DEGREE OF SATURATION ON  
COMPRESSIBILITY OF SOILS FROM THE  
DEFENCE RESEARCH ESTABLISHMENT  
SUFFIELD

by

A. J. Hendron, Jr.  
M. T. Davisson  
J. F. Parola



April 1969

Sponsored by

Defense Atomic Support Agency

Conducted for

U. S. Army Engineer Waterways Experiment Station  
CORPS OF ENGINEERS

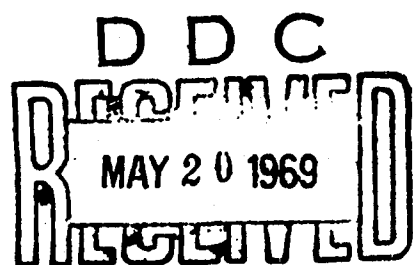
Vicksburg, Mississippi

under

Purchase Order No. WESBPJ-68-67

by

M. T. Davisson, Foundation Engineer  
Champaign, Illinois



ARMY-MRC VICKSBURG, MISS.

THIS DOCUMENT HAS BEEN APPROVED FOR PUBLIC RELEASE  
AND SALE; ITS DISTRIBUTION IS UNLIMITED

## FOREWORD

The soil properties presented herein were obtained for the purpose of clarifying the stress-strain relations which should be used in computer codes for predicting ground motions due to high pressure loading. This work is in conjunction with research on propagation of ground shock through soils being conducted by the Soils Division, U. S. Army Engineer Waterways Experiment Station, for the Defense Atomic Support Agency.

This report was requested and authorized by Mr. J. G. Jackson, Jr., Chief, Impulse Loads Section, Soil Dynamics Branch, under the direction of Mr. W. J. Turnbull, Chief of the Soils Division. The report was prepared under Purchase Order No. WESBPJ-68-67, dated 16 August 1967, issued to M. T. Davisson, Foundation Engineer, Champaign, Illinois.

Directors of the Waterways Experiment Station during the performance of this work and preparation and publication of this report were COL John R. Oswalt, Jr., CE, and COL Levi A. Brown, CE. Technical Directors were Mr. J. B. Tiffany and Mr. F. R. Brown.

## CONTENTS

	<u>Page</u>
<b>FOREWORD</b>	ui
<b>CONVERSION FACTORS BRITISH TO METRIC UNITS OF MEASUREMENT</b>	vii
<b>SUMMARY</b>	ix
<b>PART I INTRODUCTION</b>	1
Object	1
Scope	1
<b>PART II. SOILS INVESTIGATED</b>	2
Site Conditions	2
Subsurface Investigation	2
<b>PART III. TEST PROCEDURES</b>	5
Description of Apparatus	5
Experimental Procedure	7
<b>PART IV. TEST RESULTS AND INTERPRETATION OF RESULTS</b>	9
Stress-Strain Relations	9
Secant Moduli-Stress Relations	13
Axial Stress-Radial Stress Relations	15
Formulation of Three-Dimensional Stress-Strain Relations	15
<b>PART V CONCLUSIONS</b>	17
<b>LITERATURE CITED</b>	18
<b>TABLES 1-3</b>	
<b>APPENDIX A TABULATED TEST DATA</b>	
<b>APPENDIX B AXIAL STRESS VERSUS AXIAL STRAIN</b>	
<b>APPENDIX C CONSTRAINED MODULUS VERSUS AXIAL STRESS</b>	
<b>APPENDIX D RADIAL STRESS VERSUS AXIAL STRESS</b>	
<b>APPENDIX E TABULATED DATA FOR THREE-DIMENSIONAL STRESS-STRAIN RELATIONS</b>	
<b>APPENDIX F OCTAHEDRAL NORMAL STRESS VERSUS OCTAHEDRAL LINEAR STRAIN</b>	
<b>APPENDIX G OCTAHEDRAL SHEARING STRESS VERSUS OCTAHEDRAL NORMAL STRESS</b>	

## CONVERSION FACTORS, BRITISH TO METRIC UNITS OF MEASUREMENT

British units of measurement used in this report can be converted to metric units as follows

Multiply	By	To Obtain
inches	2.54	centimeters
feet	0.3048	meters
miles	1.609344	kilometers
cubic inches	16.3871	cubic centimeters
pounds	453.5924	grams
kips	453.59237	kilograms
pounds per square inch	0.070307	kilograms per square centimeter
pounds per cubic foot	16.02	kilograms per cubic meter
feet per second	30.48	centimeters per second
foot-pounds	0.138255	meter-kilograms

## SUMMARY

The soil tests reported herein were conducted to provide information on the influence of degree of saturation on high pressure stress-strain relations of undisturbed and remolded soils from the Defence Research Establishment, Suffield. These high-pressure one-dimensional test, were also to provide input data for computer codes concerning the relation between stress and strain invariants at high pressures. Some investigators were concerned that large strains might develop at high pressures in silt and clay as has been observed for sand due to grain crushing. As expected, the test results presented herein, show that large strains do not develop at high pressures in fine-grained soils such as silt and clay.

The test program consisted of 12 one-dimensional tests on 4 specimens each of undisturbed and remolded silty clay, and 4 specimens of remolded sandy silt. In all tests the radial strain was essentially zero. Axial and radial stresses and axial strain were measured. The tests were carried to an axial stress of 20,000 psi unless soil extrusion occurred at a lower stress. The following conclusions were reached:

- a. The degree of saturation and the initial void ratio are the most significant variables governing the one-dimensional stress-strain relations of soil at high pressures.
- b. For pressures exceeding 3000 psi the compacted specimens and undisturbed specimens of Suffield soil yield the same relation if the initial degree of saturation and initial void ratio are identical before loading.
- c. A lower bound to the secant modulus of deformation  $M_s$  at a given level of axial stress  $\sigma_a$  is given by

$$M_s = \frac{\sigma_a}{\left(1 - \frac{S_{ri}}{100}\right) e_i + \frac{\sigma_a}{300,000 \text{ psi}}}$$

for both compacted and undisturbed samples of fine-grained soil subjected to pressures greater than 3000 psi.

- d. The average unloading modulus of Suffield soils subjected to pressures greater than 3000 psi is approximately 10 times the loading secant modulus of deformation  $M_s$ .
- e. It is probable that the stiffness of the Suffield soils when unsaturated will be greater under dynamic loading than the static values given herein. Previous comparisons of static and dynamic values of constrained moduli of Suffield soil have shown that the dynamic values are twice the static values. This observation is consistent with similar comparisons for NTS Frenchman Flat silt.

EFFECT OF DEGREE OF SATURATION ON COMPRESSIBILITY  
OF SOILS FROM THE DEFENCE RESEARCH  
ESTABLISHMENT, SUFFIELD

PART I: INTRODUCTION

OBJECT

1. The object of this study was to determine the high-pressure, static, one-dimensional stress-strain characteristics of compacted and undisturbed soils from the Defence Research Establishment, Suffield (DRES), in Alberta, Canada. Degree of saturation was the major variable investigated. These one-dimensional tests were also to provide input data for computer codes concerning the relation between stress and strain invariants at high pressures. These high-pressure relations were especially important since some investigators were concerned that large strains might develop at high pressures in silt and clay as has been observed for sand due to grain crushing.

SCOPE

2. Two 5-in.\*-diam undisturbed Shelby tube samples and remolded samples of two different soils, which were air-dried and passed through a No. 10 sieve, were furnished by the U. S. Army Engineer Waterways Experiment Station (WES) for this study. A total of 12 static-undrained one-dimensional compression tests were performed.

3. Specifically, four tests were performed on the undisturbed samples, and four tests were performed on each of the two remolded soils, the remolded soils were compacted at predetermined water contents and dry densities. The results of the tests are presented in the form of plots of axial stress versus axial strain, secant modulus versus axial stress, and radial stress versus axial stress. The index properties for each of the different soil samples tested, and the test apparatus, experimental procedure, and an interpretation of the test results are also presented.

---

\* A table of factors for converting British units of measurement to metric units is presented on page vii.

## PART II: SOILS INVESTIGATED

### SITE CONDITIONS

#### Location and Topography

4. The location of the site is within the DRES blast range at a location known as Watching Hill. The site is approximately 30 miles north of Medicine Hat, Alberta, Canada.<sup>1</sup> Within the area of interest, the site is essentially level with a ground surface elevation of approximately 2164.0 ft msl.

#### Geology

5. A brief description of the geology of the site is available in reference 2 along with an estimate of the seismic velocities for the various layers. The site is in the southern end of the Ross Depression which, along with the areas to the south and west, has apparently been covered by a large lake. The soils to a depth of 200 ft are lacustrine deposits consisting of uniform beds of clay and silt with occasional sand lenses. However, glacio-fluvial processes and desiccation have altered approximately the upper 30 ft. In reference 2 a seismic velocity of 2200 fps has been assigned to the upper 30 ft, but indications are given that the upper 4 ft may have a velocity of 700 fps while the lower 26 ft has a velocity of 2550 fps. From 30 to 200 ft, a velocity of 5500 fps is indicated.

6. Bedrock at the site consists of Upper Cretaceous beds of the Foremost formation. These beds may be arenaceous shales and/or sandstones with many coal and carbonaceous beds. In many places the "Pale Beds" overlie the Foremost formation and consist of sandstone, shales, and sandy shales. The seismic velocity for these beds has been estimated as 7300 fps. At great depth, Mississippian limestone is found with a seismic velocity of approximately 20,000 fps.

### SUBSURFACE INVESTIGATION

#### Field Data

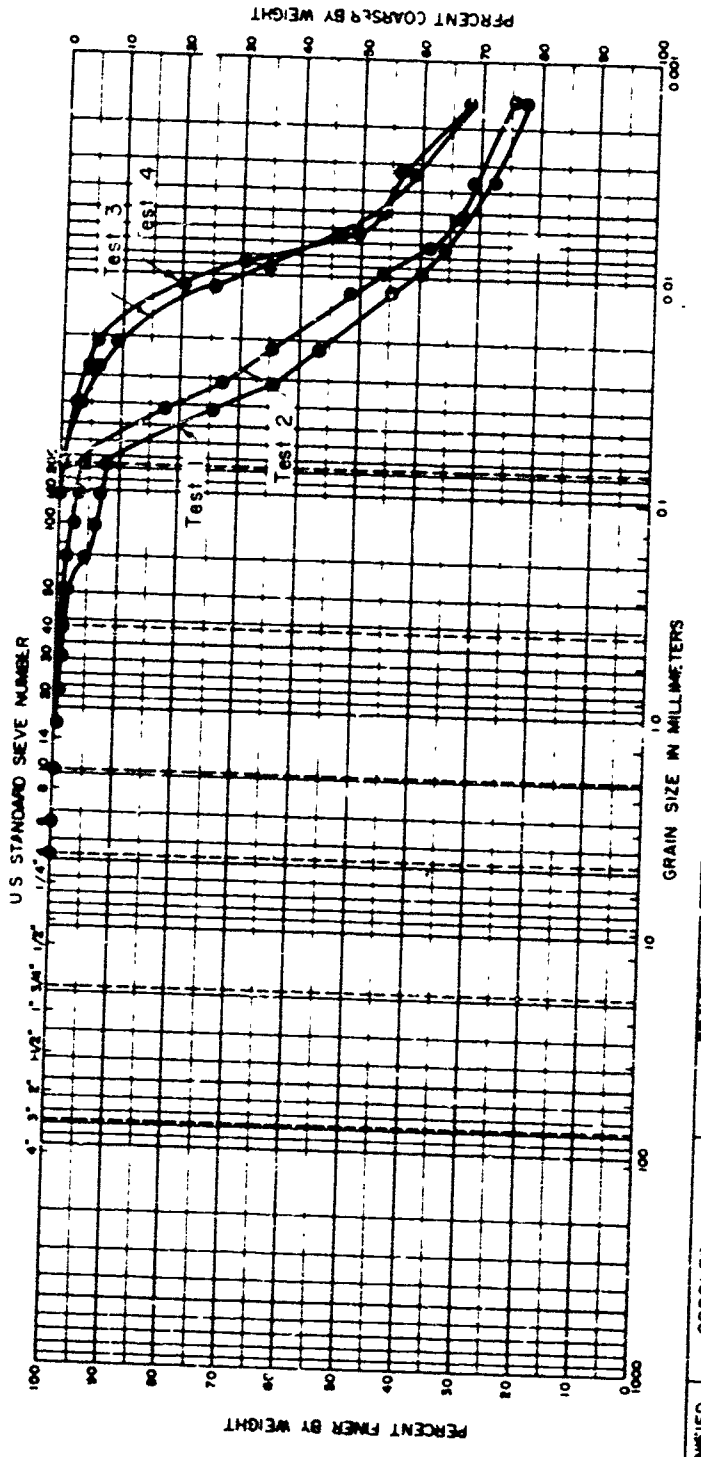
7. Two undisturbed samples from boring 2-U and two remolded samples from boring 5-U, ranging in depth from 0 to 22.5 ft, were furnished for this study. The undisturbed samples were taken with a 5-in.-diam Shelby tube and extruded immediately into 6-in.-diam fiberboard containers.<sup>3</sup> Wax was then used to fill the containers and seal the samples. The remolded samples were air-dried, mixed, and passed through a No. 10 sieve.

8. Additional information on the soil profile at the Watching Hill site can be obtained from references 4, 5, and 6.

#### Laboratory Testing

9. All soil samples received in the laboratory were subjected to routine identification and classification. The test number, sample depths, description, Unified classification, Atterberg limits, and specific gravities are listed in table 1. The gradation curves for the undisturbed and remolded samples are presented in figs. 1 and 2, respectively. All index properties for the soil samples were furnished by the WES.

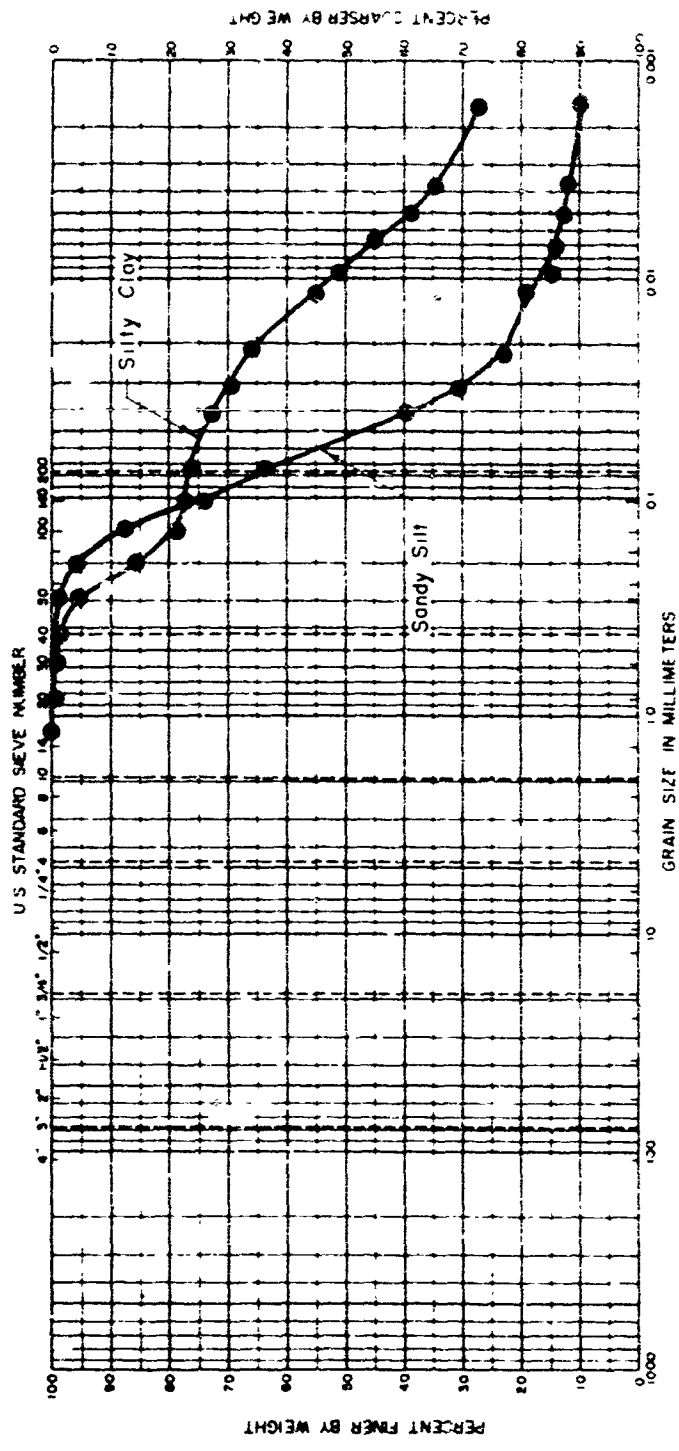
10. The initial weight-volume data for each of the 12 static test specimens are listed in table 2.



Sample No	Elev or Depth	Classification	Sp Gr	GRAIN SIZE IN MILLIMETERS			PERCENT FINE BY WEIGHT		
				COBBLES	GRAVEL	SAND	CLAY	CLAY	CLAY
1, Test 1	0 - 0.5 ft	Silty Clay (CL) w/Tr Sand	2.63	37	19	18	Project 6	Distant Plain Events 8	IA
1, Test 2	0.5 - 1 ft	Silty Clay (CL) w/Tr Sand	2.66	38	18	20	Organic Matter	Establishment, Suffield	
2, Test 3	1.2 - 1.7 ft	Silty Clay (CL) (Brown)	2.69	42	21	21	(Brown)	Area 2	Watching Hill Site
2, Test 4	1.7 - 2.3 ft	Silty Clay (CL) (Brown)	2.69	44	23	21		Boring No 2-U	

Sample No	Elev or Depth	Classification	Sp Gr	LL	PL	PI	Project	Distant Plain Events	Area	Watching Hill Site
1, Test 1	0 - 0.5 ft	Silty Clay (CL) w/Tr Sand	2.63	37	19	18	Defense Research Establishment, Suffield			
1, Test 2	0.5 - 1 ft	Silty Clay (CL) w/Tr Sand	2.66	38	18	20				
2, Test 3	1.2 - 1.7 ft	Silty Clay (CL) (Brown)	2.69	42	21	21				
2, Test 4	1.7 - 2.3 ft	Silty Clay (CL) (Brown)	2.69	44	23	21	Date 19 Sept 67			

Fig. 1. Gradation curves for undisturbed samples



UNIFIED MATERIAL	COBBLES	GRAVEL	GRAVEL	SAND	SAND	SILT	CLAY
M.I.I							

Boring No.	Elev or Depth	Classification	Sp Gr	LL	PI	Project	Division	Plan Events	6	8	1A
Bag Sample	0 - 5 ft	Silty Clay (CL)	2.69	34	16	18	Reference Reservoir	Establishment, Suffield			
5-U	5 - 22 ft	Sandy Silt (ML)	2.67	20	19	N/P	Area	Witching Hill Site			

Note: Soil air-dried, mixed and passed thru 10 sieve

Date: 20 Aug 67

Fig. 2. Gradation curves for remolded samples

## PART III TEST PROCEDURES

### DESCRIPTION OF APPARATUS

11 The apparatus used for the static one-dimensional tests, shown in fig. 3, consisted of a confining ring assembly which contained the soil specimen. The confining ring was centered on the baseplate with the aid of a lucite guide ring as shown in fig. 3. The piston was also centered on the soil specimen with the aid of a second lucite guide ring. A split ring was mounted on the piston and furnished a reaction for the dial indicator which measured the axial deformation to the nearest 0.001 in. A 300-kip universal Riehle hydraulic testing machine was used to apply the axial stress to the soil specimen through the

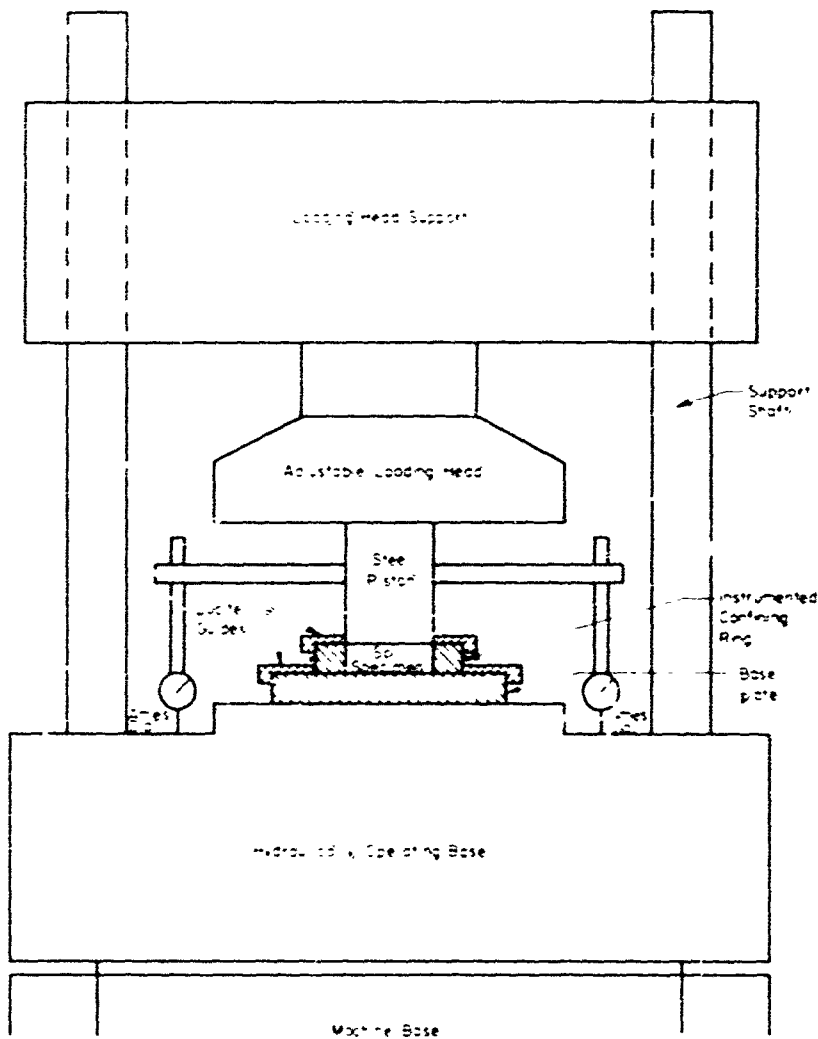
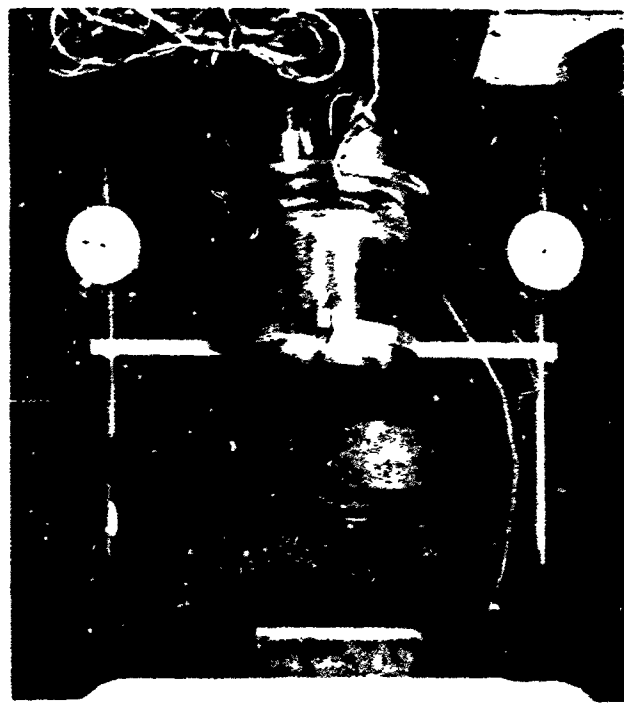


Fig. 3 Schematic of static loading machine showing axial strain instrumentation

loading piston. A photograph of this static test machine is shown in fig. 4a, a close-up of the confining ring assembly is shown in fig. 4b.



a. Static test machine



b. Close-up of confining ring assembly

Fig. 4. Test apparatus

12. A steel ring 1.0 in. high with 4-in. inside diameter and a wall thickness of 1.0 in. was used to confine the test specimens. An attempt was made to limit the radial strains to the minimum value required to facilitate accurate recording by use of the SR-4 gages. The output of the SR-4 gages was monitored with an SR-4 indicator. Calibrations of the confining rings were performed previously as described in reference 4.

## EXPERIMENTAL PROCEDURE

### Preparation of Test Specimens

13. For the tests of undisturbed samples, it was mandatory to develop a trimming operation. The trimming procedure involved placing the waxed soil sample in the hydraulic press along with the sample trimming equipment. The important feature of the trimming equipment is the trimming ring. The trimming ring has a 4-in. inside diameter, equal to that of the confining ring, but the outside face is beveled to form a sharp cutting edge. The outer face of the ring has a shoulder that fits the outside diameter of the 1.0-in.-thick confining ring. When the confining ring and the trimming ring are pressed together, an integral unit is obtained that can be forced into a soil sample in a manner similar to the use of a thin-wall sampler in a field sampling operation. Excess soil and wax were trimmed away with a knife as the trimming ring was forced into the sample. When the trimming ring had penetrated the soil a sufficient distance, the ring was carefully removed and the soil specimen was trimmed level with the height of the confining ring. Sample trimmings from each test specimen were set aside for specific gravity, Atterberg limits, and grain-size determinations. Water content samples were also taken from the Shelby tube sections before and during the trimming process.

14. The tare weight of the confining ring is known along with its dimensions. Therefore, the weight of the ring and soil specimen furnishes sufficient data to calculate the initial density of the soil. With the specific gravity and water content data, complete weight-volume determinations can be made for the test specimen.

15. The final step is to place the confining ring on the baseplate and to assemble the confining ring assembly. A height determination for the assembly is made in a dial comparator to an accuracy of 0.001 in. Because the height of the assembly itself is known, the dial comparator reading furnishes a check on the initial height of the specimen.

16. The remolded specimen was compacted into the trimming ring with a Vicksburg tamper after soil batches were properly mixed to the desired water contents and allowed to equilibrate for 24 hr. The soil specimens were compacted in two layers with nine evenly distributed blows per layer. The height of fall of the 4-lb hammer was varied to obtain the predetermined dry densities.

17. The compaction energy varied from 0.2 ft-lb/in.<sup>3</sup> to 1.1 ft-lb/in.<sup>3</sup> of soil. All remolded specimens were prepared with the compaction tamper except the sandy silt specimen at a water content of 27 percent. In order to obtain the desired density this specimen was prepared by hand-placing the soil into the confining ring. After compaction, the trimming was carried out in the same manner used for the undisturbed specimens.

### Test Procedure

18. The confining ring assembly was placed in the static test machine as shown in fig. 3. The dial indicators were set at zero under the load of the piston itself which corresponds to a stress of approximately 1 psi. Succeeding loads were applied in predetermined increments and held until the dial indicator and radial stress observations were made. A similar procedure was followed during unloading, however, at zero

applied load the soil specimen was allowed to rebound for approximately 5 min. whereas the load increments required approximately 1 min for completion. All tests were loaded to the 20,000-psi stress level or soil extrusion prior to the 20,000-psi stress.

19. Upon removing the confining ring assembly from the test machine, the height was determined with the dial comparator. This reading was compared with the initial dial comparator reading and served as a check on the residual deflection. The confining ring and specimen were removed from the assembly and a careful inspection was made for extrusion before a final water content determination was made.

## PART IV: TEST RESULTS AND INTERPRETATION OF RESULTS

20. The individual test results are tabulated in figs. A1-A12. The soil index properties are presented as well as the individual test data such as axial stress, axial strain, secant modulus, and corrected radial stress. An attempt to correct the measured radial stresses has been made by dividing the load determined from a hydraulic calibration on the full height of the ring (1 in.) by the actual height of the specimen.

21. These results have also been plotted in the form of axial stress versus corrected axial strain, constrained modulus versus axial stress, and corrected radial stress versus axial stress. The data points have not been shown on the plots because none of the points deviate from the curves. The axial stress versus axial strain plots for the 12 static tests are given in figs. B1-B12. Similarly, the constrained secant modulus versus axial stress plots are given in figs. C1-C12 and the radial stress versus axial stress plots in figs. D1-D12. The boxes in the upper left corner of the figures contain initial weight-volume data for the samples.

22. A summary of the static test data is presented in table 3. For each test the initial degree of saturation is given. At the maximum axial stress the corresponding values of axial strain and the ratio of radial stress to axial stress (denoted as  $K_0$ ) are given. A pseudo-Poisson's ratio ( $\mu$ ) has been calculated assuming that elastic theory is applicable. The residual axial strain and the ratio of residual to maximum axial strain are also presented. A notation is made in table 3 wherever soil extrusion occurred. Otherwise, the static test results can be interpreted in a straightforward manner.

### STRESS-STRAIN RELATIONS

23. A summary of the axial stress-strain relations for the undisturbed samples of silty clay, compacted samples of silty clay, and compacted samples of sandy silt are shown in figs. 5, 6, and 7, respectively. The axial stress-strain curves for all static tests were concave toward the stress axis throughout the complete loading cycle; therefore, the compressibility decreases as the stress level is increased. The absence of the small initial concave downward curvature in the stress-strain diagram of the compacted samples is believed to be caused by the negligible preload effect because of the low compaction energy necessary to yield the desired dry densities of 80-88pcf. The unloading portions of the stress-strain curves, which are shown on the individual test plots in Appendix B, are very steep at high stress ranges, but the slope decreases at a stress of approximately 500 psi. Table 3 is a list of the maximum axial strains and ratio of the residual strain to maximum strain for all tests. The maximum strain at the peak stress of 20,000 psi varied from 0.299 to 0.457 in./in. The ratio of residual to maximum strain varied from 0.85 to 0.96 for all test specimens.

24. The stress-strain relations of the compacted or remolded samples of silty clay given in fig. 6 show the effect of the initial degree of saturation for a dry density similar to field conditions. As the initial degree of saturation increases, the strain at which the stress-strain curve turns abruptly upward is reduced because of the amount of pore air decrease. However, the stress-strain curves shift downward toward the strain axis at low stress levels for samples with increasing degrees of saturation. Thus at low stress levels the samples with a high degree of saturation are more compressible than those with a low degree of saturation. However, the wetter specimens reach 100% saturation at lower strains and become stiffer than the dryer specimens at lower strains, resulting in a crossover of the stress-strain curves as illustrated by tests 7 and 8 in fig. 6. Also, variation of the dry density at a particular initial degree of saturation indicates a more compressible soil structure at a lower dry density as shown by tests 6 and 7, fig. 6. The behavior of the compacted specimens of sandy silt is similar to that of the silty clay;

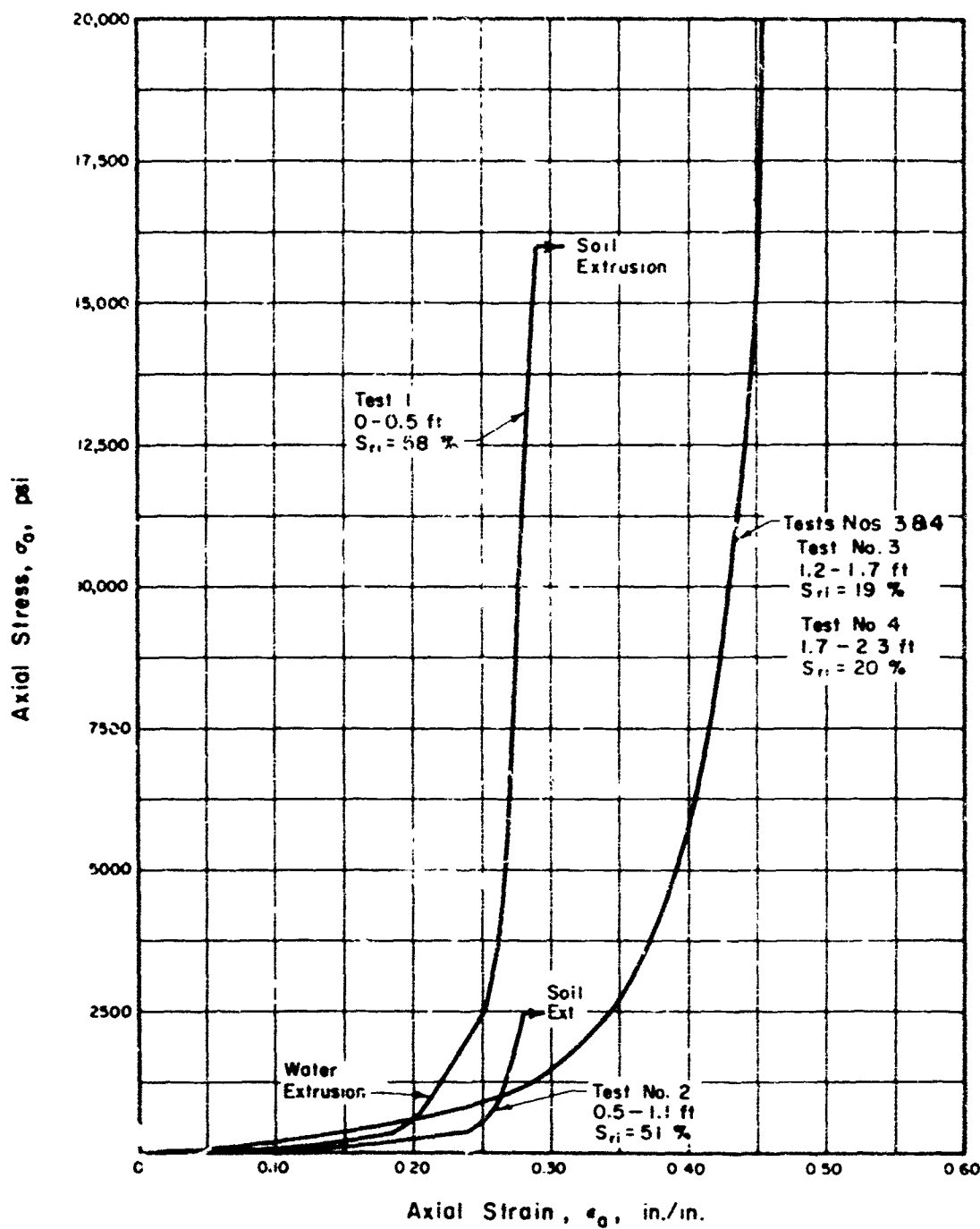


Fig. 5. Summary of stress-strain curves for the undisturbed samples of silty clay

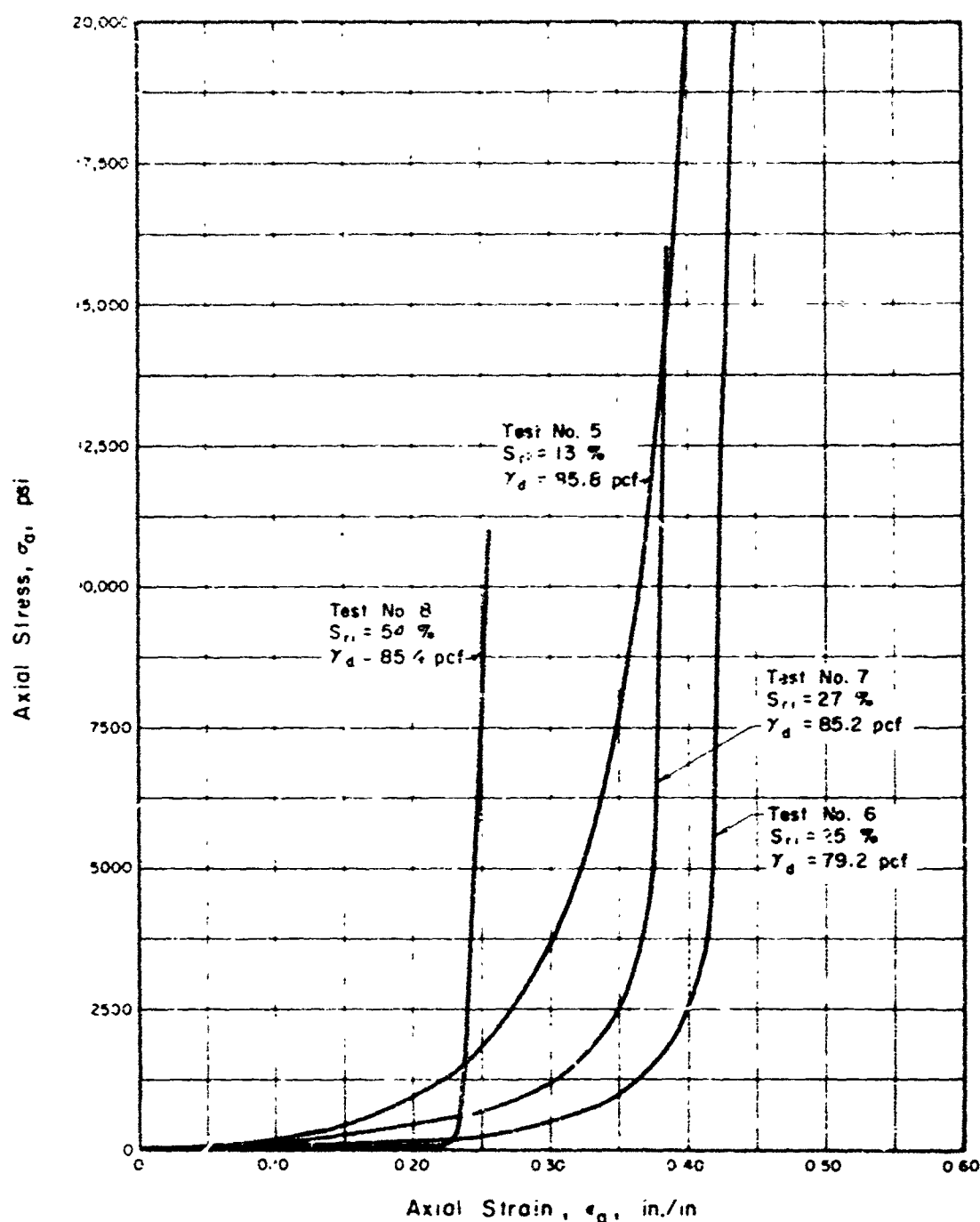


Fig. 6. Summary of stress-strain curves for the compacted samples of silty clay

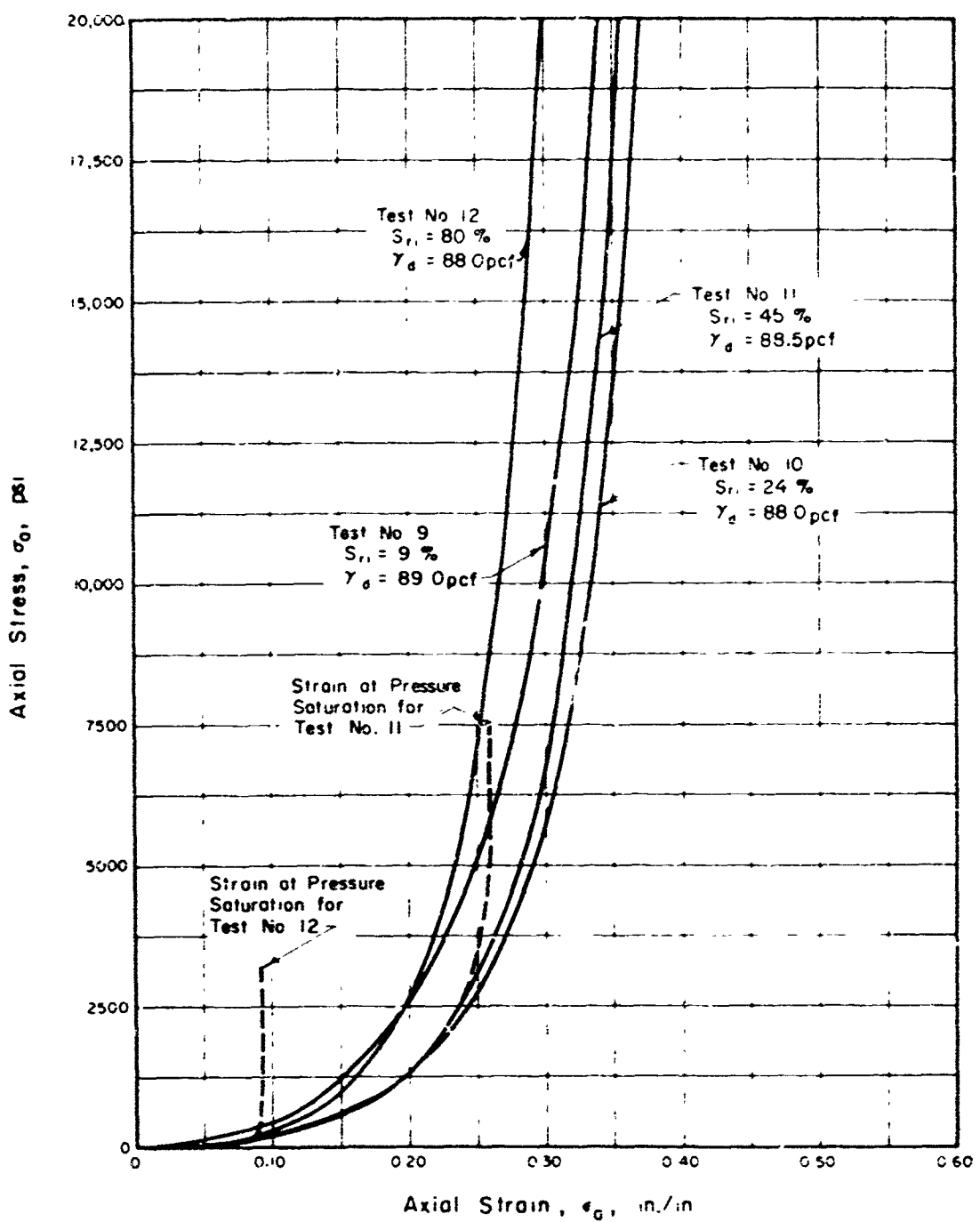


Fig. 7. Summary of stress-strain curves for the compacted samples of sandy silt

however, extrusion of the specimens with a high initial degree of saturation (tests 11 and 12) distorts the true confined stress-strain curves (fig. 7). The calculations of strain at pressure saturation indicate a modification of the stress-strain curves for tests 11 and 12. The strain at saturation can be readily calculated as

$$\epsilon = \frac{\Delta e}{1 + e_i} = \frac{\left(1 - \frac{S_n}{100}\right) e_i}{1 + e_i} \text{ in./in.}$$

where  $e_i$  is the initial void ratio,  $S_n$  is the initial degree of saturation, and  $\epsilon$  is the axial strain at saturation of the specimen

25. The stress-strain curves for the remolded samples approximate the shape of the curves for the undisturbed samples as shown in fig. 5, but the behavior is different. Tests 3 and 4 were plotted as one curve because the difference between them was not distinguishable. In general the behavior of the undisturbed samples is similar to that of the compacted samples of silty clay except that the undisturbed samples are less compressible in the low stress ranges (less than 2500 psi).

26. The shape of the stress-strain curves (concave upward) for the undisturbed samples at the shallow depths is indicative of uncemented soils. This behavior is contrary to the behavior at greater depths as reported previously.<sup>4</sup> The data in reference 4 indicate an initial concave downward stress-strain diagram and then a change in curvature as the stress level increases. With an increase in stress, the stress strain diagram is concave upward as the initial stiffness due to preload is destroyed.

27. A typical variation of degree of saturation with depth for the Watchung Hill site is presented in fig. 6 as determined from undisturbed specimens reported in references 4 and 5. These data are given for the purpose of enabling one to select the appropriate stress-strain curve from this report that is consistent with the degree of saturation at the particular depth for which the high-pressure moduli are desired.

#### SECANT MODULI-STRESS RELATIONS

28. Many of the ground motion problems in protective construction can be approximated by assuming that the displacements occur in the direction of the stress-wave propagation. Under these imposed strain conditions, the constrained modulus is the significant property of the soil controlling the ground motions. A constrained secant modulus of deformation  $M_s$  is by definition the ratio of the axial stress to the axial strain under conditions of zero radial strain.

29. All the graphs of the secant modulus versus axial stress are shown in figs C1-C12. The shapes of the modulus-stress curves follow directly from the changes of the stress-strain curves just examined, and thus require little additional discussion. The secant moduli vary linearly with axial stress for both the loading and unloading curve. The secant moduli are dependent on the initial degree of saturation, initial void ratio and the axial stress level. The lower bound secant modulus of deformation for stress levels above 3000 psi can be approximated by

$$M_s = \frac{S_n}{\left(1 - \frac{S_n}{100}\right) e_i} \text{ in.}^2 / 300,000 \text{ psi}$$

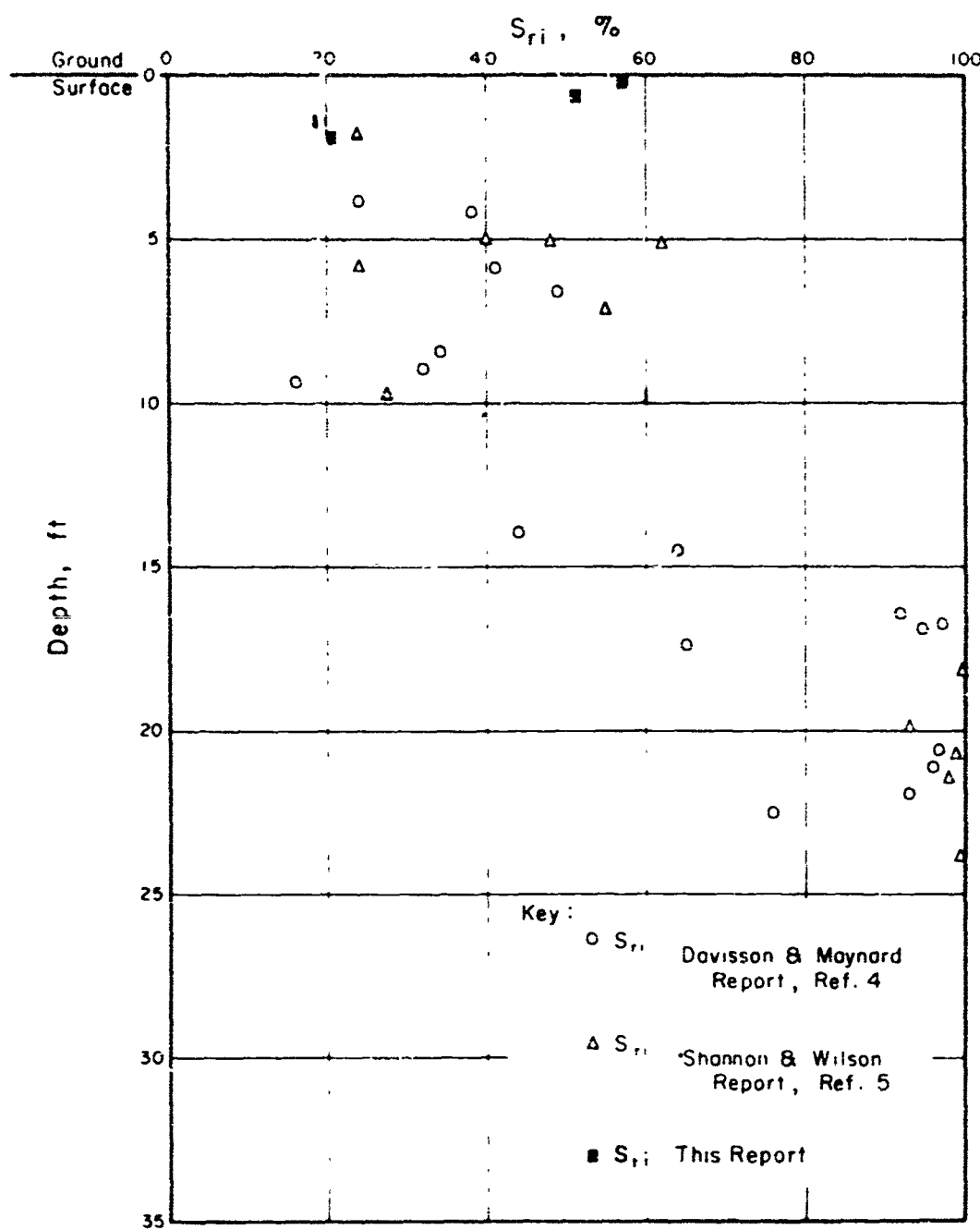


Fig. 8. Soil profile data from referenced reports

for the soils tested in this study. The average unloading secant modulus from the residual strain intercept is given by

$$M_u = 10M_s$$

#### AXIAL STRESS-RADIAL STRESS RELATIONS

30. At any given stress level, the ratio of radial stress to axial stress is denoted as  $K_o$ . In this series of one-dimensional static tests full drainage could not occur; therefore, the ratio of radial stress to axial stress determined for these tests is essentially in terms of total stresses.

31. In general, the value of  $K_o$  is closely related to the degree of saturation. As the degree of saturation increases, the value of  $K_o$  increases and approaches a value of unity for saturated soils. Because the degree of saturation depends on the axial strain, the value of  $K_o$  can vary continuously throughout the test. The values of  $K_o$  presented in table 3 vary from 0.38 to 1.00, and a pseudo-Poisson's ratio varied from 0.28 to 0.50.

32. In situ,  $K_o$  may be considered as unity for soils below the water table. For soils above the water table having high degrees of saturation, by capillarity or otherwise, the value of  $K_o$  will be nearly unity. Where the water table fluctuates, as it does at the DRES, the values of  $K_o$  (and secant modulus) will depend on the applied stress and the degree of saturation existing at the time a field test is performed.

33. During the unloading cycle, the radial stresses are reduced at a slower rate than the axial stress, this causes a concave downward curve that lies above the loading curve. Therefore, values of  $K_o$  often exceed unity during unloading.

#### FORMULATION OF THREE-DIMENSIONAL STRESS-STRAIN RELATIONS

34. The test data given in Appendix A have been used to compute: (a) octahedral shearing stress, (b) octahedral normal stress, and (c) octahedral linear strain; tabulated data for each test are presented in Appendix E. From these data, graphs have been prepared of octahedral normal stress versus octahedral linear strain; the graphs are presented in Appendix F. The relations between octahedral shearing stress and octahedral normal stress are given in Appendix G in the form of graphs.

35. A detailed discussion of the data in Appendixes F and G is beyond the scope of this report; only general comments will be made. Such data are useful in the formulation of generalized stress-strain relations for soils. For instance, the graphs shown in Appendix F show the average principal strain or octahedral linear strain which results from the average principal stress or octahedral normal stress. The slope of these curves is equal to three times that of the bulk modulus of the specimen. Note that in all instances the curves in Appendix F become very steep at some value of the strain. This value of strain is essentially that required for the soil to become fully saturated. The numerical value of the strain at this point is dependent upon the initial degree of saturation and the initial void ratio. At higher strains the bulk modulus is equal to or greater than that of water.

36. The data presented graphically in Appendix G are useful in establishing yield criteria to be used in multidimensional computer programs. Note the curves for tests 9, 10, 11, and 12 which show a nearly linear relation between octahedral shearing stress and octahedral normal stress during loading. This is not surprising since these samples were silty sand, and the shearing resistance of sand increases linearly with

normal pressure. Note that the specimens of relatively dry silty clay, tests 3, 4, and 5, showed the same behavior because the initial degree of saturation was low and the specimens probably never became saturated. Thus the shear strength increased with pressure throughout the entire test. Note the results of test 2, 6, 7 and 8, however, where the octahedral shearing stress approaches a constant as the octahedral normal stress increases. In each case the specimen has become saturated and is behaving as if  $\sigma_3 = 0$  beyond the pressure at which the curve turns horizontal. In each of these cases the soil is a silty clay with a relatively high initial degree of saturation.

## PART V CONCLUSIONS

- 37 The following conclusions were drawn from the investigation
- a The degree of saturation and the initial void ratio are the most significant variables governing the one-dimensional stress-strain relations of soil at high pressures
  - b For pressures exceeding 3000 psi the compacted specimens and undisturbed specimens of Suffield soil yield the same relation if the initial degree of saturation and initial void ratio are identical before loading
  - c A lower bound to the secant modulus of deformation  $M_s$  at a given level of axial stress  $\sigma_a$  is given by

$$M_s = \frac{\sigma_a}{\left(1 - \frac{S_n}{100}\right)e_i + \frac{\sigma_a}{300,000 \text{ psi}}}$$

for both compacted and undisturbed samples of fine-grained soil subjected to pressures greater than 3000 psi.

- d The average unloading modulus of Suffield soils subjected to pressures greater than 3000 psi is approximately 10 times the loading secant modulus of deformation  $M_s$ .
- e It is probable that the stiffness of the Suffield soils when unsaturated will be greater under dynamic loading than the static values given in this report. Previous comparisons of static and dynamic values of constrained moduli of Suffield soils (reference 4) have shown that the dynamic values are twice the static values. This observation is consistent with similar comparisons for NTS Frenchman Flat silt (reference 7)

## LITERATURE CITED

1. "Operation Snowball," Technical and Administrative Information for Operation Snowball, United States Participation with Canada and Great Britain in a Nuclear Weapons Effects 500-ton High Explosive Experimental Program.
2. Jones, G. H. S., "Strong Motion Seismic Effects of the Suffield Explosions," Suffield Report No 208, 1963, Suffield Experimental Station, Ralston, Alberta, Canada.
3. Hvorslev, M. J., "Subsurface Exploration and Sampling of Soils for Civil Engineering Purposes," Nov 1948, Research Project of the Committee on Sampling and Testing, Soil Mechanics and Foundations Division, American Society of Civil Engineers, published by U. S. Army Engineer Waterways Experiment Station, CE, Vicksburg, Miss.
4. Davison, M. T. and Maynard, T. R., "Static and Dynamic Compressibility of Suffield Experimental Station Soils," Technical Report No. WL-TR 64-118, April 1965, Air Force Weapons Laboratory, Kirtland Air Force Base, N. Mex.
5. Shannon and Wilson, Inc., "Soil Vibration Tests, Suffield Experimental Station, Canada," Contract Report No. 1-125, July 1964, U. S. Army Engineer Waterways Experiment Station, CE, Vicksburg, Miss.
6. Hendron, A. J., Jr., "Correlation of Operation Snowball Ground Motions with Dynamic Properties of Test Site Soils," Miscellaneous Paper No. 1-745, Oct 1965, U. S. Army Engineer Waterways Experiment Station, CE, Vicksburg, Miss.
7. Hendron, A. J., Jr., and Davison, M. T., "Static and Dynamic Behavior of a Playa Sil in One-Dimensional Compression," Technical Documentary Report No. RTD TDR-63-3078, Sept 1964, Air Force Weapons Laboratory, Kirtland Air Force Base, N. Mex.

**Table 1**

Table 2  
Initial Specimen Data

<u>Test No.</u>	<u>Type of Sample</u>	<u>Dry Density</u> $\gamma_d$ ,pcf	<u>Water Content</u> $w_i$ ,%	<u>Degree of Saturation</u> $S_n$ ,%	<u>Void Ratio</u> $e_i$	<u>Specific Gravity</u> $G_s$
1	Undisturbed, 0-0.5 ft	86.2	19.9	58.0	0.902	2.63
2	Undisturbed, 0.5-1.1 ft	83.3	19.1	51.2	0.993	2.66
3	Undisturbed, 1.2-1.7 ft	77.5	8.3	19.1	1.170	2.69
4	Undisturbed, 1.7-2.3 ft	76.2	9.0	20.1	1.200	2.69
5	Remolded silty clay, 0-5 ft	85.8	4.8	13.5	0.960	2.69
6		79.2	9.7	25.3	1.120	2.69
7		85.2	9.8	27.1	0.972	2.69
8		85.4	19.6	54.3	0.970	2.69
9	Remolded sandy silt, 5-22 ft	89.0	3.1	9.4	0.876	2.67
10		88.0	8.1	24.1	0.898	2.67
11		88.5	15.0	45.0	0.888	2.67
12		88.0	27.2	80.3	0.898	2.67

Table 3  
Summary of Static Test Data

Test No.	Sample Type and Location	Initial Value $S_1$ , %	$\sigma_a$ , psi	Initial Peak $\epsilon_{a_{max}}$ , in./in.	$K_o$	Poisson's Ratio $\mu$	Residual Strain $\epsilon_{a_{resid}}$ , in./in.	Ratio of Residual Strain to Maxi- mum Strain	
								$\epsilon_{a_{resid}}/\epsilon_{a_{max}}$	$\epsilon_{a_{resid}}/\epsilon_{a_{max}}$
1*	Undisturbed, 0.05 ft	58.0	16,000	0.292					
2*	Undisturbed, 0.511 ft	51.2	2,500	0.284	0.94		0.48		
3	Undisturbed, 1.217 ft	19.1	20,000	0.454	0.55		0.35	0.424	0.93
4	Undisturbed, 1.723 ft	20.1	20,000	0.457	0.39		0.28	0.424	0.93
5		13.5	20,000	0.399	0.48		0.32	0.37	0.94
6	Remolded silty clay, 0.5 ft	25.3	20,000	0.437	0.89		0.47	0.418	0.96
7		27.1	16,000	0.385	0.89		0.47	0.366	0.95
8**		54.3	11,000	0.273	1.00		0.50	0.244	0.96
9	Remolded sandy silt, 5.22 ft	9.4	20,000	0.340	0.41		0.29	0.305	0.90
10		24.1	20,000	0.370	0.41		0.29	0.316	0.85
11**		45.0	20,000	0.358	0.47		0.32	0.304	0.85
12**		80.3	20,000	0.299	0.38		0.28	0.262	0.88

\* Soil extrusion at initial peak axial stress.  
\*\* Water extrusion.

**APPENDIX A: TABULATED TEST DATA**

## ONE-DIMENSIONAL STATIC TEST DATA

Test No 1 Soil Type Undisturbed Soil Location Depth 0 - 0.5 ft.  
Silty Clay Racing 24, Distant Plain 6  
 w. 19.9 % S., 58.2 % Y, 103.2pcf Y<sub>d</sub>, 86.2pcf S<sub>s</sub>, 2.93 e, - 0.902  
 L. 37 % P, 19 % Classification Brewer Silty Clay w/ 2000 e.s. traces  
of organic matter (CL)

Axial Stress $\sigma_a$	Axial Strain $\epsilon_a$	Secant Modulus $M_s$	Radial Stress $\sigma_r$	Degree of Saturation $S_r$	Axial Stress $\sigma_a$	Axial Strain $\epsilon_a$	Secant Modulus $M_s$	Radial Stress $\sigma_r$	Degree of Saturation $S_r$
psi	in/in	psi	psi	%	psi	in/in	psi	psi	%
0	0	-	0	580	1000	0.352	2840		
10	0.009	1110	-		500	0.351	1420		
200	0.154	1300			200	0.351	570		
400	0.194	2060			0	0.344	0		
600	0.205	2930			0(smu)	0.344	0	-	
800	0.211	3780							
1000	0.216	4620							
1500	0.229	6550							
2000	0.242	8250							
2500	0.252	9900							
3000	0.257	11700							
3500	0.260	13450							
4000	0.263	15200							
5000	0.266	18800							
6000	0.269	22200							
7000	0.271	25800							
8000	0.274	29200							
9000	0.275	32800							
10000	0.277	36200							
11000	0.279	39500							
12000	0.281	42600							
13000	0.284	46800							
14000	0.286	49000							
15000	0.288	52000							
16000	0.292	54800							
Soil Extrusion									
4000	0.351	11400							
3000	0.354	8500							
2000	0.353	5660							

Note: Water Extrusion at  $\sigma_a = 10000$  psi.

Radial Stress was not recorded for this test.

About 6 gms of water was extruded during the test.

Fig. A1

## ONE-DIMENSIONAL STATIC TEST DATA

Test No. 2 Soil Type Undisturbed Soil Location Depth 0.5 - 11 ft.  
Silty Clay Bearing 2.14, Distant Plain 6  
 $w_i = 19.1\%$   $s_i = 51.2\%$   $\gamma_i = 99.1 \text{pcf}$   $\gamma_d = 83.3 \text{pcf}$   $S_i = 266$   $e_i = 0.993$   
 $L_w = 38\%$   $P_w = 18\%$  Classification Brown Silty Clay w/ trace of sand. (CL)

Axial Stress $\sigma_a$	Axial Strain $\epsilon_a$	Secant Modulus $M_s$	Radial Stress $\sigma_r$	Degree of Saturation $S_r$	Axial Stress $\sigma_a$	Axial Strain $\epsilon_a$	Secant Modulus $M_s$	Radial Stress $\sigma_r$	Degree of Saturation $S_r$
psi	in/in	psi	psi	%	psi	in/in	psi	psi	%
0	0	-	0						
10	0.008	1250	0						
50	0.054	840	10						
100	0.120	834	50						
200	0.188	1060	98						
300	0.221	1355	130						
400	0.240	1670	210						
500	0.250	2000	264						
600	0.255	2350	358						
800	0.259	3090	515						
1000	0.262	3820	710						
1500	0.269	5500	1290						
2000	0.276	7250	1830						
2500	0.294	8500	2340						
Soil Extrusion									
2000	0.374	5350	1980						
1500	0.448	3350	1547						
1000	0.486	2060	1110						
800	0.487	1640	933						
600	0.487	1230	750						
400	0.486	820	560						
300	0.486	620	468						
200	0.485	410	374						
100	0.484	206	298						
50	0.484	104	278						
10	0.482	21	222						
0	0.478	0	220						

Fig. A2

### ONE-DIMENSIONAL STATIC TEST DATA

Test No 3 Soil Type Undisturbed Soil Location Depth 1.2 - 17 ft.  
Silty Clay Boring 2-U, Distant Plain  
w. 8.3 % S<sub>r</sub> 19.1 %  $\gamma$ , 84.0 pcf  $\gamma_d$ , 77.5 pcf S<sub>s</sub>, 2.69 e, 1.170  
L, 42 % P, 21 % Classification Brown Silty Clay (CL)

Axial Stress $\sigma_a$	Axial Strain $\epsilon_a$	Secant Modulus $M_s$	Radial Stress $\sigma_r$	Degree of Saturation $S_r$	Axial Stress $\sigma_a$	Axial Strain $\epsilon_a$	Secant Modulus $M_s$	Radial Stress $\sigma_r$	Degree of Saturation $S_r$
psi	in/in	psi	psi	%	psi	in/in	psi	psi	%
0	0	-	0		17000	0.450	37800	9600	
10	0.004	2500	0		18000	0.451	39900	10100	
50	0.016	3120	29		19000	0.452	42000	10500	
100	0.036	2780	88		20000	0.454	44000	11000	
200	0.090	2220	128		17500	0.454	38600	10200	
300	0.135	2260	201		15000	0.454	33000	9190	
400	0.167	2400	266		12500	0.452	27700	8070	
500	0.193	2590	357		10000	0.451	22100	7150	
600	0.213	2820	388		8000	0.449	17700	6250	
800	0.243	3290	447		6000	0.447	13410	5230	
1000	0.265	3770	655		4000	0.444	9070	4270	
1500	0.302	4970	905		2000	0.441	4540	2960	
2000	0.327	5120	1140		1000	0.436	2290	2210	
2500	0.345	7250	1450		500	0.432	1160	1690	
3000	0.359	8360	1640		200	0.429	466	1372	
3500	0.369	9480	1840		100	0.429	233	1270	
4000	0.379	10520	2140		50	0.428	116	1160	
5000	0.393	12700	2530		0	0.424	0	1030	
6000	0.403	14900	3020						
7000	0.412	17000	3590						
8000	0.419	19100	4100						
9000	0.424	21200	4610						
10000	0.430	23200	-						
11000	0.435	25300	5630						
12000	0.439	27400	6410						
13000	0.442	29400	7150						
14000	0.445	31500	7900						
15000	0.447	33600	8500						
16000	0.449	36700	9060						

Fig 1.3

## ONE-DIMENSIONAL STATIC TEST DATA

Test No 4 Soil Type Undisturbed Soil Location Depth 1.7-2.3 ft.  
Silty Clay Boring 2-4, Distant Plain  
W<sub>i</sub> 9.0 % S<sub>r</sub>, 20.1 % Y<sub>i</sub>, 83.1pcf Y<sub>d</sub>, 76.2pcf S<sub>s</sub>, 2.69 e, 1.200  
L<sub>w</sub> 44 % P, 23 % Classification Brown Silty Clay (CL)

Axial Stress $\sigma_a$	Axial Strain $\epsilon_a$	Secant Modulus $M_s$	Radial Stress $\sigma_r$	Degree of Saturation $S_r$	Axial Stress $\sigma_a$	Axial Strain $\epsilon_a$	Secant Modulus $M_s$	Radial Stress $\sigma_r$	Degree of Saturation $S_r$
psi	in/in	psi	psi	%	psi	in/in	psi	psi	%
0	0	-	0		17000	0.452	37600	6810	
10	0.002	5000	0		18000	0.454	39700	7000	
50	0.008	6260	10		19000	0.455	41700	7400	
100	0.018	5550	20		20000	0.457	43700	7800	
200	0.067	2990	103		17500	0.456	38400	7440	
300	0.119	2520	141		15000	0.455	33000	6860	
400	0.169	2520	216		12500	0.455	27500	6380	
500	0.187	2670	236		10000	0.453	22100	5750	
600	0.209	2870	266		6000	0.449	13400	4350	
800	0.240	3340	391		4000	0.447	8950	3500	
1000	0.262	3820	520		2000	0.443	4500	2410	
1500	0.300	5000	712		1000	0.439	2280	1880	
2000	0.324	6160	990		500	0.437	1140	1360	
2500	0.342	7310	1160		200	0.432	460	-	
3000	0.356	8430	1470		100	0.431	230	-	
3500	0.368	9500	1660		50	0.429	120	920	
4000	0.378	10600	1860		0	0.424	-	830	
5000	0.391	12820	2350						
6000	0.402	14950	2740						
7000	0.410	17000	3170						
8000	0.418	19100	3680						
9000	0.423	21200	3970						
10000	0.429	23300	4340						
11000	0.434	25400	4650						
12000	0.439	27400	5110						
13000	0.443	29300	5420						
14000	0.446	31300	5750						
15000	0.449	33200	6060						
16000	0.451	35500	6450						

Fig. A4

### ONE-DIMENSIONAL STATIC TEST DATA

Test No 5 Soil Type Remolded Silty Clay Soil Location Depth 0-5 ft.  
Bag Sample, Distinct Phase  
 $\epsilon_s = 4.8\%$   $S_s = 13.5\%$   $\gamma = 98.0 \text{ pcf}$   $\gamma_d = 83.0 \text{ pcf}$   $S_r = 2.67$   $\sigma_i = 0.960$   
 $L_w = 34\%$   $P_w = 16\%$  Classification Brown Silty Clay (cc)

Axial Stress $\sigma_a$ psi	Axial Strain $\epsilon_a$ in/in.	Secant Modulus $M_s$ psi	Radial Stress $\sigma_r$ psi	Degree of Saturation $S_r$ %	Axial Stress $\sigma_a$ psi	Axial Strain $\epsilon_a$ in/in.	Secant Modulus $M_s$ psi	Radial Stress $\sigma_r$ psi	Degree of Saturation $S_r$ %
0	0		0		17000	0.391	43500	8070	
10	0.011	1000	0		18000	0.393	46000	8500	
50	0.037	1300	10		19000	0.397	48000	9090	
100	0.062	1600	71		20000	0.399	50000	9600	
200	0.097	2100	106		17500	0.399	43800	9350	
300	0.122	2500	131		15000	0.398	37700	8850	
400	0.141	2800	212		12500	0.397	31500	8250	
500	0.153	3300	225		10000	0.396	25300	7500	
600	0.167	3600	287		6000	0.392	15300	5500	
800	0.188	4200	365		4000	0.390	10200	4350	
1000	0.205	4900	495		2000	0.388	5200	3050	
1500	0.233	6500	750		1000	0.385	2600	2230	
2000	0.256	7800	1001		500	0.383	1300	1760	
2500	0.272	9200	1260		200	0.382	500	1400	
3000	0.286	10500	1470		100	0.382	300	1320	
3500	0.296	11800	1700		50	0.380	100	1220	
4000	0.307	13000	1950		0	0.377	0	1000	
5000	0.323	15500	2420						
6000	0.333	18000	2910						
7000	0.343	20400	3360						
8000	0.351	22800	3820						
9000	0.357	25200	4300						
10000	0.363	27600	4870						
11000	0.369	29800	5470						
12000	0.374	32100	5630						
13000	0.378	34400	6040						
14000	0.382	36700	6500						
15000	0.386	39000	7000						
16000	0.389	41200	7500						

Fig A5

### ONE-DIMENSIONAL STATIC TEST DATA

Test No. 6 Soil Type Rewarded Soil Location Depth 0 - 5 ft.  
Silty Clay Aug Sample, Distant Plain  
 $\gamma_1 = 9.7 \text{ } \text{lb/in}^3$   $S_1 = 25.3 \%$   $\gamma_1 = 26.8 \text{ } \text{pcf}$   $\gamma_{\text{sat}} = 79.8 \text{ } \text{pcf}$   $\delta = 2.69$   $c_i = 1.122$   
 $L_s = 24 \%$   $P_s = 16 \%$  Classification Brown Silty Clay (CL)

Axial Stress $\sigma_a$ psi	Axial Strain $\epsilon_a$ in./in.	Secant Modulus $M_a$ psi	Radial Stress $\sigma_r$ psi	Degree of Saturation $S_r$ %
0	0	—	0	
10	0.003	1000	0	
50	. .81	600	21	
100	0.147	700	56	
200	0.219	900	122	
300	0.255	1200	167	
400	0.284	1400	253	
500	0.301	1700	272	
600	0.313	1900	290	
800	0.336	2400	433	
1000	0.352	2800	470	
1500	0.374	4000	760	
2000	0.390	5100	975	
2500	0.401	6200	1260	
3000	0.408	7300	1490	
3500	0.413	8500	1790	
4000	0.416	9600	2130	
5000	0.419	12000	2800	
6000	0.420	14300	3450	
7000	0.422	16600	4600	
8000	0.423	19000	5520	
9000	0.423	21200	6330	
10000	0.424	23600	7300	
11000	0.425	25900	8250	
12000	0.426	28100	9180	
14000	0.428	32700	11400	
15000	0.430	35000	12600	
16000	0.430	37300	—	
17000	0.431	39500	—	

Axial Stress $\sigma_a$ psi	Axial Strain $\epsilon_a$ in./in.	Secant Modulus $M_a$ psi	Radial Stress $\sigma_r$ psi	Degree of Saturation $S_r$ %
18000	0.432	41800	—	
19000	0.435	43700	—	
20000	0.437	45800	—	
17500	0.436	40000	—	
15000	0.435	34500	—	
12500	0.434	28800	—	
10000	0.433	23100	—	
8000	0.432	18500	—	
6000	0.431	14000	—	
4000	0.430	9300	—	
2000	0.430	4600	—	
1000	0.428	2300	—	
500	0.426	1200	—	
200	0.425	500	—	
100	0.424	200	—	
50	0.423	100	—	
0	0.418	0	—	

Note: Strain gages on the  
confining ring yielded at an  
axial stress of 14,000 psi.

Fig. A6

# ONE-DIMENSIONAL STATIC TEST DATA

Test No. 7 Soil Type Ramended Silty Clay Soil Location Depth 0-5 ft.  
Bag Samak, Durant Plain  
 $w_i = 9.8\%$   $S_i = 27.1\%$   $\gamma_i = 93.8 \text{ pcf}$   $\gamma_o = 85.2 \text{ pcf}$   $S_s = 2.69$   $\epsilon_i = 0.978$   
 $L_i = 34\%$   $P_i = 14\%$  Classification Brown Silty Clay (c)

Axial Stress psi	Axial Strain $\epsilon_a$	Secant Modulus $M_s$	Radial Stress $\sigma_r$	Degree of Saturation $S_s$	Axial Stress psi	Axial Strain $\epsilon_a$	Secant Modulus $M_s$	Radial Stress $\sigma_r$	Degree of Saturation $S_s$
psi / in		psi	psi	%	psi	in/in.	psi	psi	%
0	0	-	0		15000	0.385	39000	14000	
10	0.003	2000	0		12500	0.384	32600	12200	
50	0.024	2100	56		10000	0.383	26100	11800	
100	0.087	1100	101		8000	0.381	21000	8750	
200	0.152	1300	119		4000	0.380	10500	5350	
300	0.193	1500	182		2000	0.378	5300	3900	
400	0.220	1800	248		1000	0.376	2700	2510	
500	0.244	2000	280		500	0.373	1300	1930	
600	0.257	2300	372		200	0.371	500	1620	
700	0.280	2900	512		100	0.370	300	1480	
1000	0.295	3400	587		50	0.368	100	1390	
1500	0.322	4700	895		0	0.366	0	1190	
2000	0.338	5900	1250						
2500	0.349	7200	1550						
3000	0.360	8300	1920						
3500	0.365	9600	2260						
4000	0.368	10900	2780						
5000	0.372	13400	3830						
6000	0.374	16000	4900						
7000	0.377	18600	6080						
8000	0.378	21100	7550						
9000	0.380	23700	8000						
10000	0.380	26300	8950						
11000	0.381	28900	9700						
12000	0.382	31500	10600						
13000	0.383	34000	11500						
14000	0.383	36600	12300						
15000	0.384	39100	13200						
16000	0.385	41500	14200						

Note: Axial load was stopped at 16,000 psi because of capacity of strain gages on confining ring.

Fig A7

### ONE-DIMENSIONAL STATIC TEST DATA

Test No. 8 Soil Type Ramakid Soil Location Depth 0-5 ft.  
Silty Clay Bag Sample Distant Plateau  
 $\pi_1 = 12.6 \text{ lb/in}^2$   $S_r = 54.3 \%$   $\gamma_1 = 102.2 \text{ psf}$   $\gamma_{\text{sat}} = 88.4 \text{ psf}$   $\phi_s = 26.9$   $c_s = 0.970$   
 $L_s = 34 \text{ %}$   $P_s = 16 \text{ %}$  Classification Brewer Silty Clay (CL)

Axial Stress $\sigma_a$	Axial Strain $\epsilon_a$	Secant Modulus $M_a$	Radial Stress $\sigma_r$	Degree of Saturation $S_s$
50	In./in.	psi	psi	%
0	0	0	0	
10	0.022	500	0	
50	0.186	300	0	
100	0.220	500	12	
150	0.228	700	48	
200	0.230	900	96	
300	0.231	1300	191	
400	0.232	1700	276	
500	0.232	2200	358	
600	0.233	2600	480	
700	0.234	3000	588	
800	0.234	3400	685	
900	0.234	3900	744	
1000	0.234	4300	850	
1100	0.235	4700	890	
	0.235	-	975	
1150	0.235	4900	1000	
1275	0.236	5400	1110	
1500	0.237	6300	1340	
1600	0.238	6700	1460	
1800	0.238	7870	1640	
2000	0.239	8400	1830	
2250	0.239	9400	2080	
2500	0.240	10400	2370	
2750	0.240	11500	2660	
3000	0.240	12500	2920	
3500	0.242	14500	3400	
4000	0.244	16400	3900	
5000	0.246	20300	5000	

Axial Stress $\sigma_a$	Axial Strain $\epsilon_a$	Secant Modulus $M_a$	Radial Stress $\sigma_r$	Degree of Saturation $S_s$
psi	In./in.	psi	psi	%
6000	0.247	24300	6000	
7000	0.248	28200	7000	
8000	0.250	32000	7970	
9000	0.251	36000	8880	
10000	0.252	39700	9850	
11000	0.253	43500	11000	
8500	0.252	31700	8000	
6000	0.250	24000	6000	
4000	0.249	16000	4040	
3000	0.248	12100	3070	
2000	0.247	8100	2070	
1000	0.246	4100	1010	
500	0.246	2000	600	
200	0.246	800	256	
100	0.246	400	134	
50	0.246	200	97	
0	0.244	0	36	

Note: Water extraction at  
 $\sigma_a = 400 \text{ psi} < 2 \text{ gms of water}$ .  
 Loading was stopped at  
 11,000 psi because of  
 capacity of strain gages  
 on the confining ring.

Fig. A8

### ONE-DIMENSIONAL STATIC TEST DATA

Test No 9      Soil Type Remolded      Soil Location Depth 5-22 ft  
Sandy Silt      Boring 5-U. instant Plane 6  
w. 31 % S., 9.4 % Y, 97.0pcf  $\gamma_d$ , 89.0pcf  $\gamma_s$ , 2.67 e, 0.876  
L. 20 % P, 19 % Classification: Brown Sandy Silt (ml)

Axial Stress $\sigma_a$ psi	Axial Strain $\epsilon_a$ in/in	Secant Modulus $M_s$ psi	Radial Stress $\sigma_r$ psi	Degree of Saturation $S_s$ %	Axial Stress $\sigma_a$ psi	Axial Strain $\epsilon_a$ in/in	Secant Modulus $M_s$ psi	Radial Stress $\sigma_r$ psi	Degree of Saturation $S_s$ %
0	0	—	0		17000	.330	51500	6860	
10	.008	1250	0		18000	.333	54000	7240	
50	.033	1515	37.1		19000	.336	56600	7640	
100	.050	2000	48.4		20000	.340	58800	8150	
200	.066	3030	108		17500	.339	51600	7950	
300	.083	3620	150.5		15000	.338	44400	7580	
400	.095	4220	173		12500	.338	37000	7020	
500	.105	4750	247		10000	.338	29600	6310	
600	.114	5250	270		8000	.336	23800	5670	
800	.129	6200	370		6000	.332	18100	4910	
1000	.141	7100	450		4000	.331	12100	4280	
1500	.163	9200	615		2000	.328	6100	3080	
2000	.184	10900	834		1000	.323	3100	2380	
2500	.199	12600	998		500	.320	1560	1960	
3000	.212	14150	1225		200	.317	630	1550	
3500	.225	15600	1440		100	.316	316	1400	
4000	.232	17150	1630		50	.314	159	1280	
5000	.248	20100	2020		0	.305	—	980	
6000	.261	23000	2430						
7000	.272	25700	2850						
8000	.281	28500	3270						
9000	.289	31100	3590						
10000	.296	33800	4000						
11000	.303	36300	4410						
12000	.309	38800	4750						
13000	.315	41400	5160						
14000	.320	43700	5640						
15000	.323	46400	6140						
16000	.327	49000	6360						

Fig A9

### ONE-DIMENSIONAL STATIC TEST DATA

Test No 10 Soil Type Revetted Soil Location Depth 5-22 ft.  
Sandy Silt Boring 5-4, Distant Plain 6  
 $w_s$  8.1 %  $S_r$  24.1 %  $\gamma$  95.3 pcf  $\gamma_o$  88.0 pcf  $S_a$  2.67  $e$  0.898  
 $L$  20 %  $P$  19 % Classification Brown Sandy Silt (ml)

Axial Stress $\sigma_a$ psi	Axial Strain $\epsilon_a$ in/in	Secant Modulus $M_s$ psi	Radial Stress $\sigma_r$ psi	Degree of Saturation $S_s$ %	Axial Stress $\sigma_a$ psi	Axial Strain $\epsilon_a$ in/in	Secant Modulus $M_s$ psi	Radial Stress $\sigma_r$ psi	Degree of Saturation $S_s$ %
0	0	-	0		17000	.362	47000	6770	
10	.007	1430	46.4		18000	.365	49400	7020	
50	.031	1610	85.5		19000	.367	51700	7550	
100	.059	1695	98		20000	.370	54000	8050	
200	.093	2160	132		17500	.370	47400	7750	
300	.115	2610	188		15000	.369	41900	7400	
400	.131	3050	212		12500	.369	33900	6830	
500	.142	3520	226		10000	.367	27800	6120	
600	.151	3970	304		8000	.366	21800	5540	
800	.171	4670	346		6000	.364	16500	4780	
1000	.183	5460	450		4000	.362	1050	3900	
1500	.210	7140	641		2000	.358	5590	2760	
2000	.230	8700	839		1000	.354	2820	1995	
2500	.244	10250	1035		500	.349	1430	1410	
3000	.257	11700	1240		200	.345	580	1160	
3500	.267	13100	1435		100	.342	292	726	
4000	.276	14450	1660		50	.339	147	588	
5000	.290	17250	2050		0	.316	0	337	
6000	.301	19900	2420						
7000	.312	22400	2830						
8000	.320	25000	3250						
9000	.326	27600	3580						
10000	.335	30000	4000						
11000	.339	32500	4340						
12000	.344	34900	4760						
13000	.348	37400	5170						
14000	.352	39800	5550						
15000	.356	42100	5850						
16000	.360	44500	6300						

Fig. A10

## ONE-DIMENSIONAL STATIC TEST DATA

Test No 11 Soil Type Remolded Soil Location Depth 5-22 ft.  
Sandy Silt Boring 5-4, Distant Plate  
w. 15.0 % S., 45.0 % Y, 101.8 pcf  $\gamma_c$ , 28.5 pcf  $S_s$ , 2.67 e, 0.888  
L. 2.0 % P, 19 % Classification Brown Sandy Silt (ML)

Axial Stress $\sigma_a$	Axial Strain $\epsilon_a$	Secant Modulus $M_s$	Radial Stress $\sigma_r$	Degree of Saturation $S_s$
psi	in/in	psi	psi	%
0	0	—	0	
10	.010	1000	0	
50	.046	1090	9.3	
100	.074	1355	67.6	
200	.101	1980	199	
300	.120	2500	256	
400	.136	2940	314	
500	.144	3470	330	
600	.153	3920	397	
800	.167	4800	442	
1000	.184	5420	552	
1500	.208	7200	688	
2000	.223	8960	926	
2500	.237	10550	1110	
3000	.250	12000	1345	
3500	.258	13550	1550	
4000	.268	14900	1900	
5000	.283	17100	2070	
6000	.293	20500	2570	
7000	.303	23100	3040	
8000	.310	25800	3470	
9000	.316	28400	3980	
10000	.320	31300	4530	
11000	.326	33800	4950	
12000	.331	36300	5470	
13000	.336	38700	5960	
14000	.341	41000	6190	
15000	.344	43600	6750	
16000	.348	46000	7270	

Axial Stress $\sigma_a$	Axial Strain $\epsilon_a$	Secant Modulus $M_s$	Radial Stress $\sigma_r$	Degree of Saturation $S_s$
psi	in/in	psi	psi	%
17000	.350	48500	7800	
18000	.353	51000	8190	
19000	.355	53500	8710	
20000	.358	55900	9300	
17500	.358	48900	8730	
15000	.358	41900	8150	
12500	.358	34900	7500	
10000	.355	28200	6590	
8000	.354	22600	5860	
6000	.352	19000	5090	
4000	.349	11400	4310	
2000	.346	5770	3060	
1000	.342	2920	2240	
500	.337	1485	1675	
200	.333	600	1230	
100	.330	303	947	
50	.326	153.5	822	
0	.304	0	461	

Note: Water extrusion at  
 $\sigma_a = 2500 \text{ psi.} \approx 16 \text{ g/cm}^2$  of  
water extruded during test.

Fig. A11

# ONE-DIMENSIONAL STATIC TEST DATA

Test No 12 Soil Type Recalded Soil Location Depth 5-22 ft.  
Sandy Silt Boring 5-14, Distant Plain 6  
W<sub>1</sub> 27.2 % S<sub>r</sub> 80.3 % T<sub>1</sub> 112.2 pcf T<sub>0</sub> 88.0 pcf S<sub>0</sub> 267 e<sub>0</sub> 0.898  
L<sub>0</sub> 20 % P<sub>0</sub> 19 % Classification Brown Sandy Silt (ML)

Axial Stress $\sigma_a$	Axial Strain $\epsilon_a$	Secant Modulus $M_s$	Radial Stress $\sigma_r$	Degree of Saturation $S_r$	Axial Stress $\sigma_a$	Axial Strain $\epsilon_a$	Secant Modulus $M_s$	Radial Stress $\sigma_r$	Degree of Saturation $S_r$
psi	in/in	psi	psi	%	psi	in/in	psi	psi	%
0	0	—	0		9000	.258	34000	3360	
10	.032	321	0		10000	.263	38000	3740	
50	.058	860	0		11000	.270	40700	4100	
100	.076	1318	9.5		12000	.274	43400	4450	
150	.088	1700	9.8		13000	.278	46800	4850	
200	.094	2130	29.9		14000	.282	49600	5300	
250	.101	2480	50.5		15000	.286	52500	5550	
300	.107	2800	81.2		16000	.288	55500	5950	
350	.112	3120	92		17000	.291	58500	6350	
400	.117	3420	103		18000	.294	61100	6630	
450	.121	3720	104		19000	.295	64500	7050	
500	.124	4030	115		20000	.299	66900	7470	
600	.131	4580	126		17500	.299	58500	7080	
700	.137	5100	192		15000	.293	50400	6700	
800	.143	5600	215		12500	.298	42000	6270	
900	.147	6120	237		10000	.296	33800	5610	
1000	.152	6560	312		8000	.295	27100	4960	
1250	.162	7700	425		6000	.292	20500	4250	
1500	.171	8780	500		4000	.291	15700	3450	
1750	.178	9840	560		2000	.288	6950	2380	
2000	.185	10800	677		1000	.284	3520	1675	
2500	.196	12750	860		500	.280	1790	1260	
3000	206	14560	1042		200	.278	719	882	
3500	214	16350	1270		100	.276	362	650	
4000	223	17900	1420		50	.274	182	607	
5000	232	21600	1800		0	.262	—	375	
6000	241	24900	2190		Note: Water extrusion at				
7000	247	28400	2580		$\epsilon_a = 10 \text{ psi} \approx 48 \text{ gms}$ of water extruded during test.				
8000	253	31600	2970						

Fig. A12

**APPENDIX B AXIAL STRESS VERSUS AXIAL STRAIN**

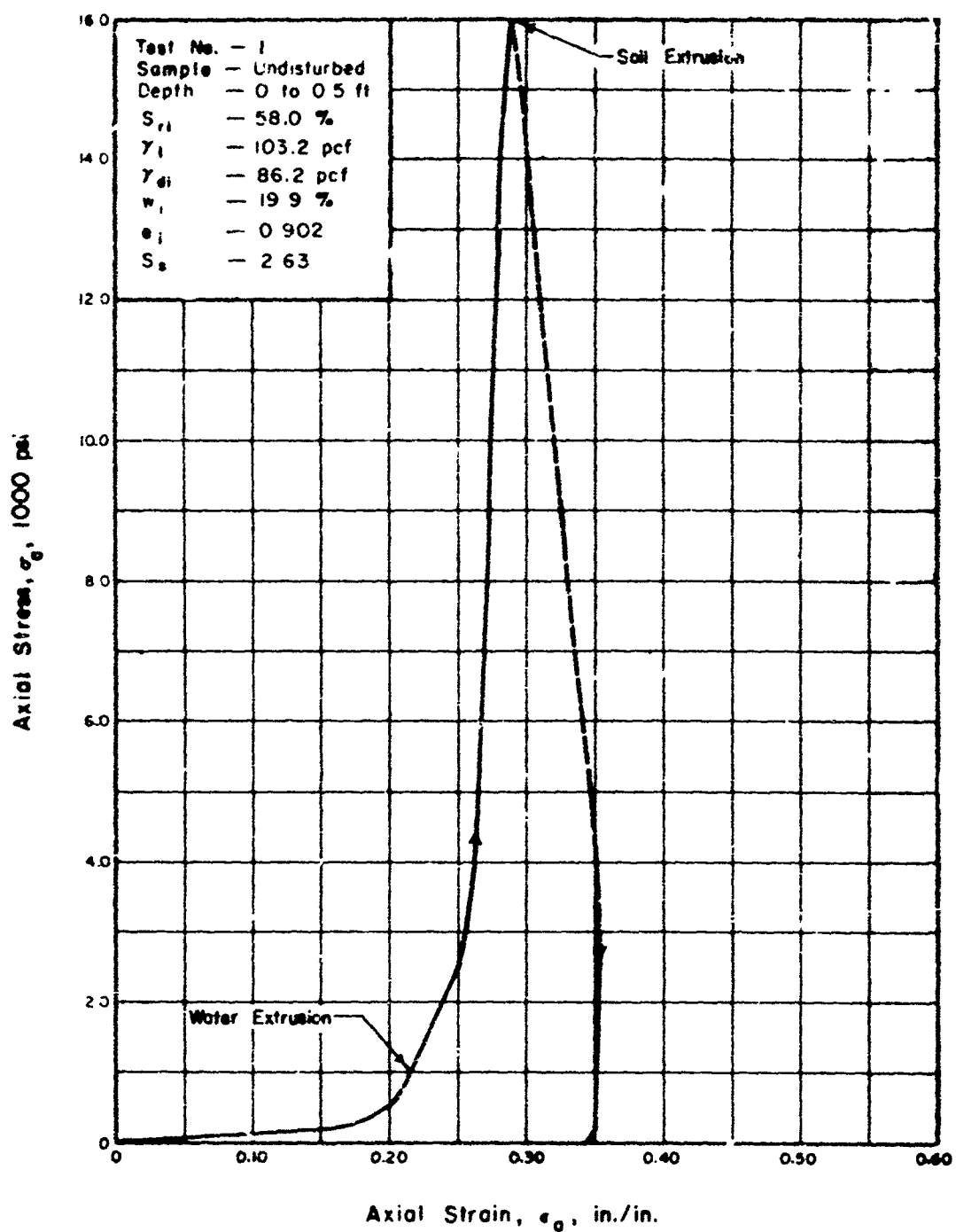


Fig B1. Stress-strain relation in one-dimensional compression, test 1

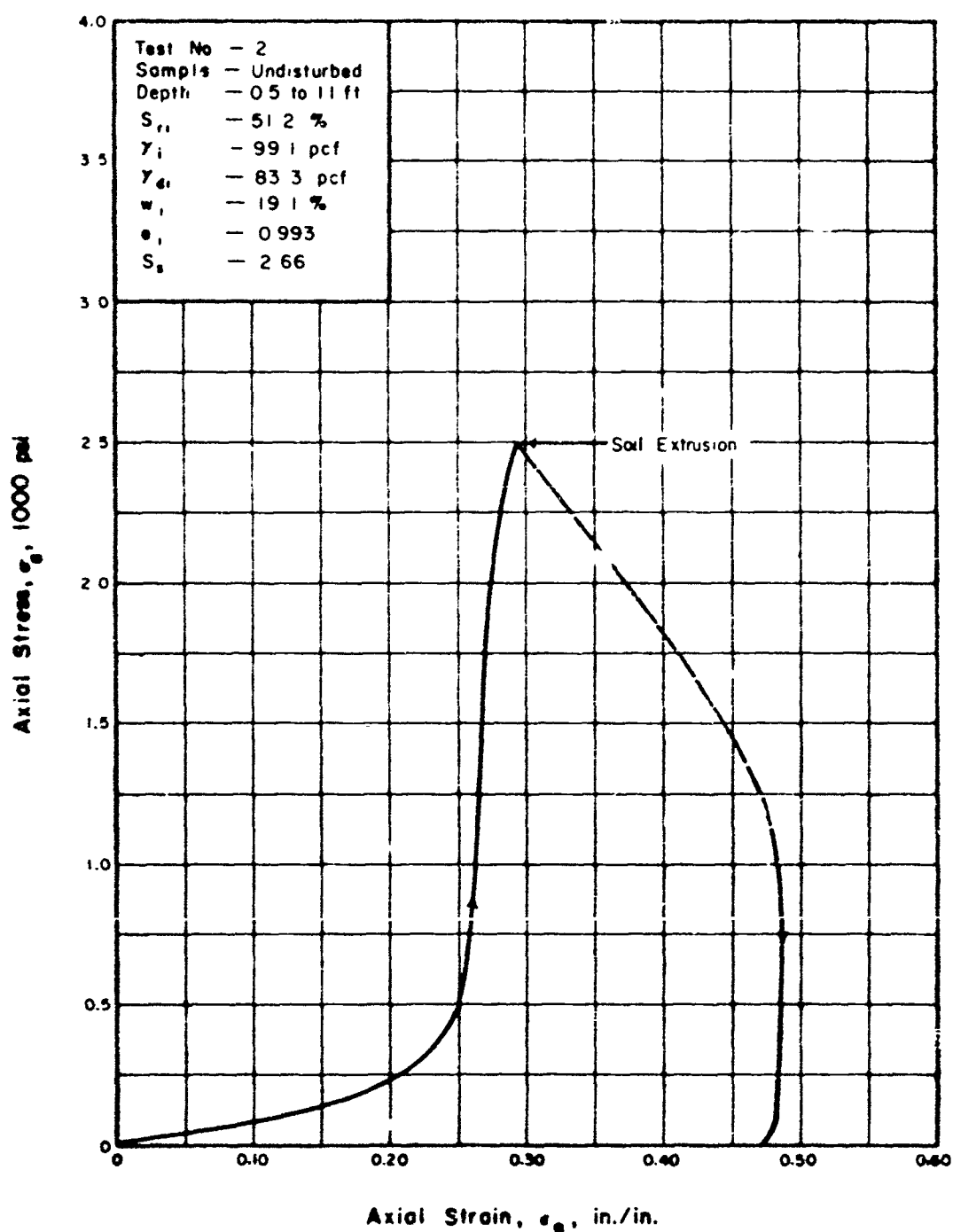


Fig. B2. Stress-strain relation in one-dimensional compression, test 2

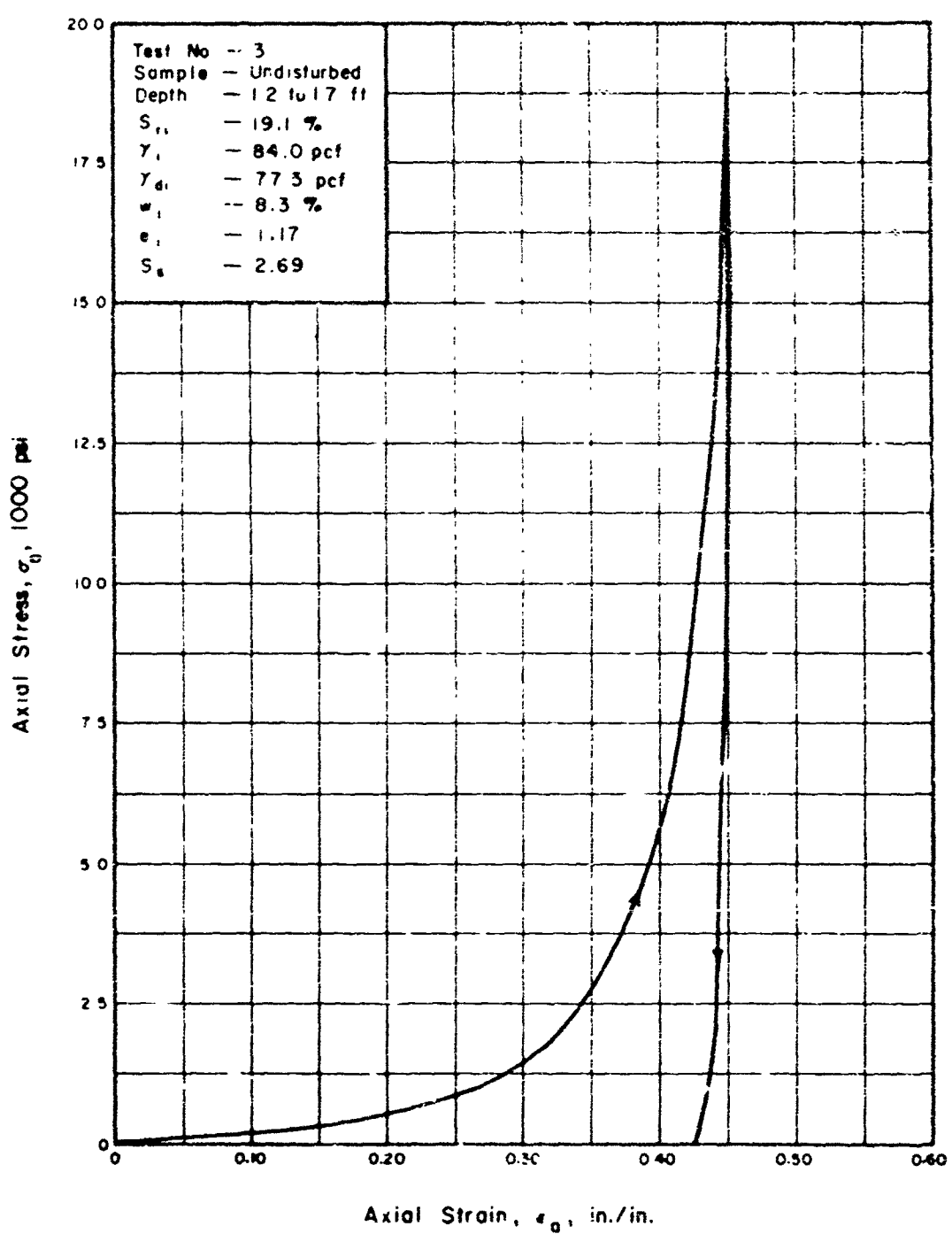


Fig B3. Stress-strain relation in one-dimensional compression, test 3

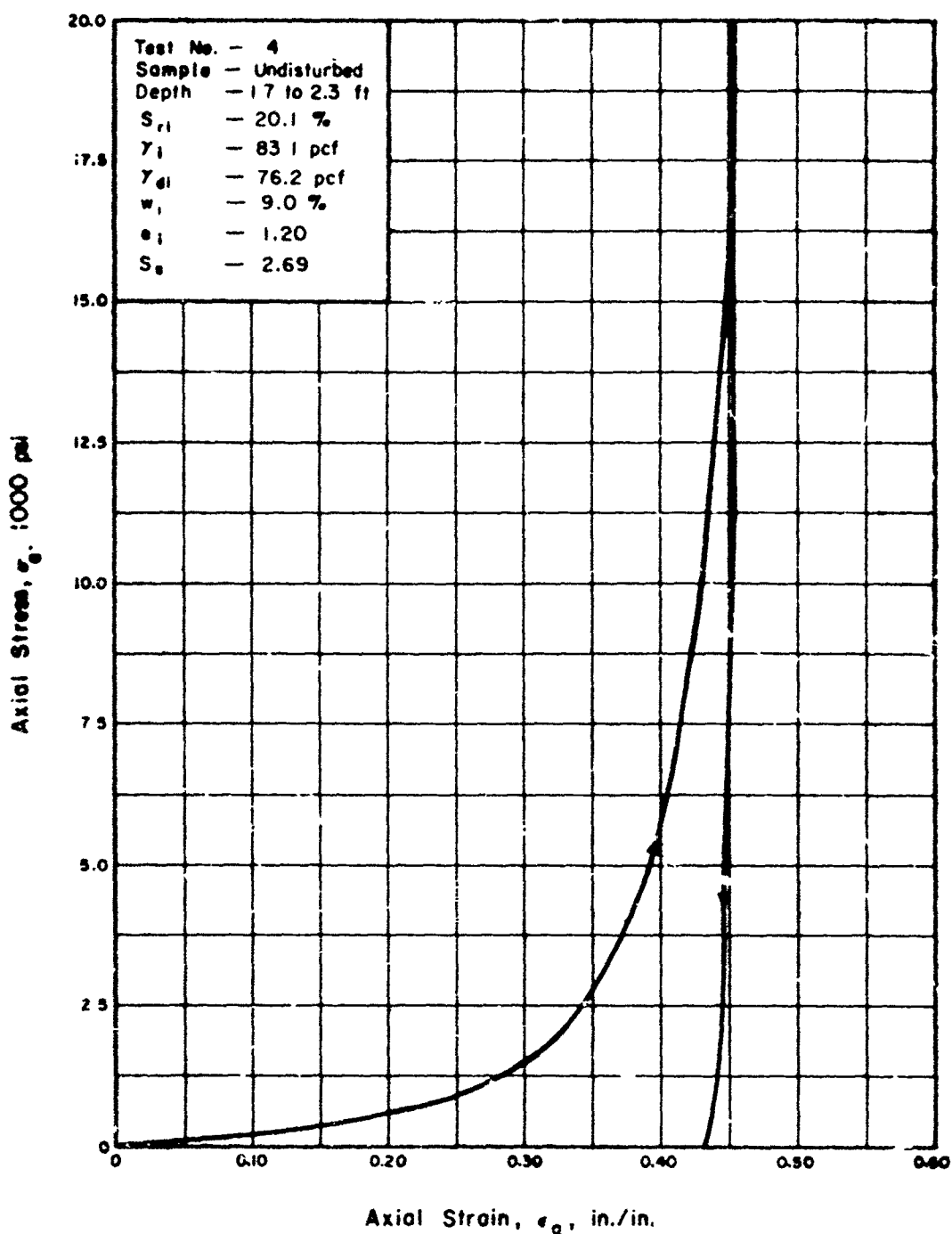


Fig. B4. Stress-strain relation in one-dimensional compression test 4

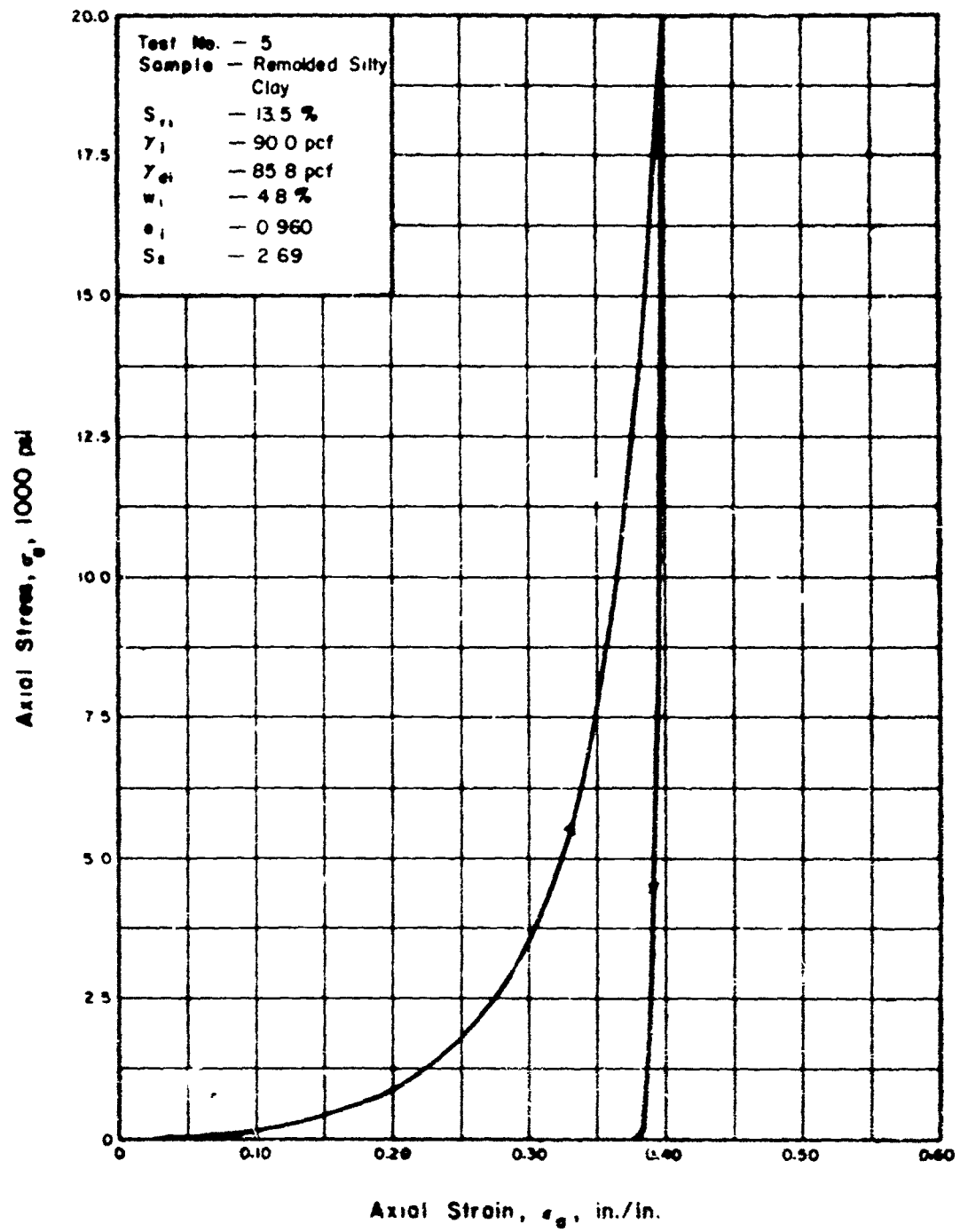


Fig. B5 Stress-strain relation in one-dimensional compression test 5

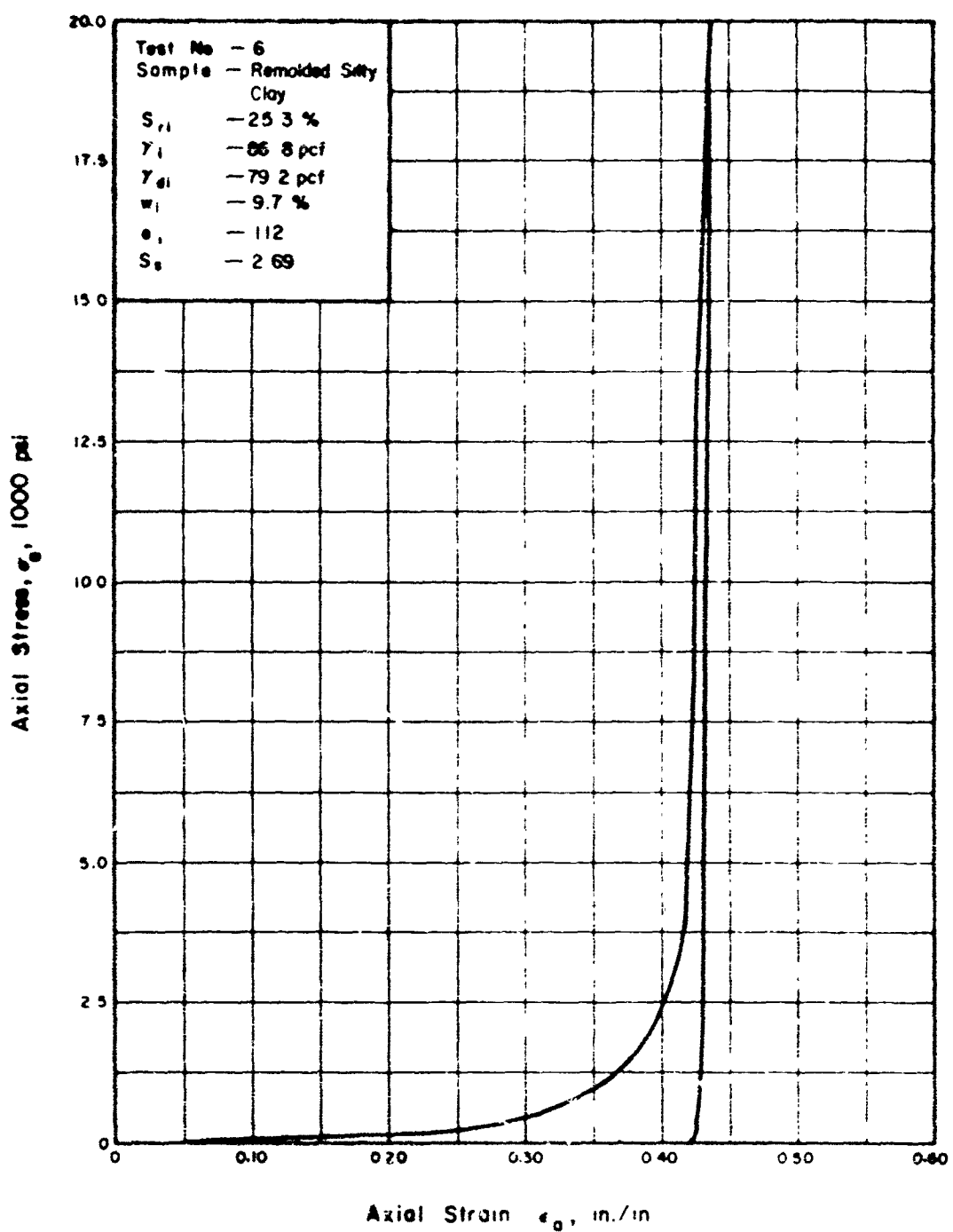


Fig B6 Stress-strain relation in one dimensional compression test 6

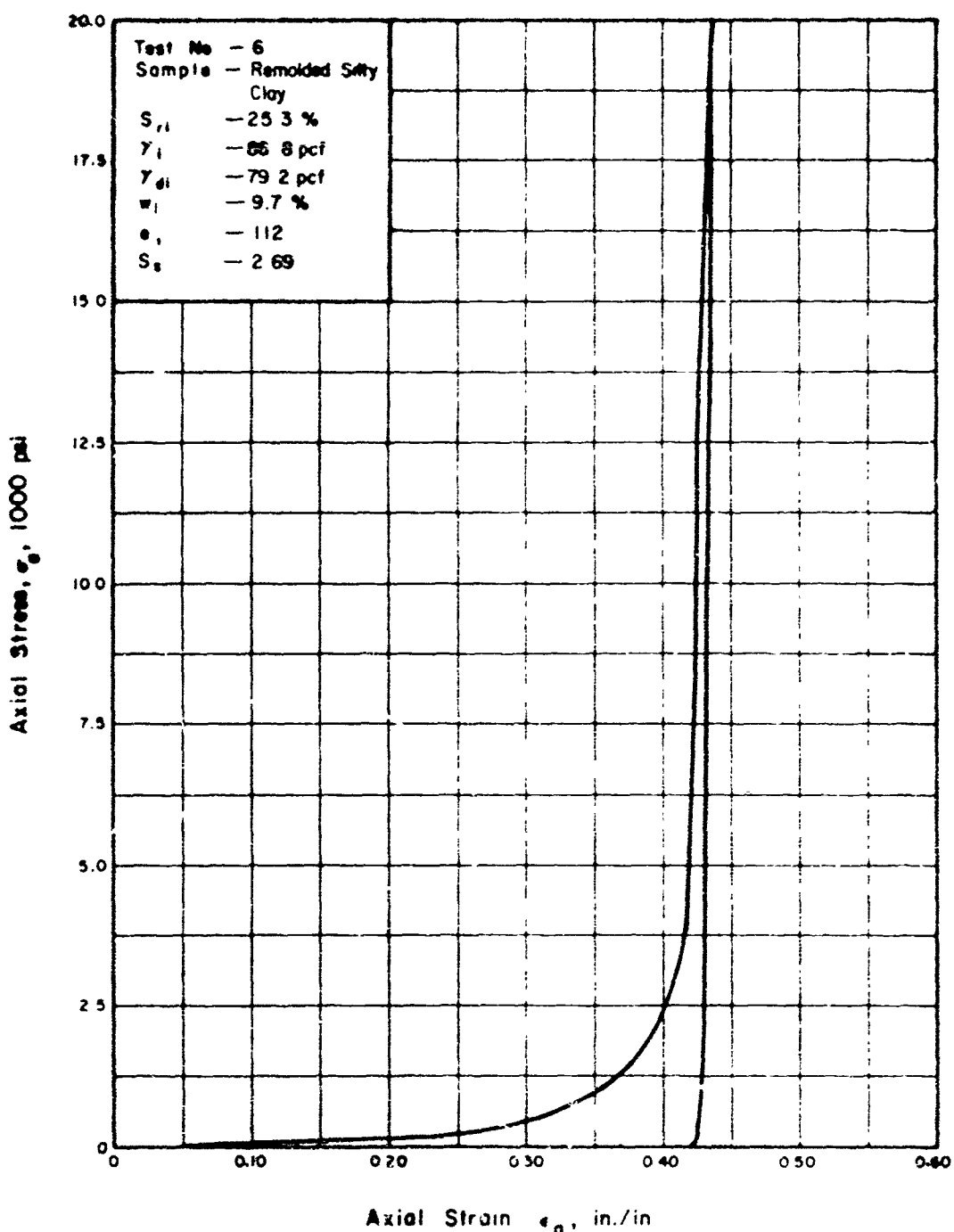


Fig. B6 Stress-strain relation in one dimensional compression test 6

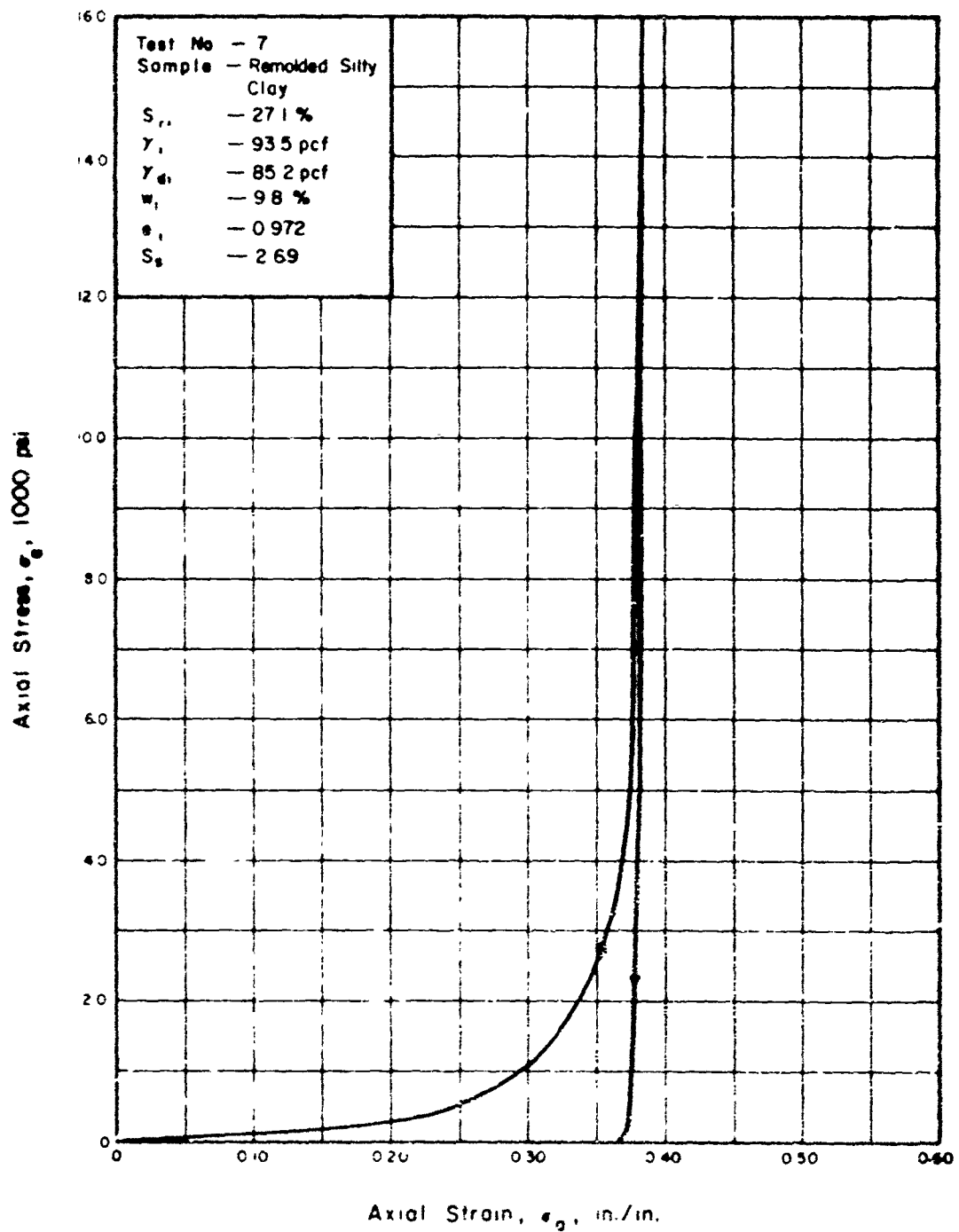


Fig. B7 Stress-strain relation in one dimensional compression, test 7

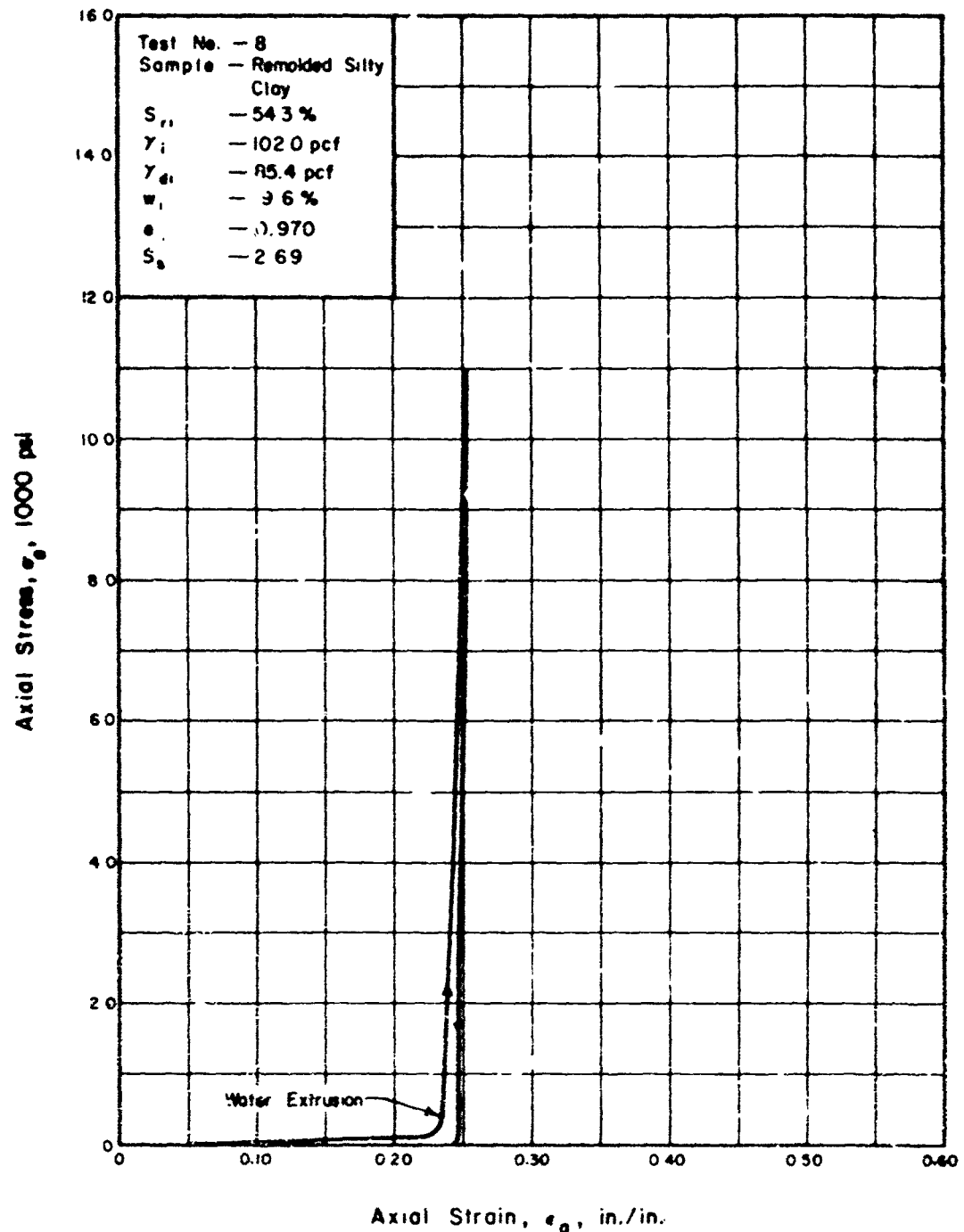


Fig. B8 Stress-strain relation in one-dimensional compression, test 8

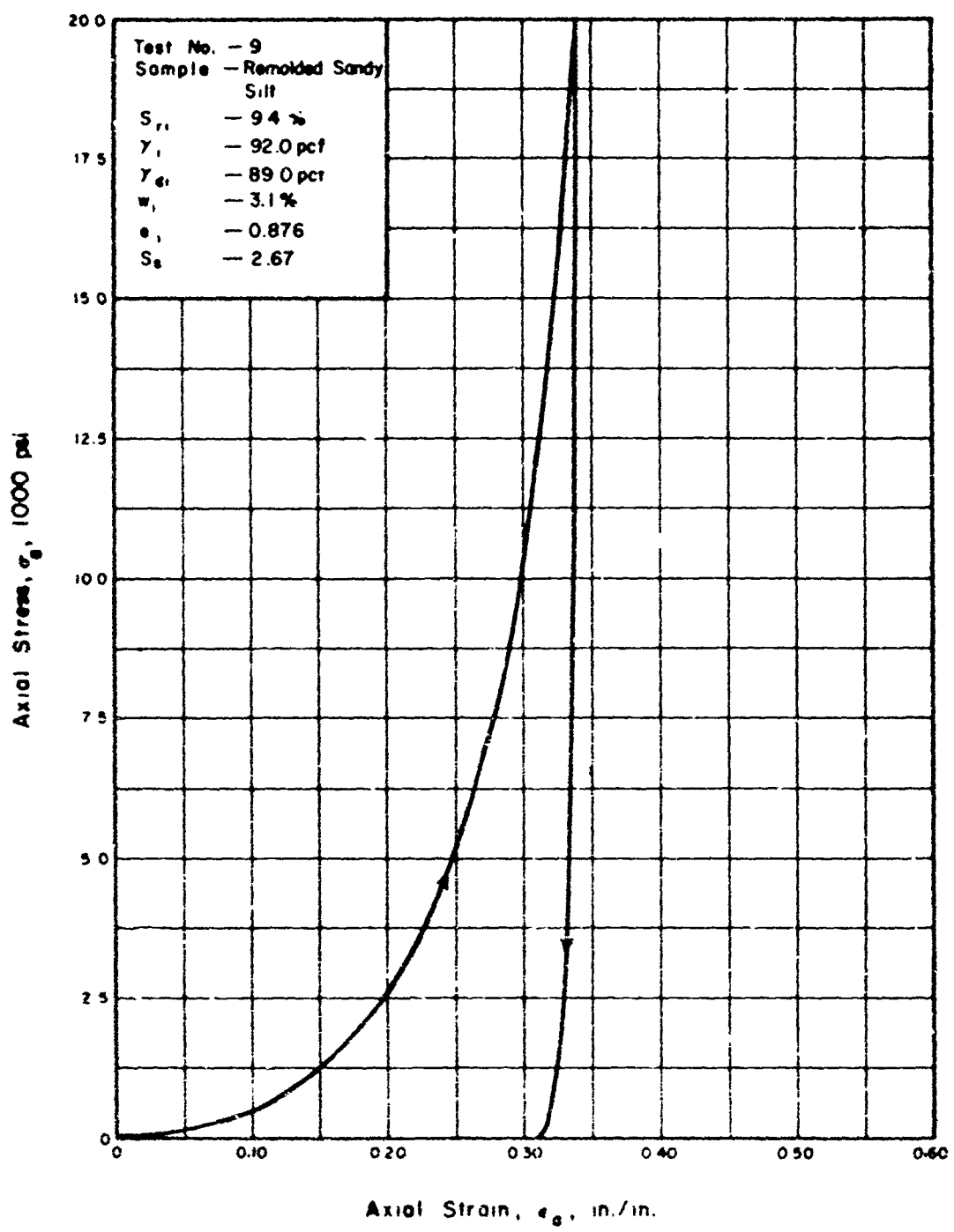


Fig. B9. Stress-strain relation in one-dimensional compression test 9

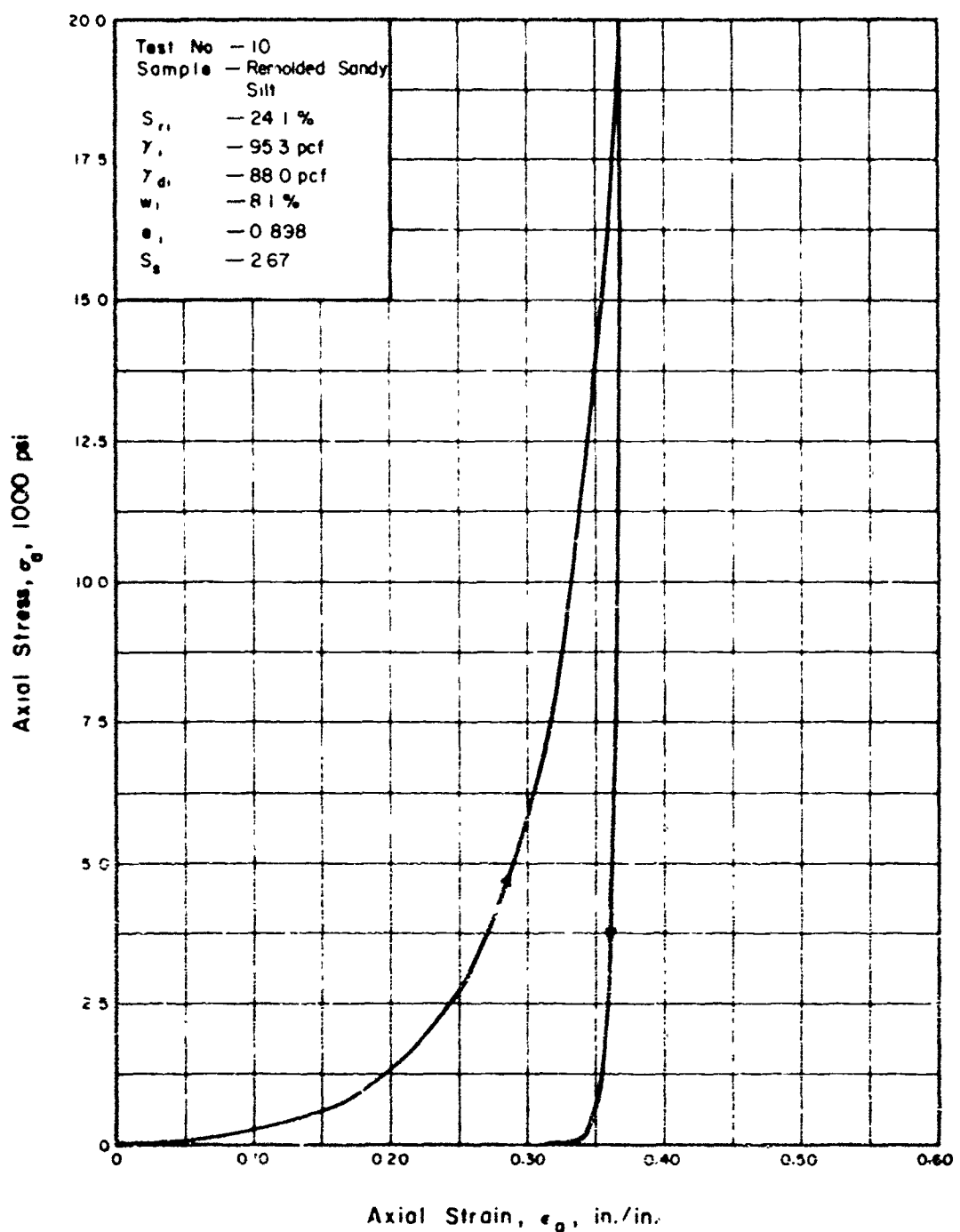


Fig B10 Stress-strain relation in one dimensional compression, test 10

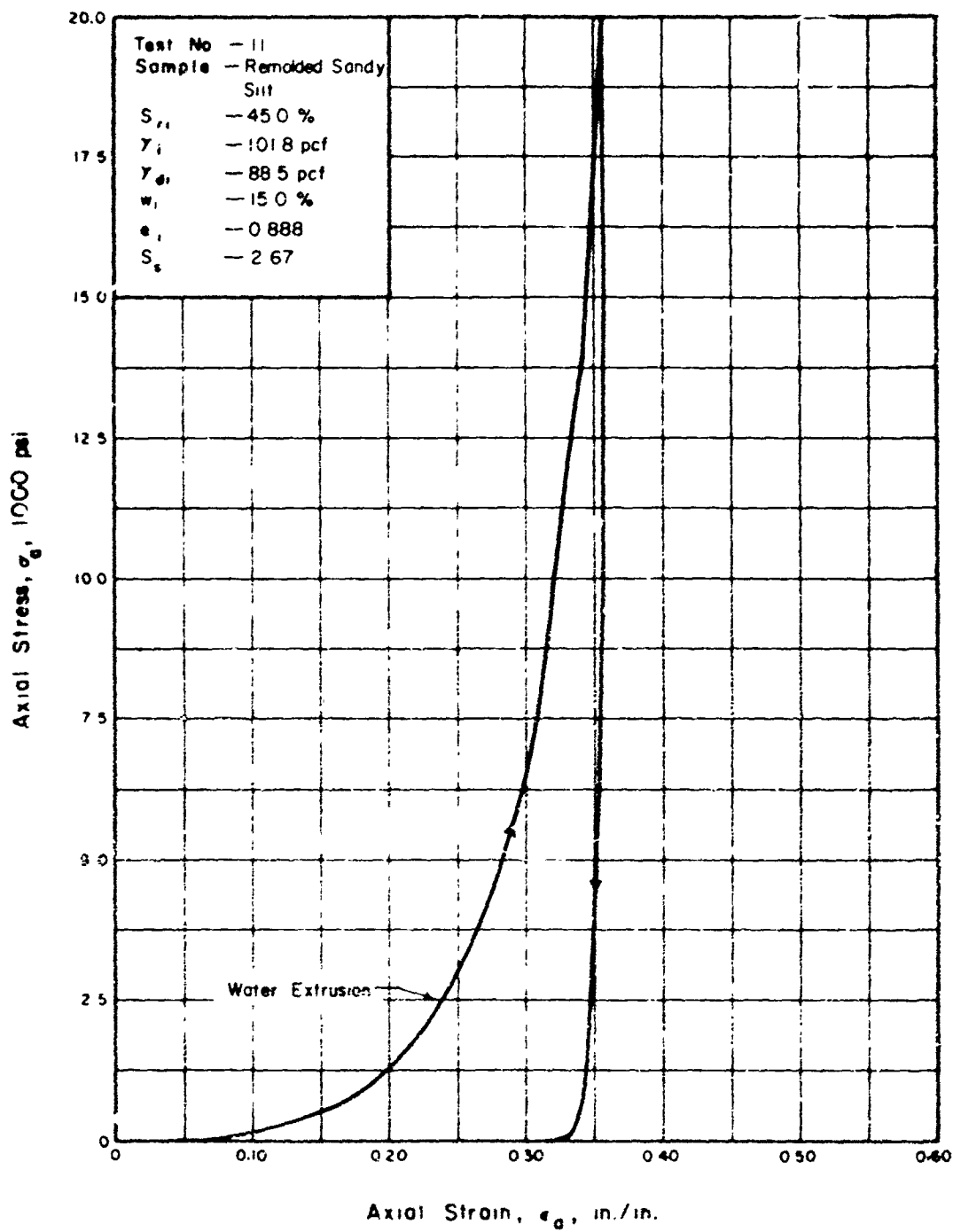


Fig B11 Stress-strain relation in one-dimensional compression, test 11

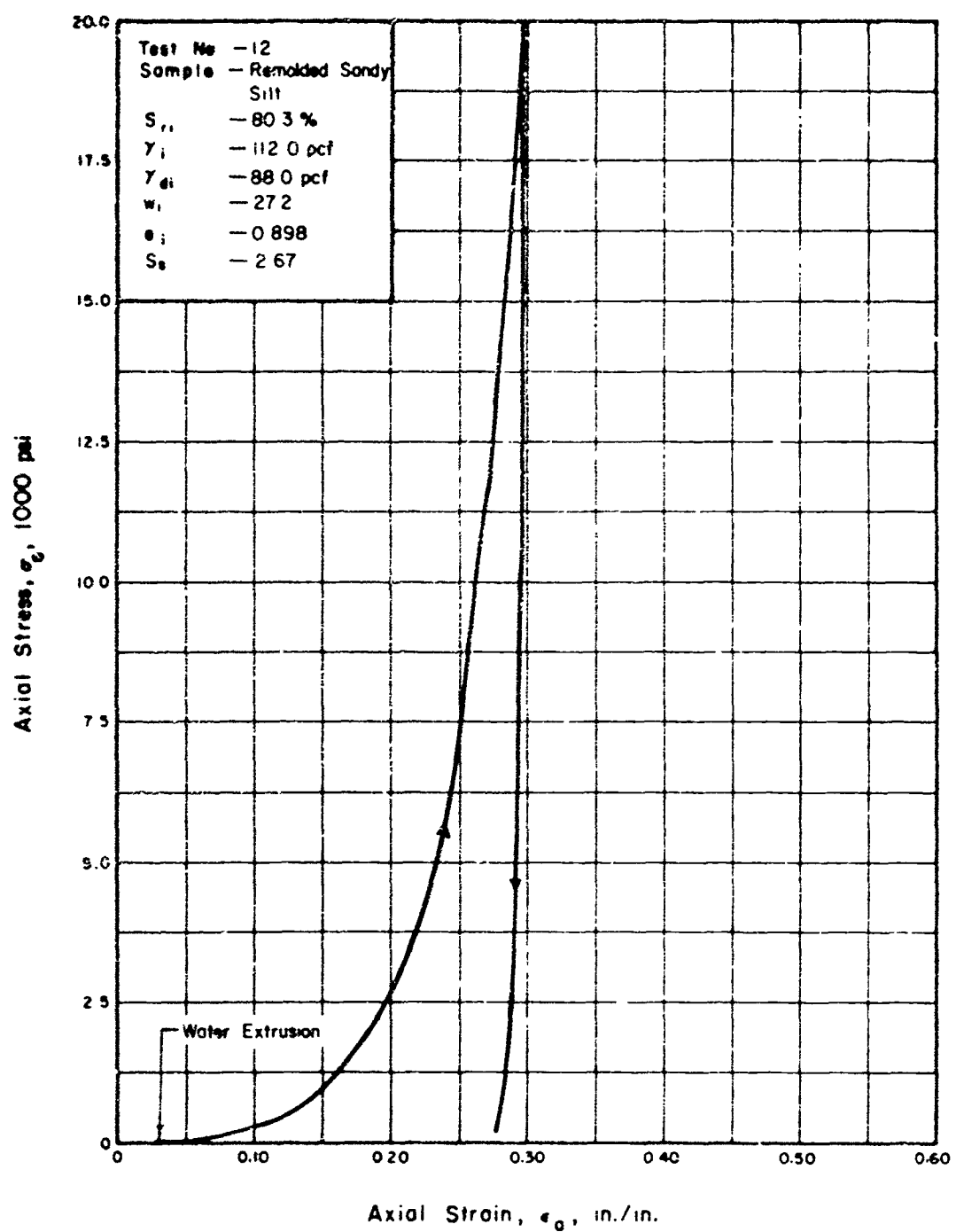


Fig. B12. Stress-strain relation in one-dimensional compression, test 12

APPENDIX C. CONSTRAINED MODULUS VERSUS AXIAL STRESS.

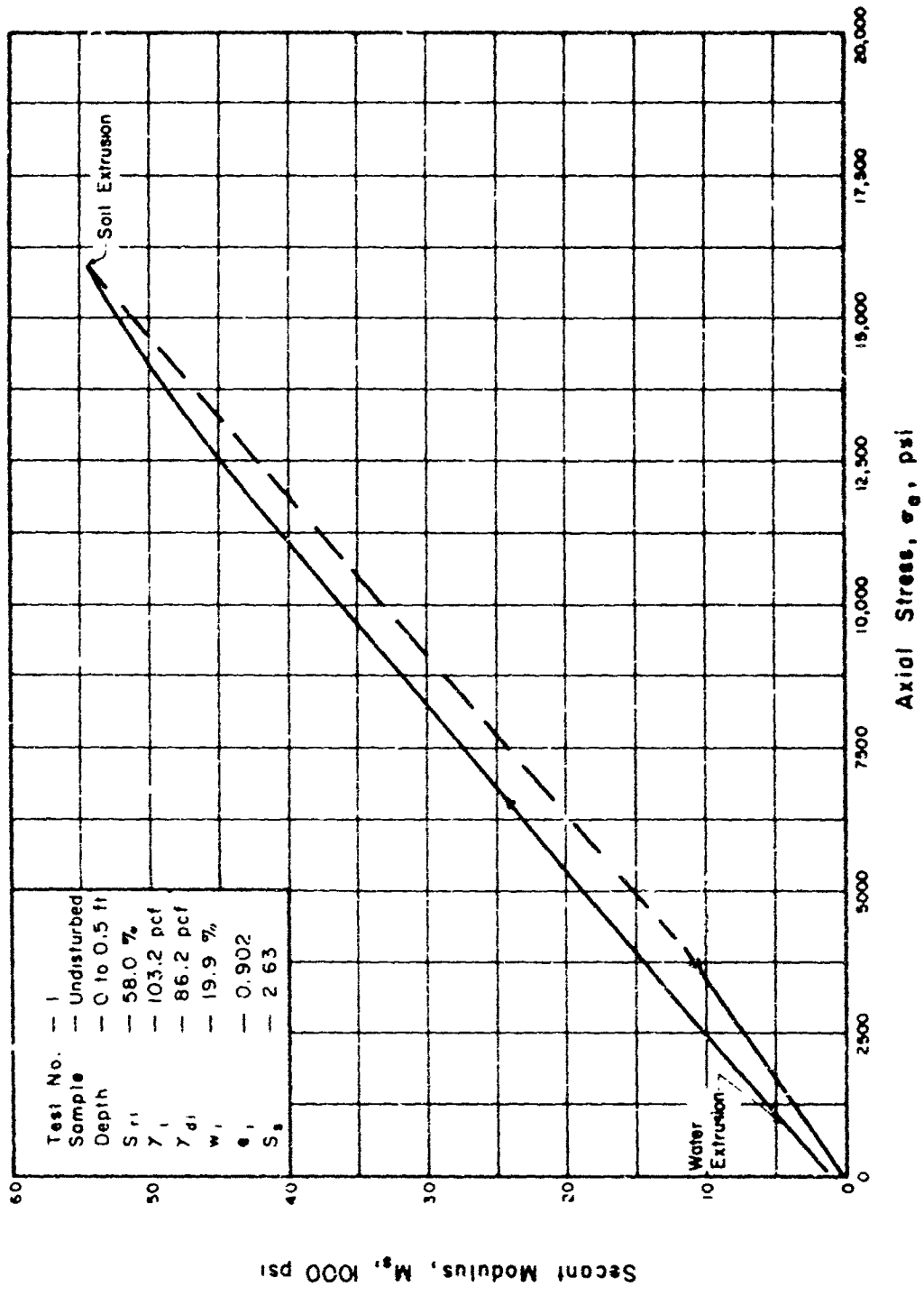


Fig C1: Relation between secant modulus and axial stress, test 1

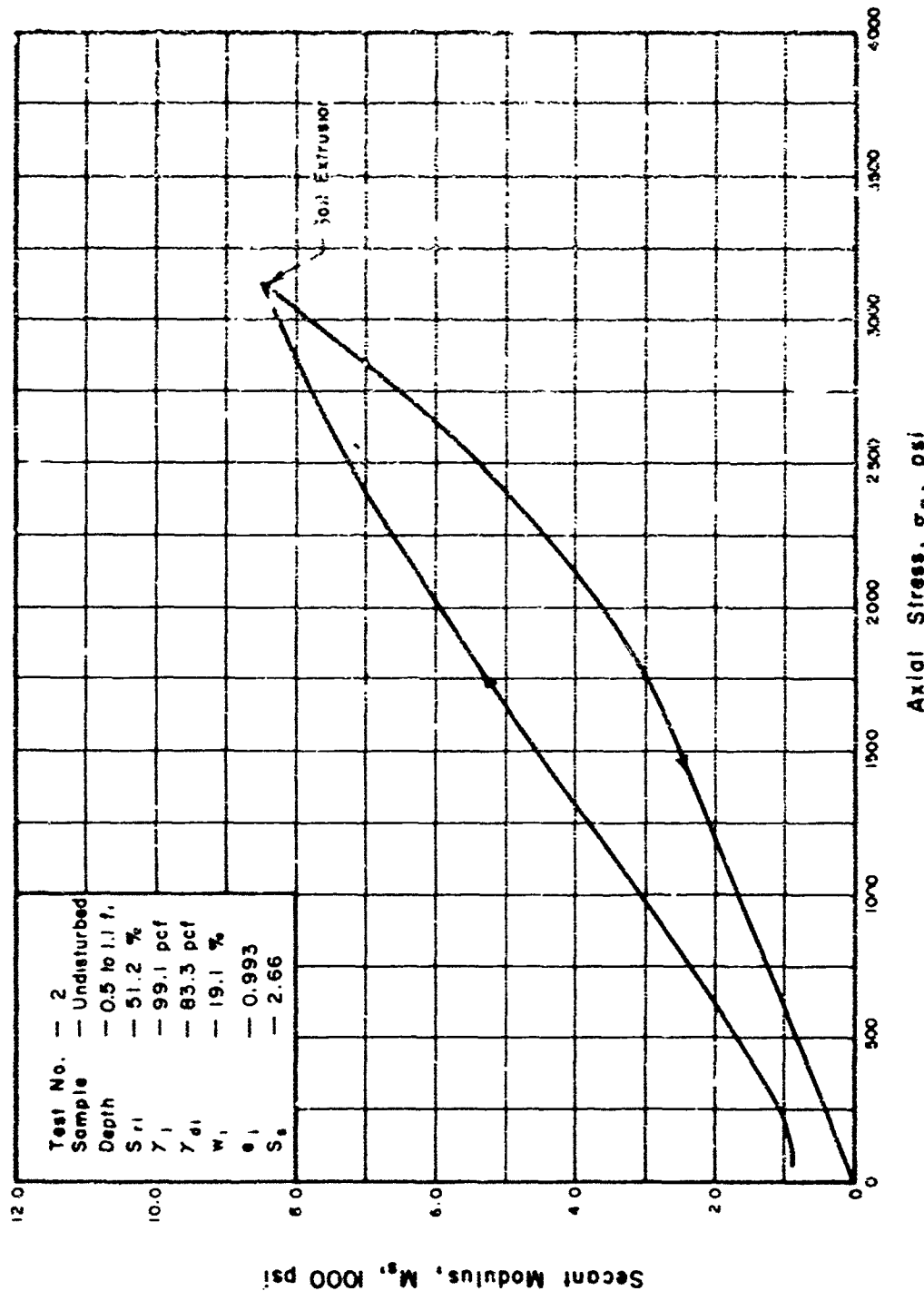


Fig. C2. Relation between secant modulus and axial stress, test 2

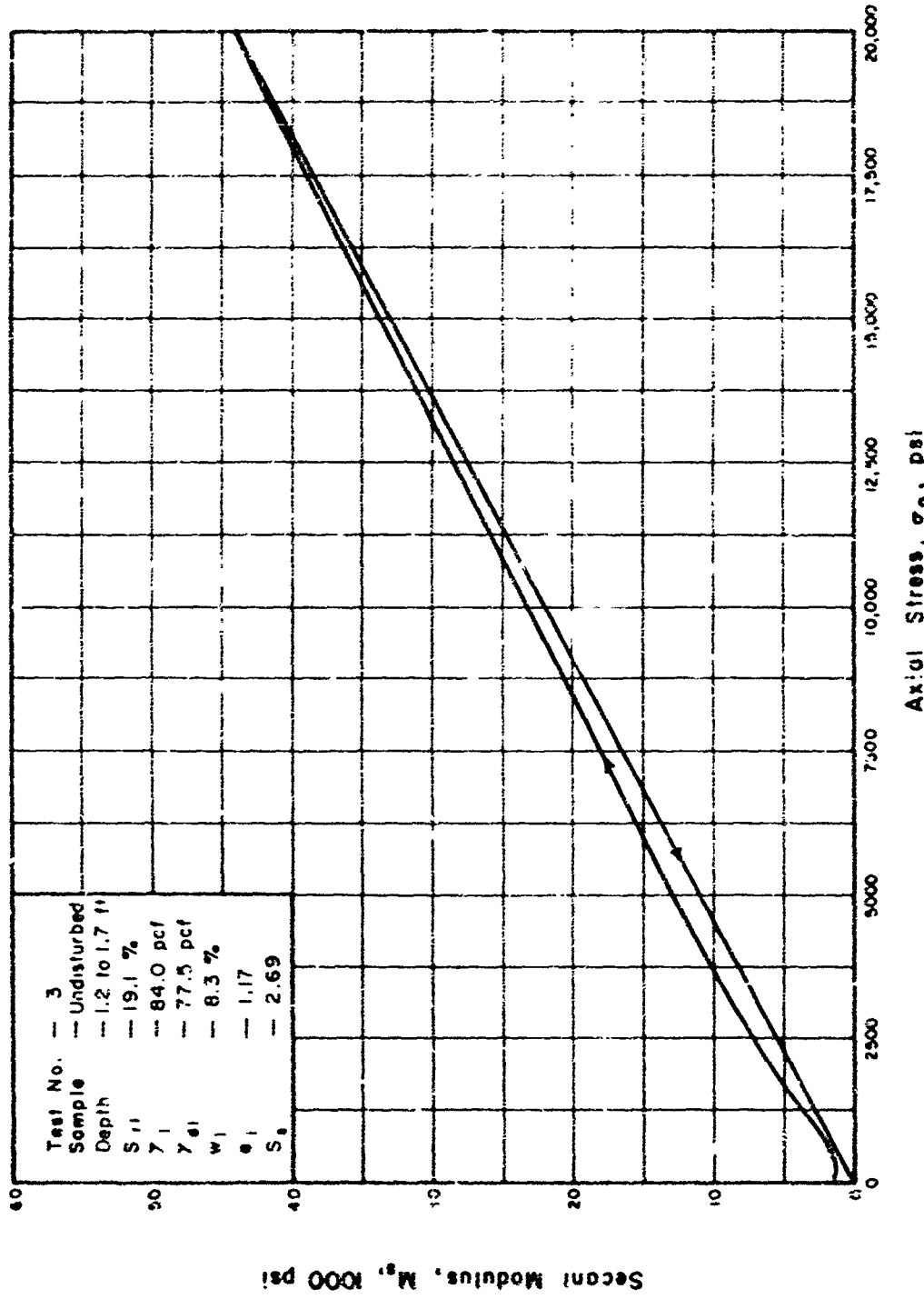


Fig. C3. Relation between secant modulus and axial stress, test 3

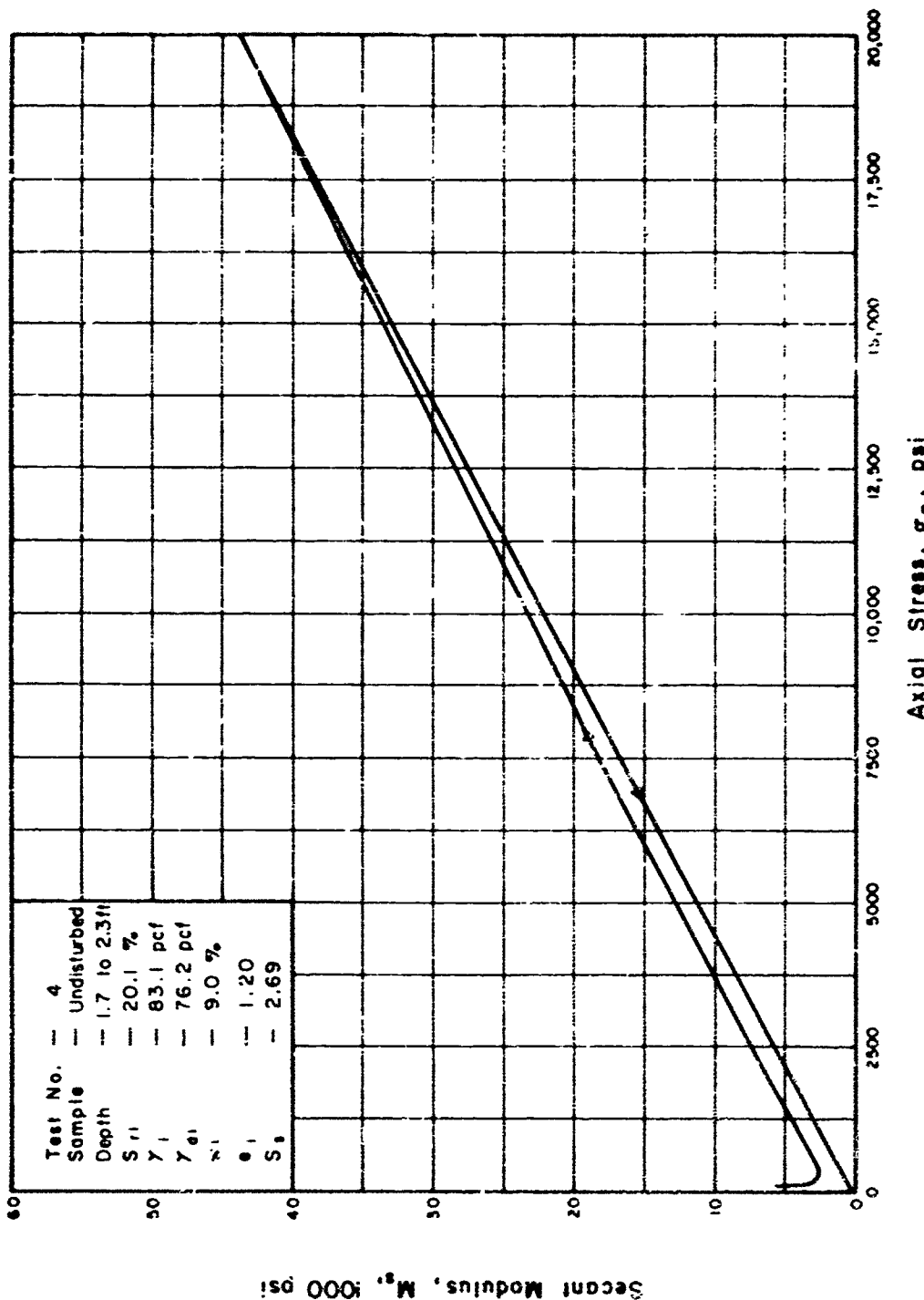


Fig. C4. Relation between secant modulus and axial stress, test 4

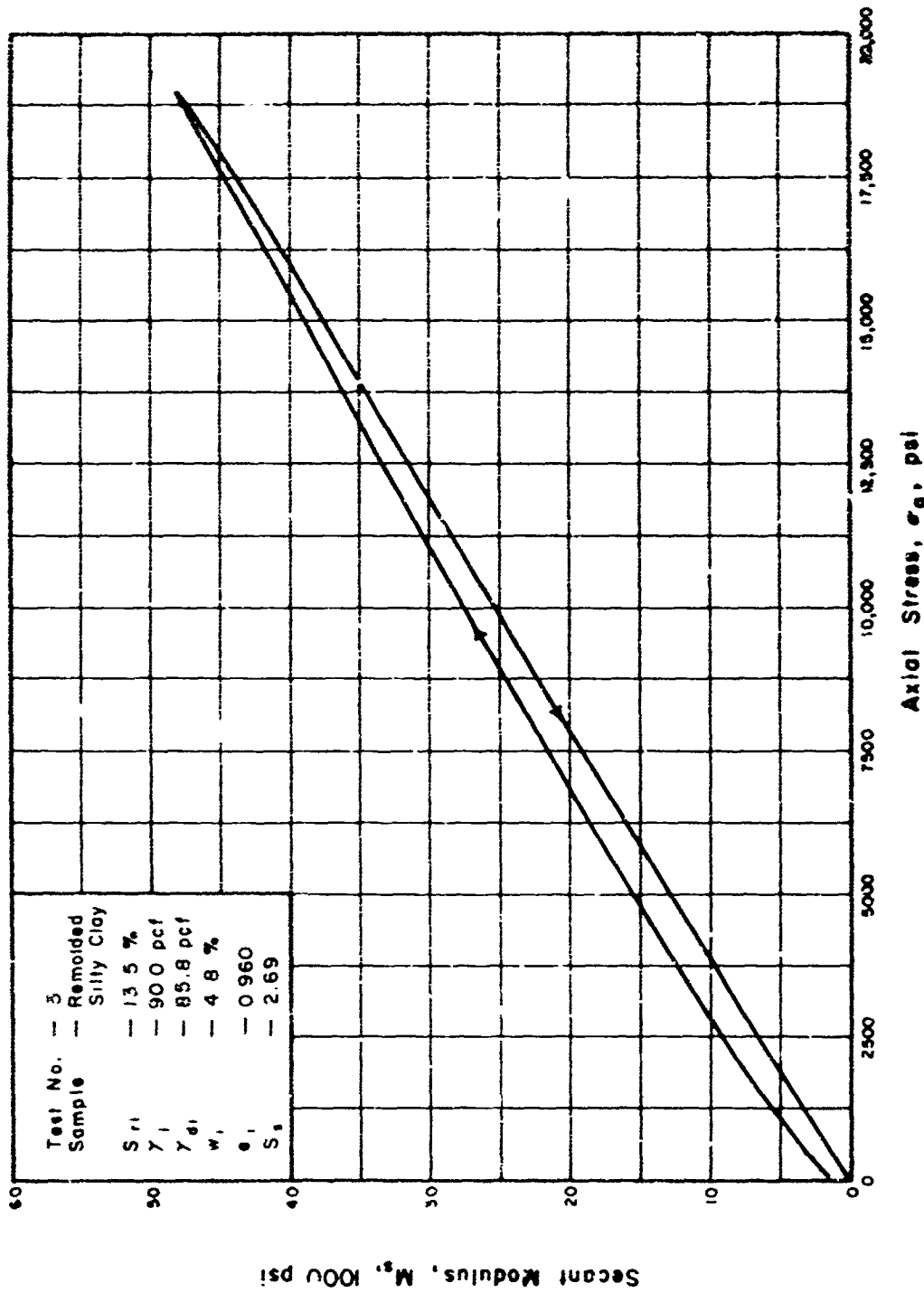


Fig. C5. Relation between secant modulus and axial stress, test 5

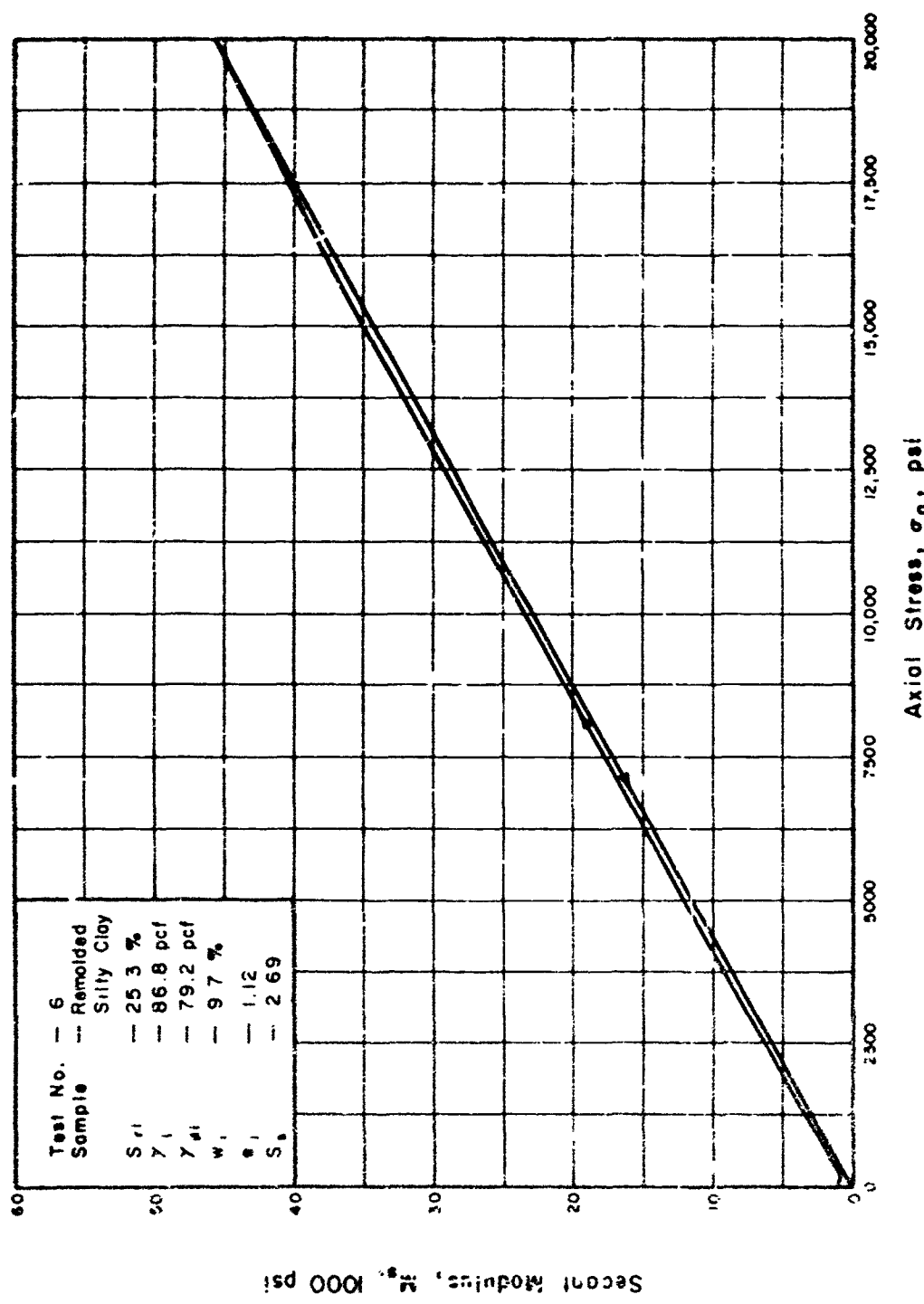


Fig. C6. Relation between secant modulus and axial stress, test 6

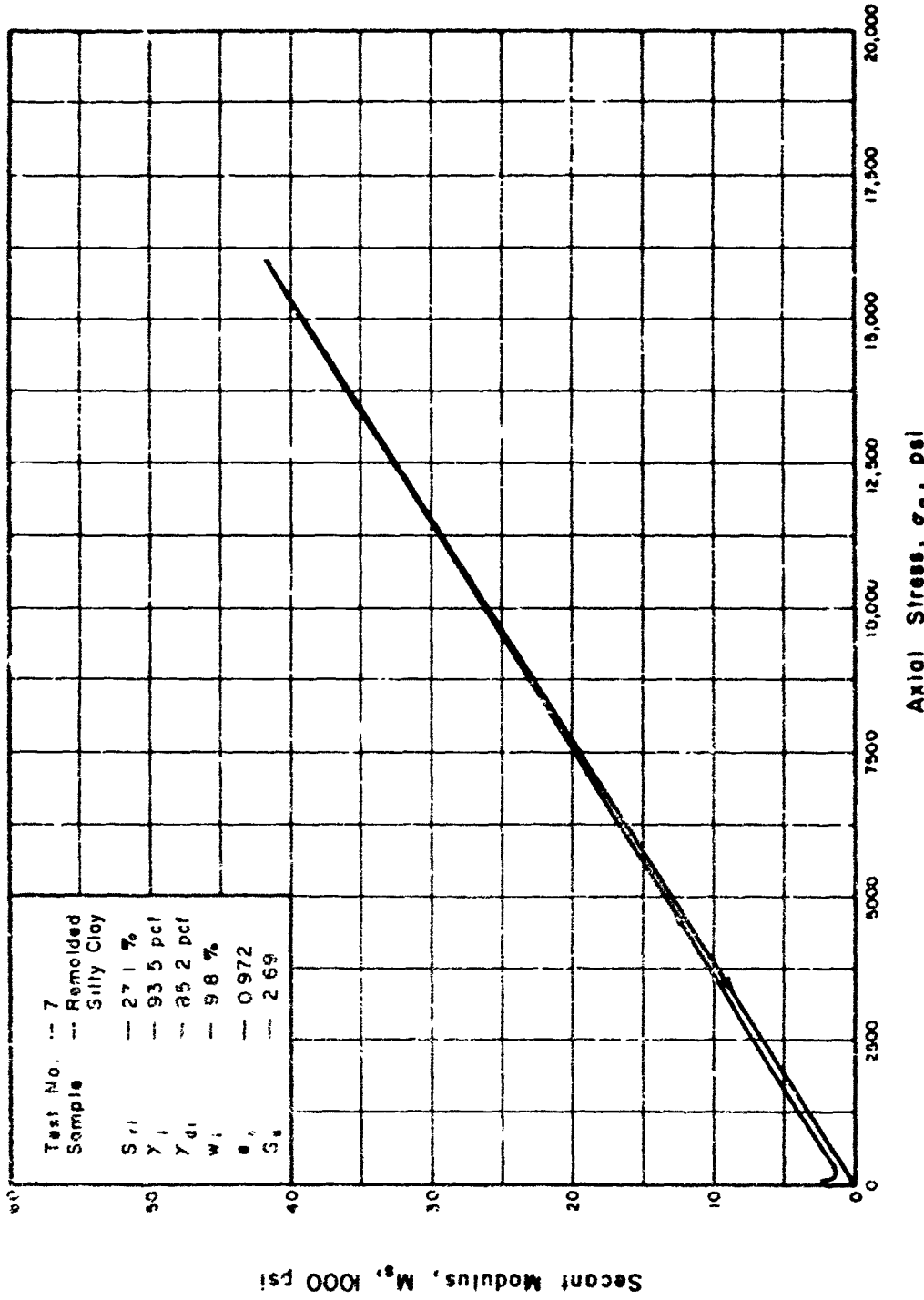


Fig. C7. Relation between secant modulus and axial stress, test 7

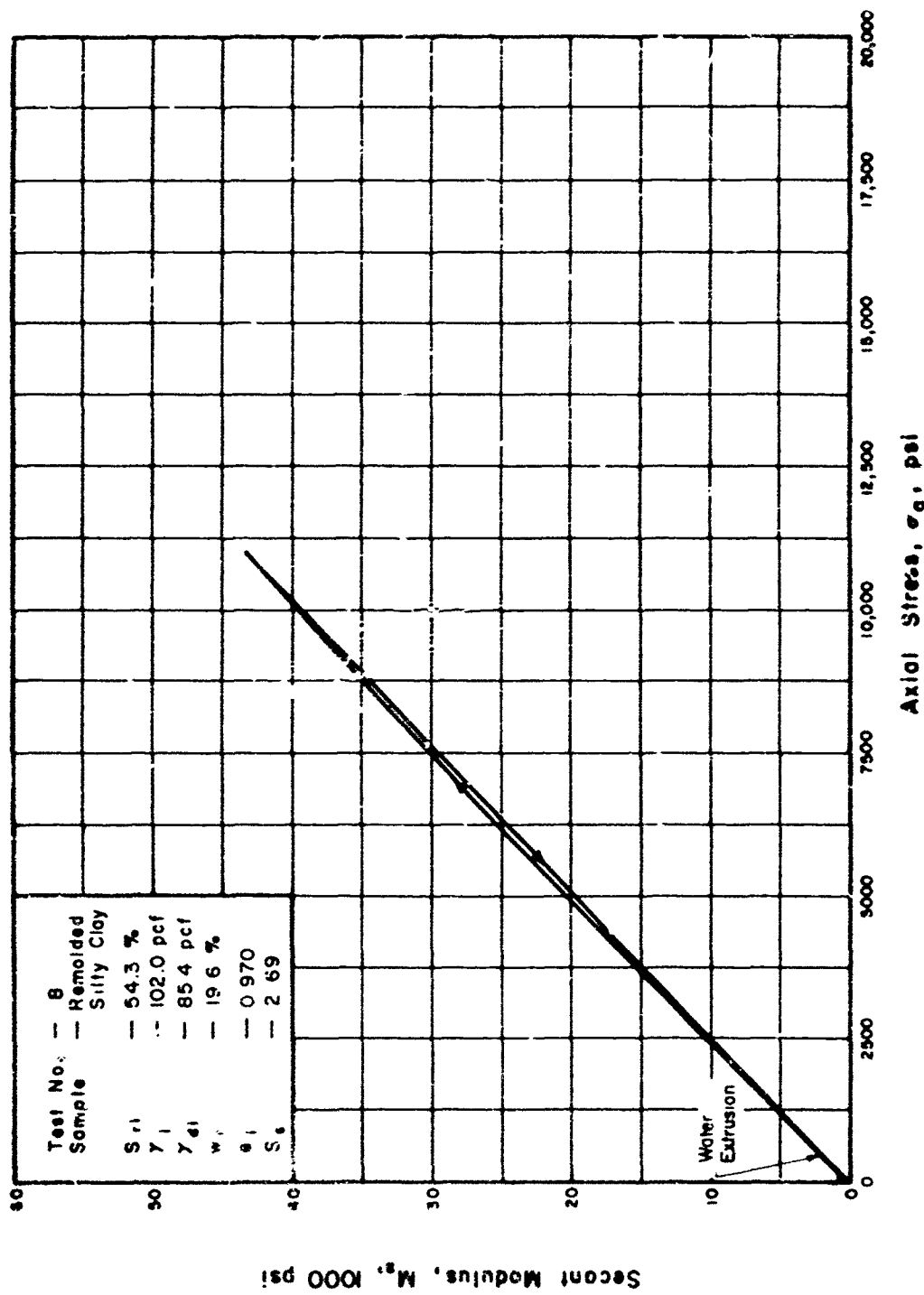


Fig. C8. Relation between secant modulus and axial stress, test 8

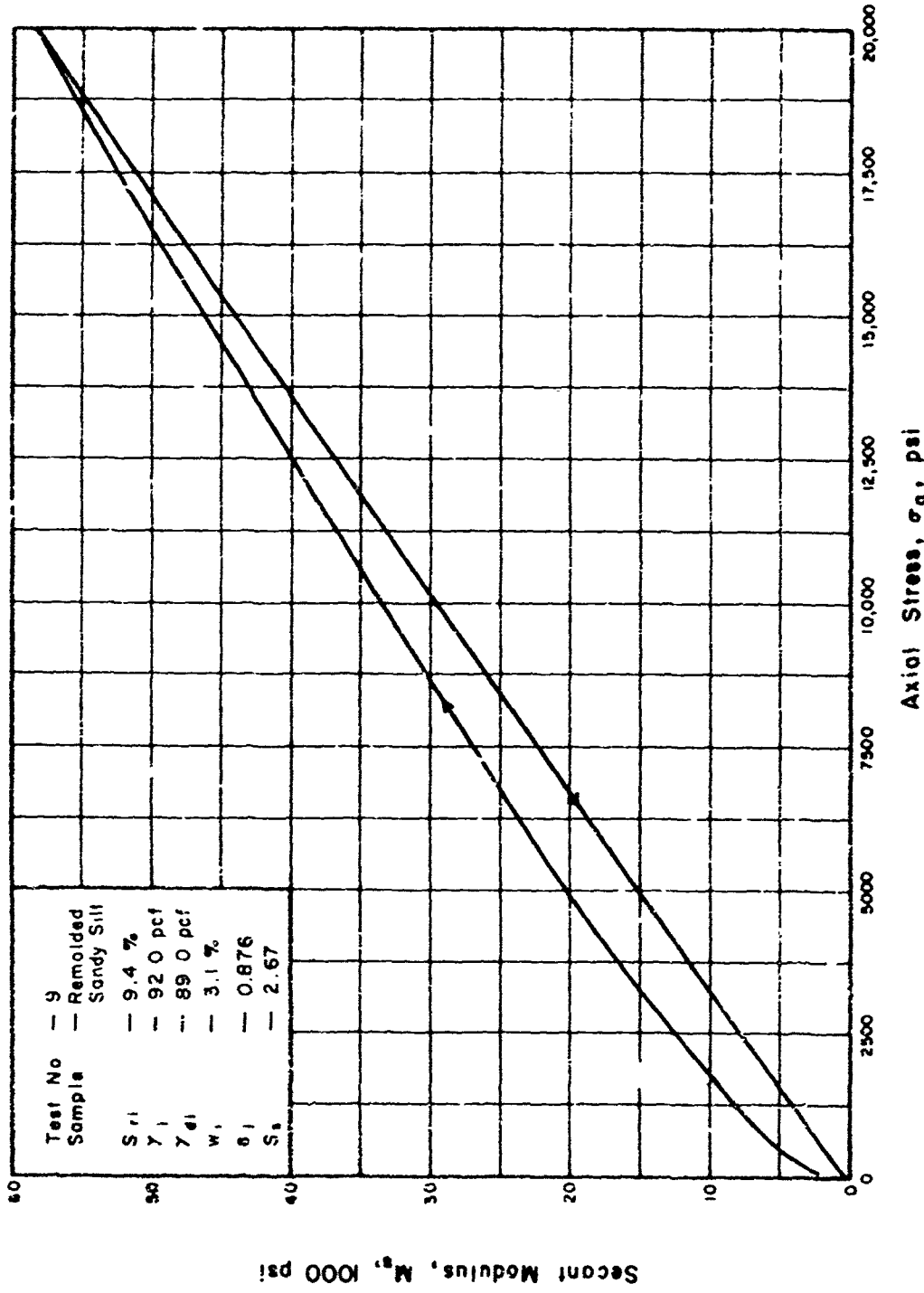


Fig. C9. Relation between secant modulus and axial stress, test 9

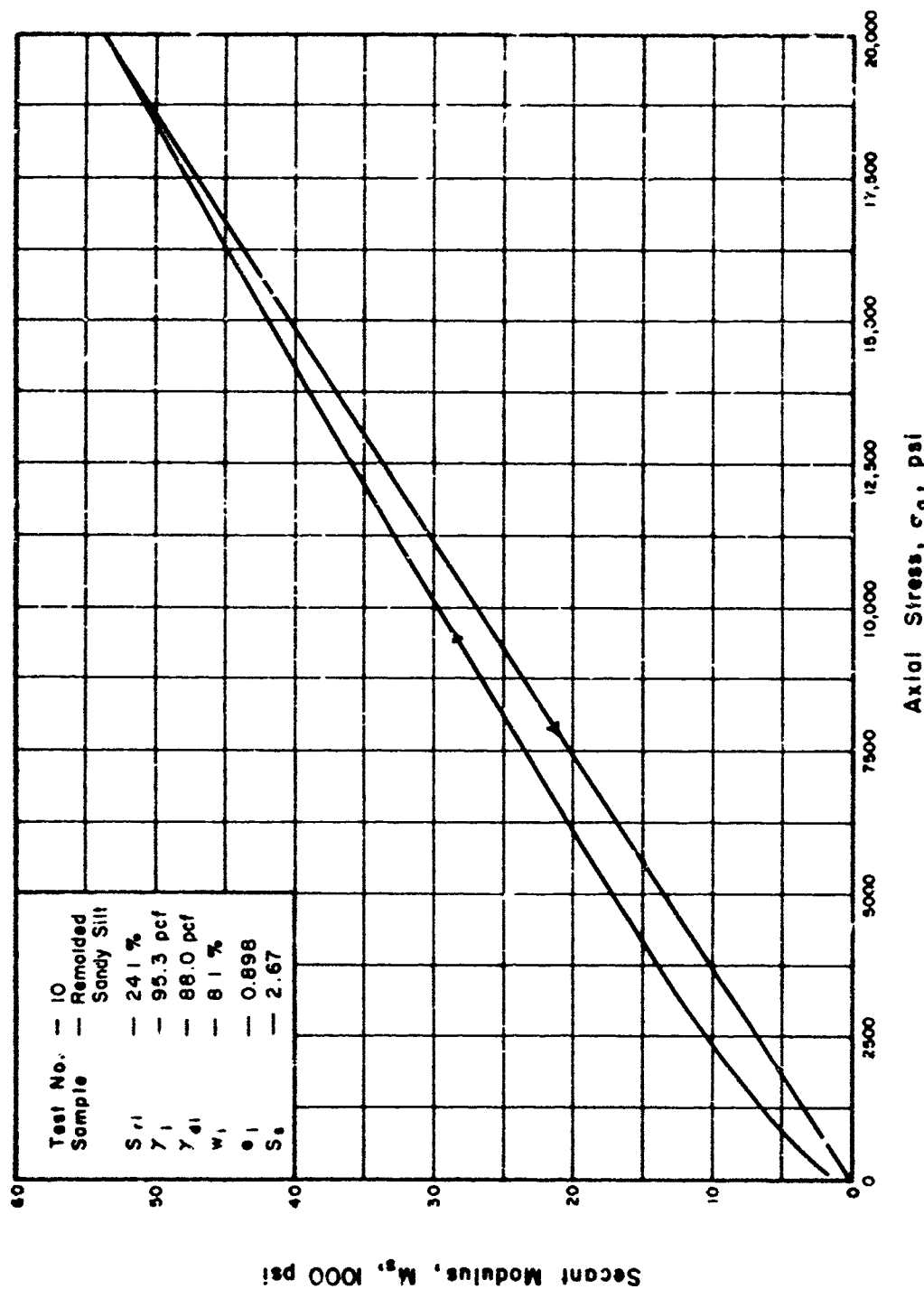


Fig. C10. Relation between secant modulus and axial stress test 10

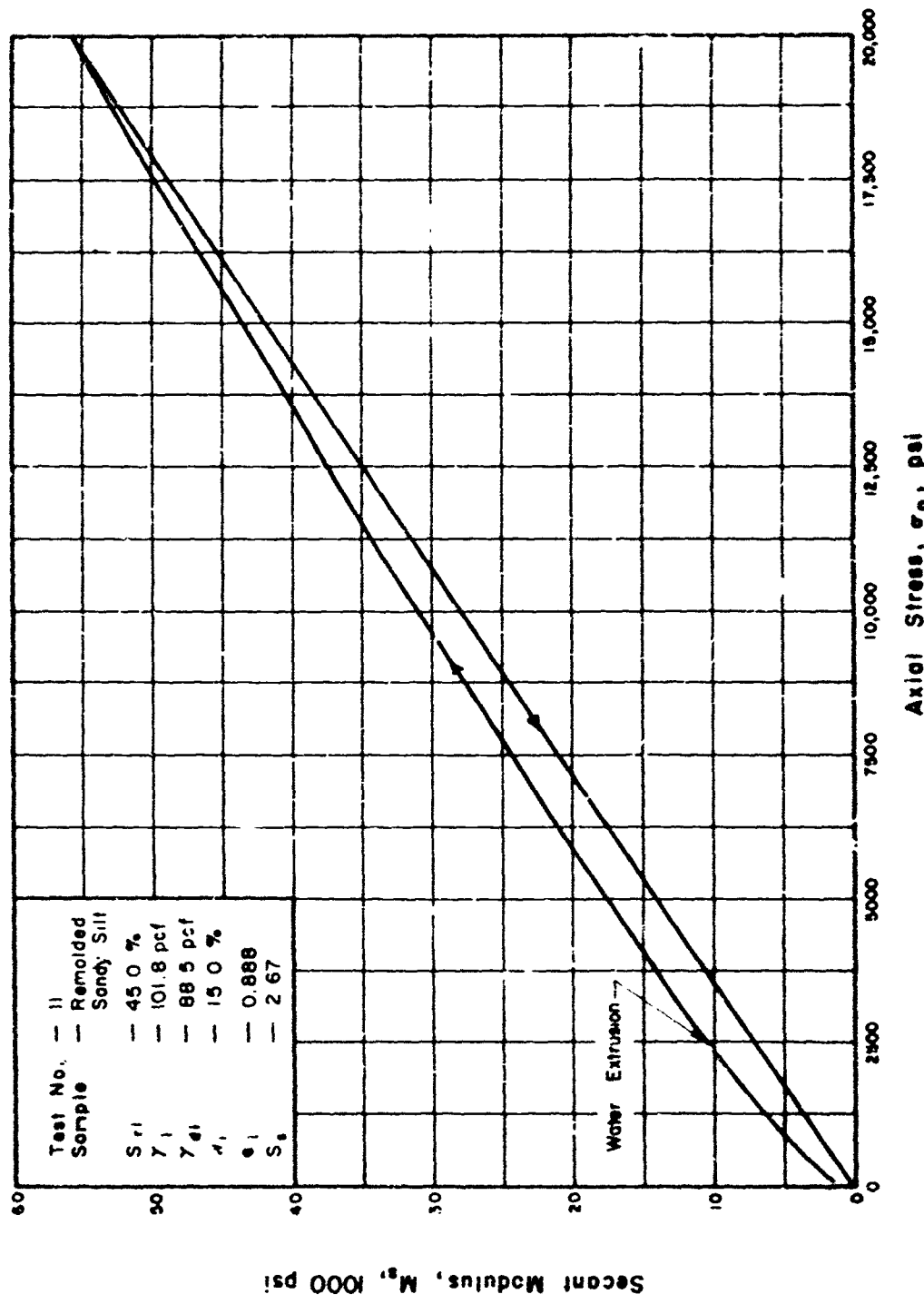


Fig. C11. Relation between secant modulus and axial stress, test 11

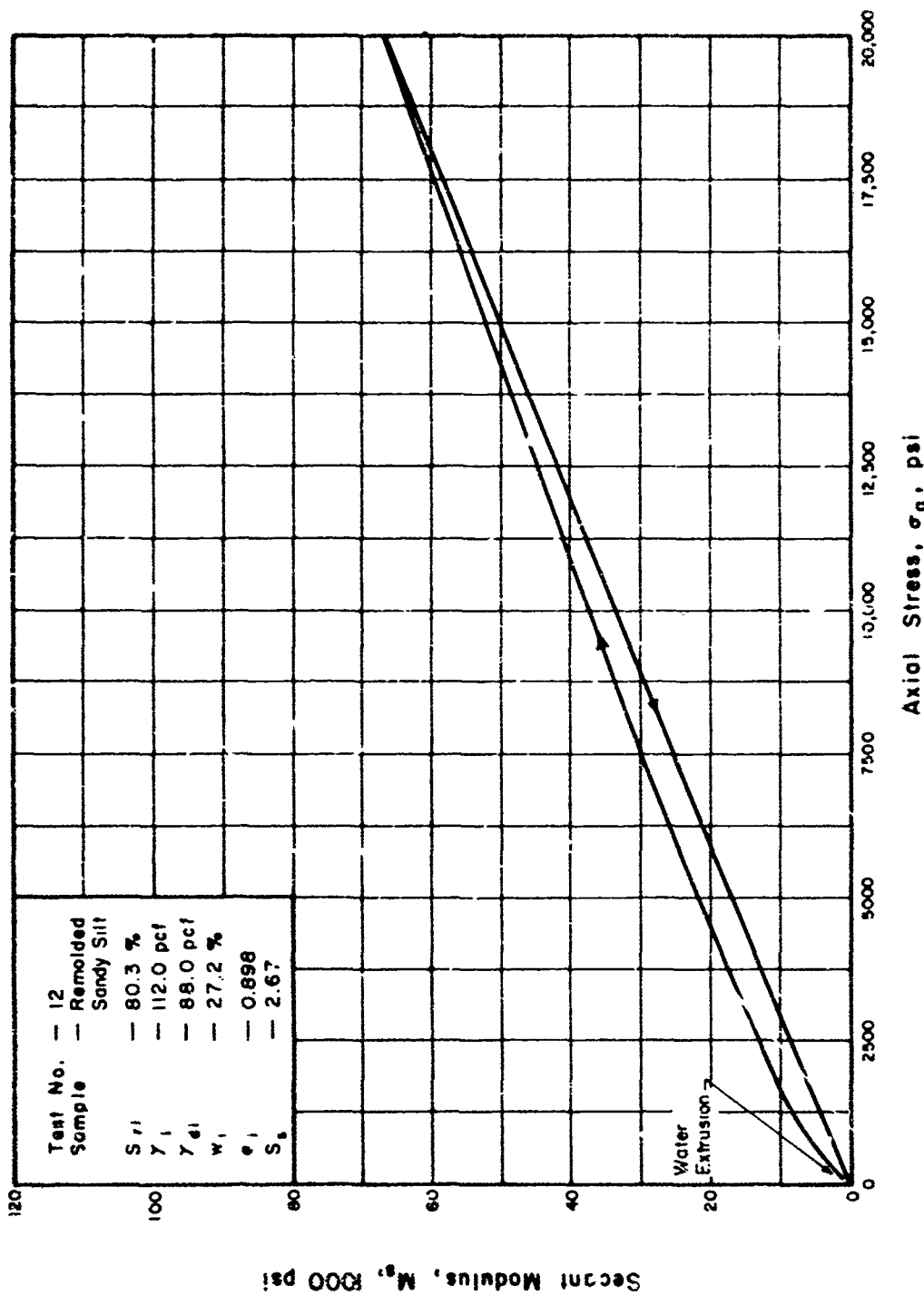


Fig C12. Relation between secant modulus and axial stress, test 12.

**APPENDIX D RADIAL STRESS VERSUS AXIAL STRESS**

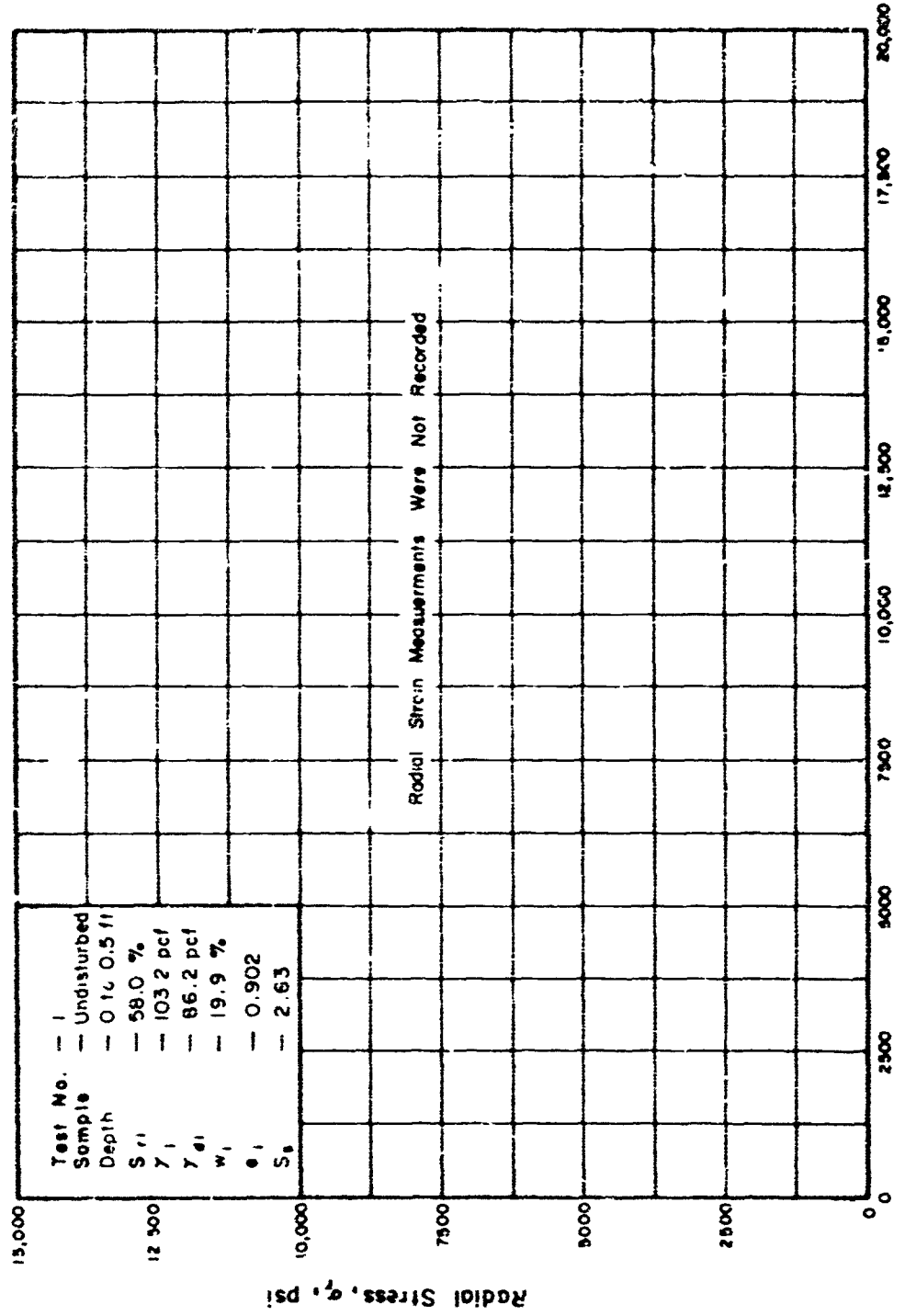


Fig. D1. Relation between radial and axial stress, test 1

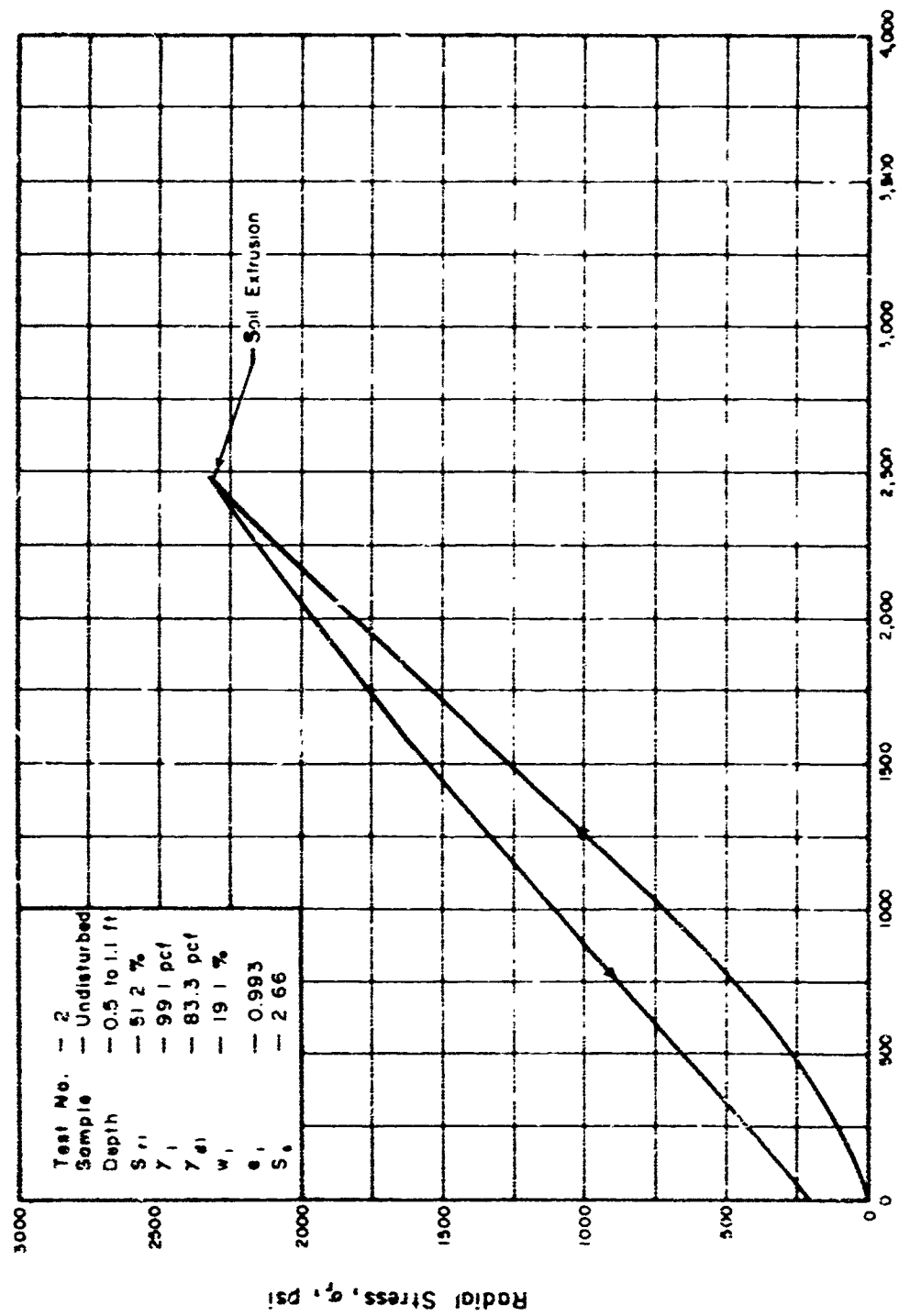


Fig D2. Relation between radial and axial stress, test 2.

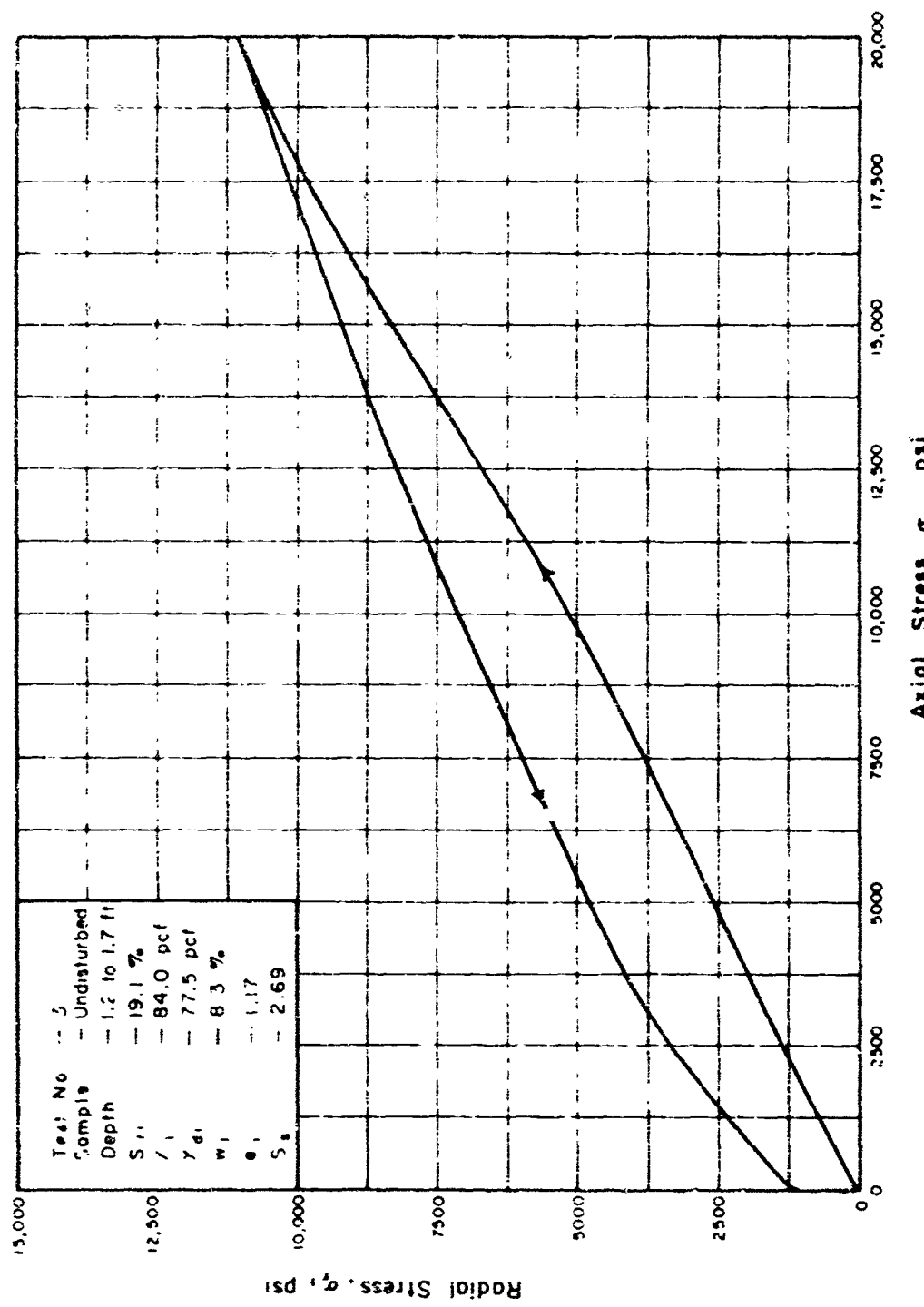


Fig. D3. Relation between radial and axial stress, test 3

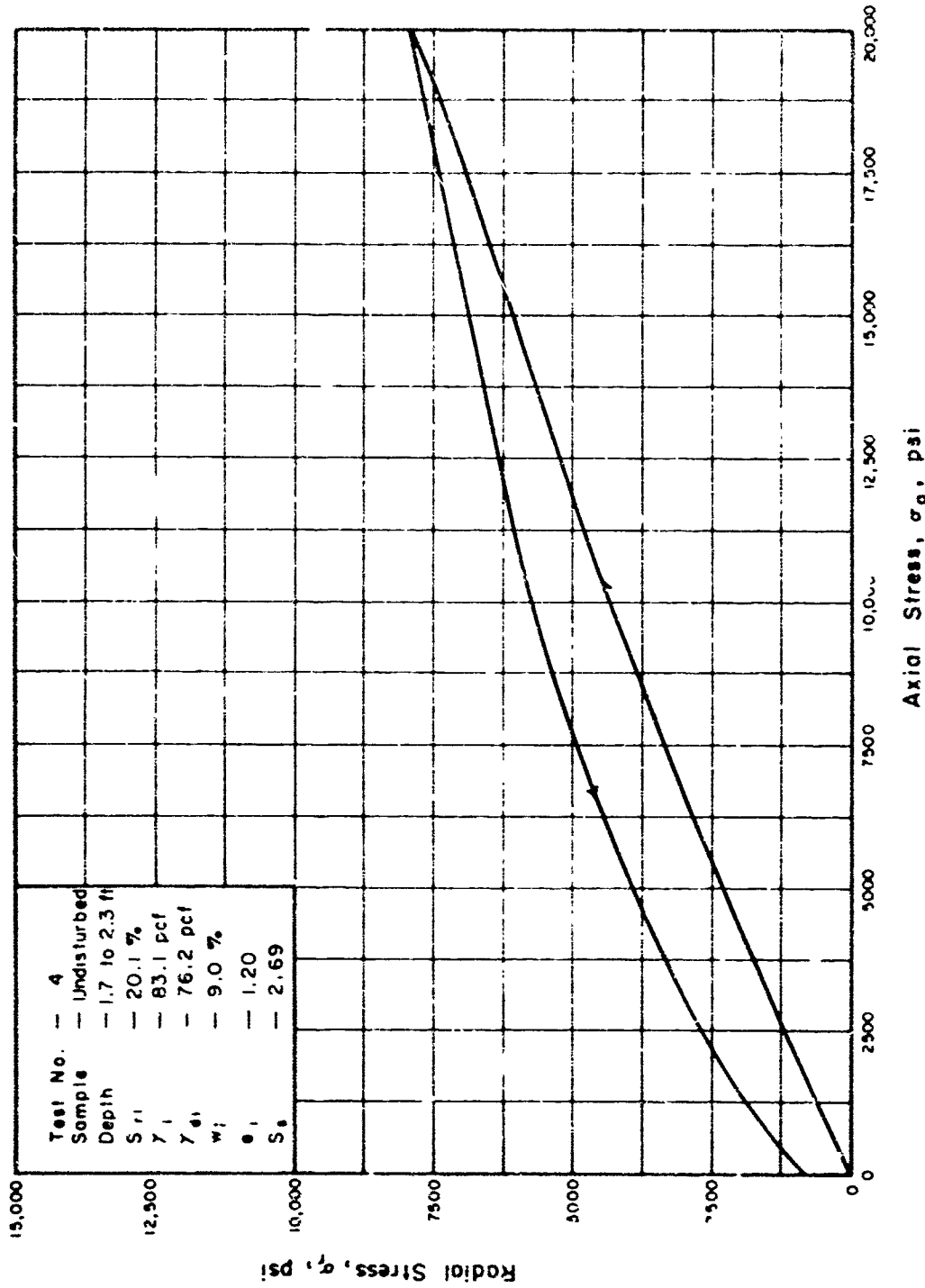


Fig. D4. Relation between radial and axial stress, test 4.

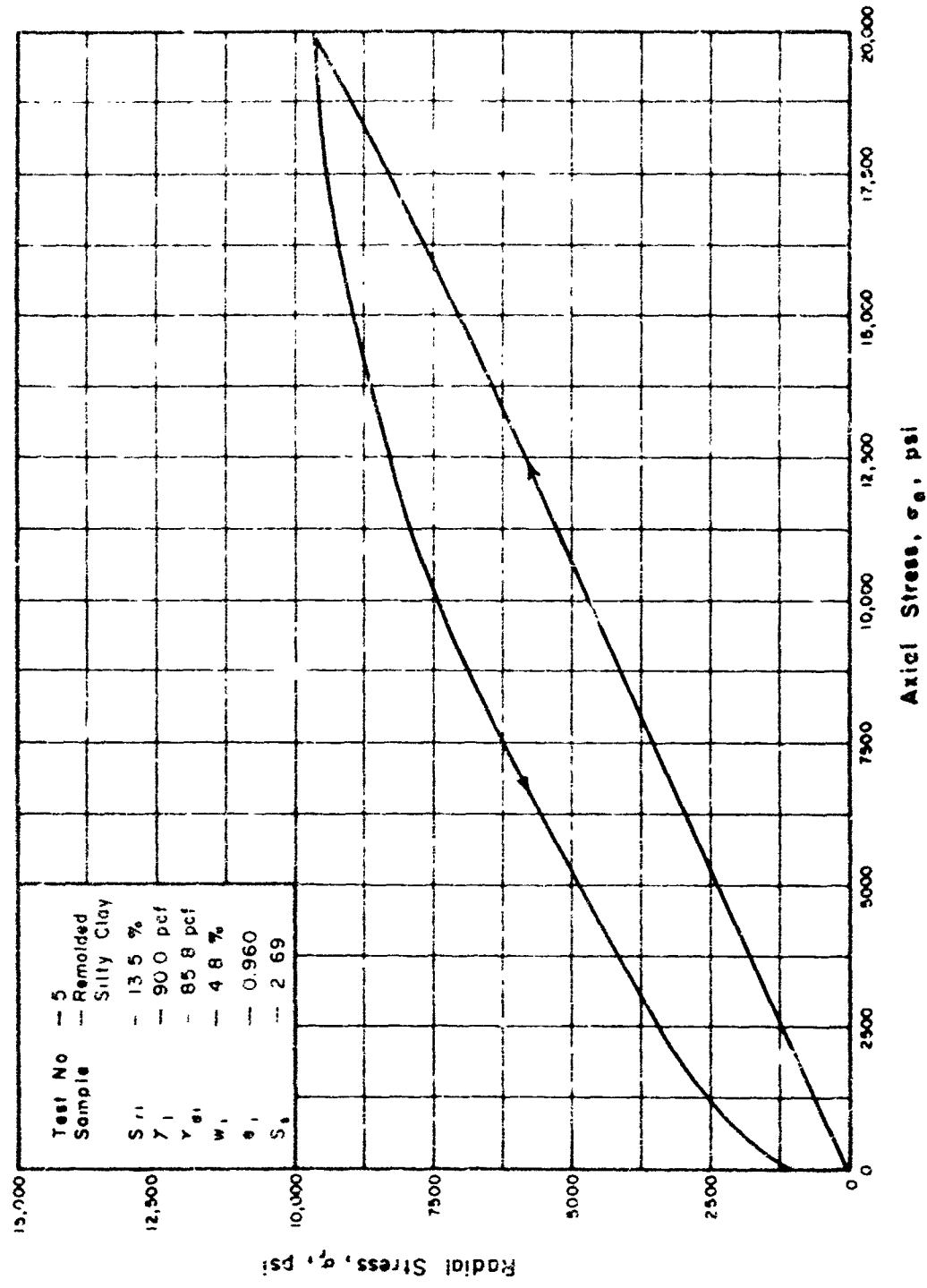


Fig. D5. Relation between radial and axial stress, test 5

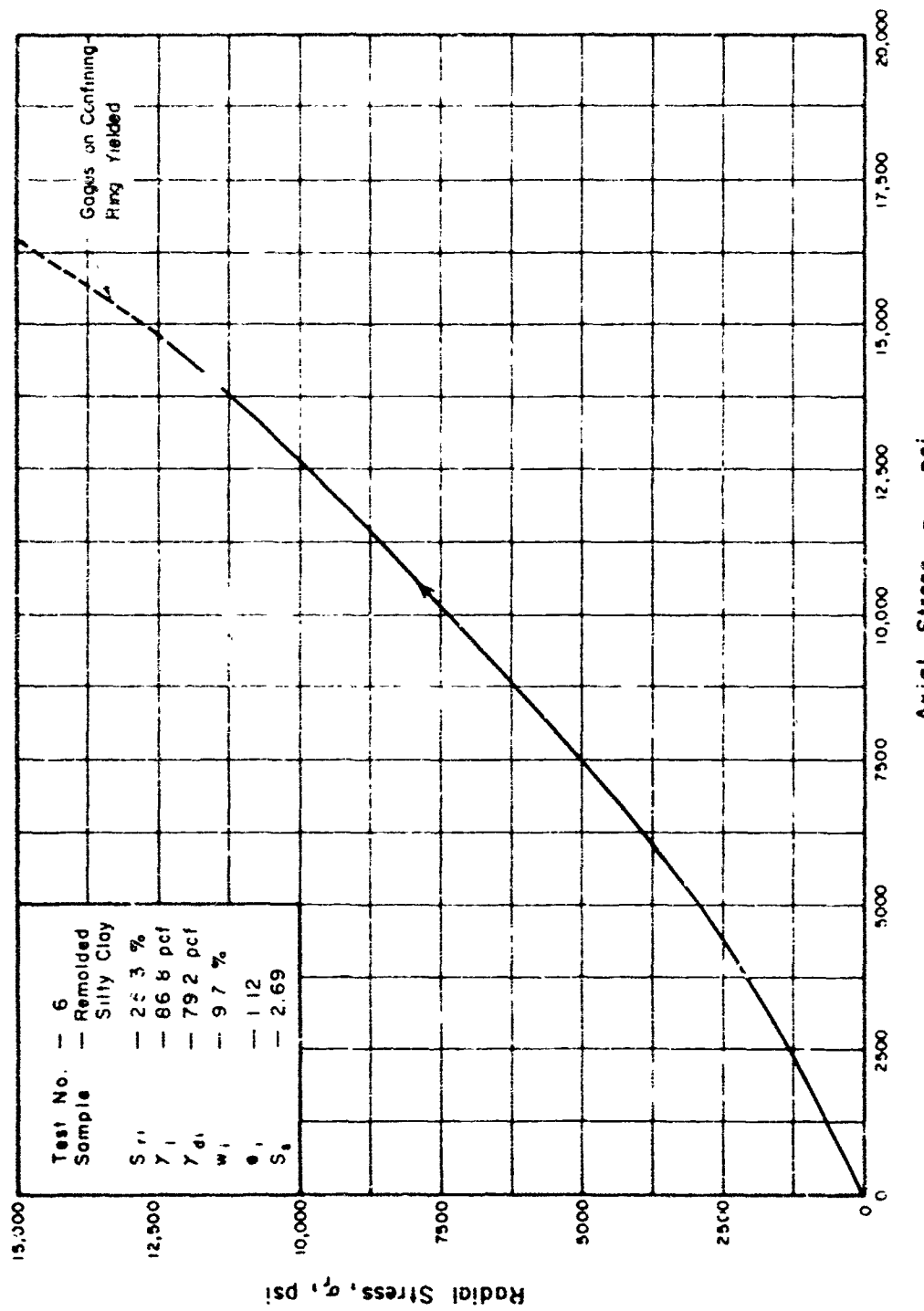


Fig. D6. Relation between radial and axial stress, test 6

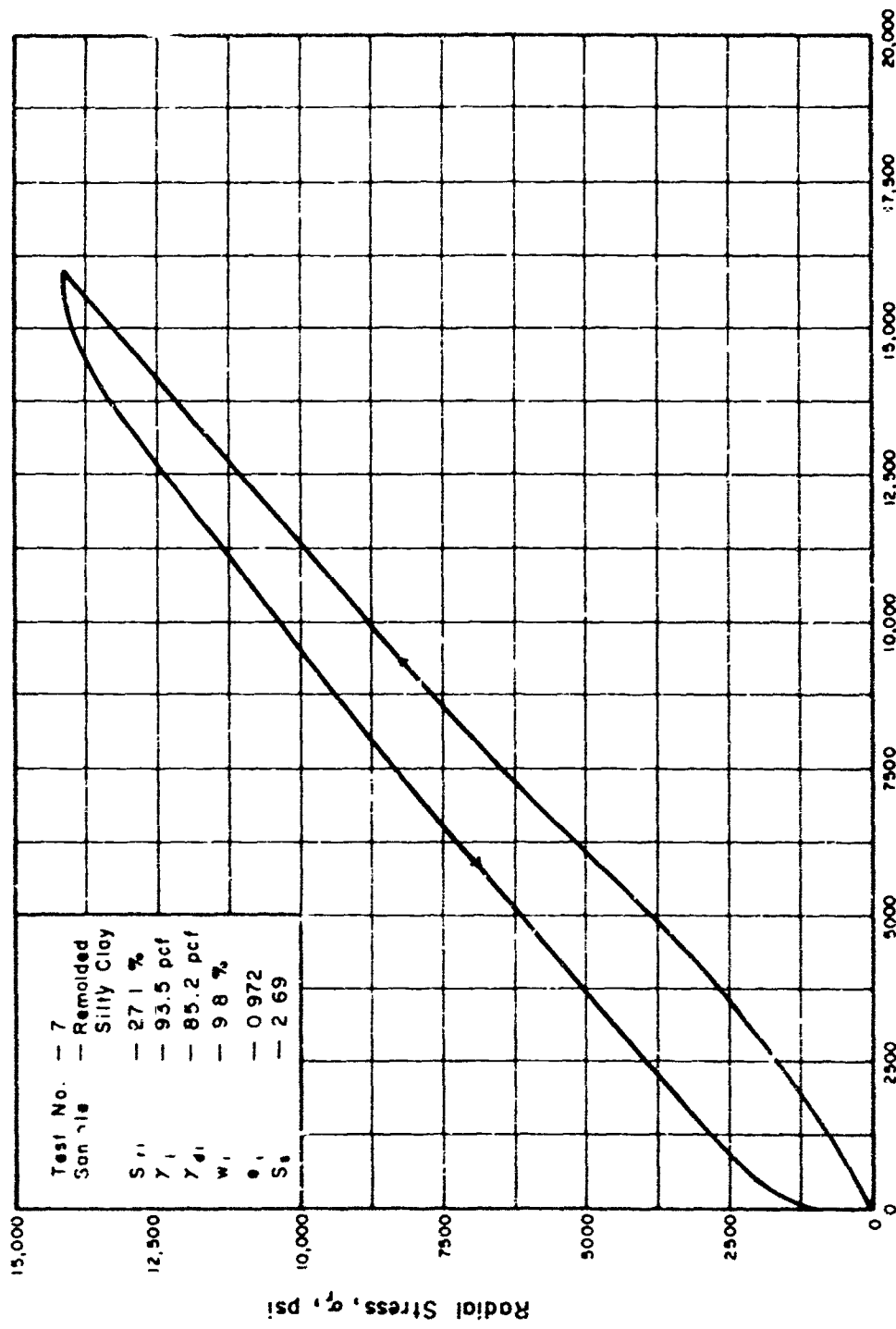


Fig. D7. Relation between radial and axial stress, test 7

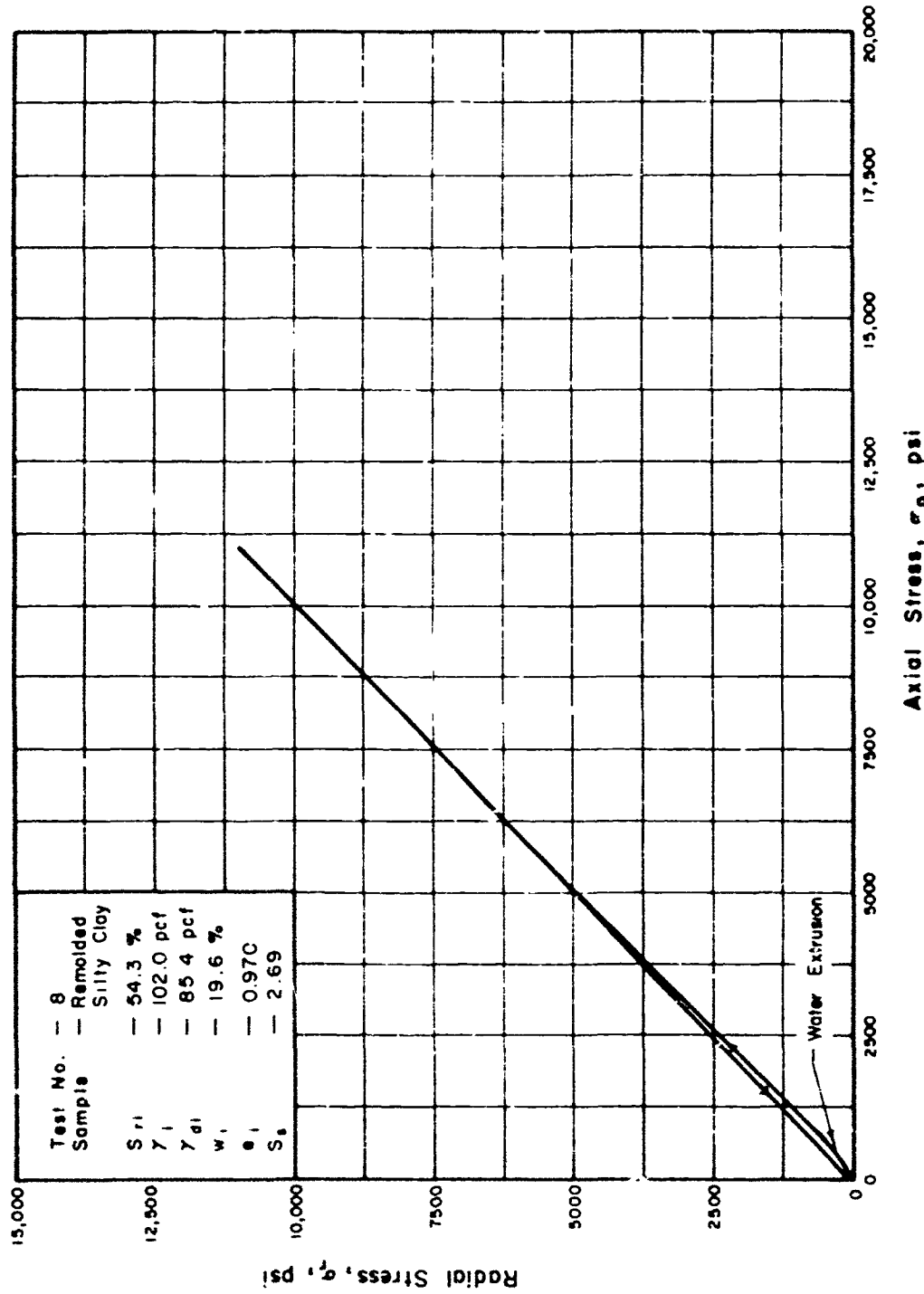


Fig. D8. Relation between radial and axial stress, test 8

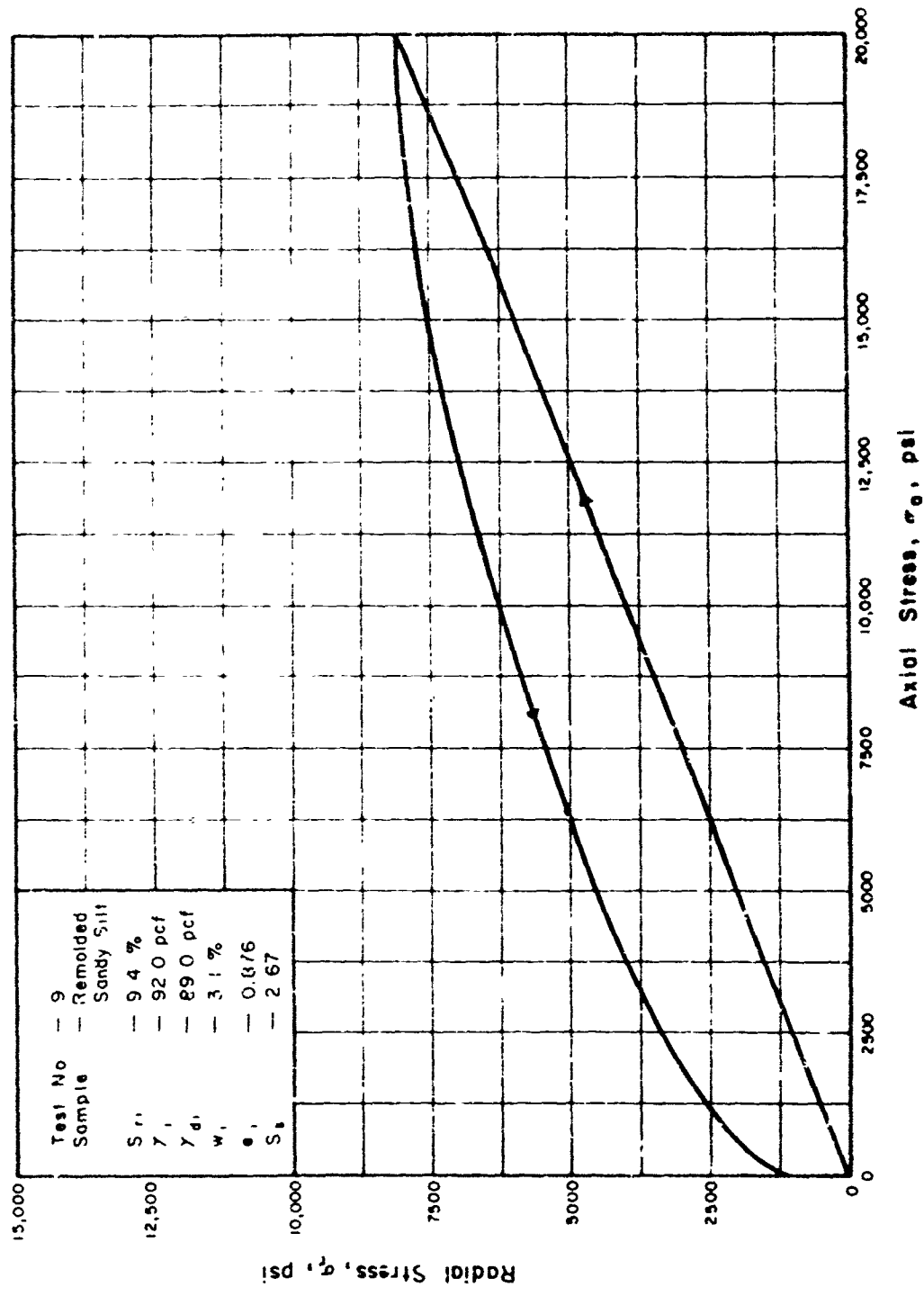


Fig. D9. Relation between radial and axial stress, test 9

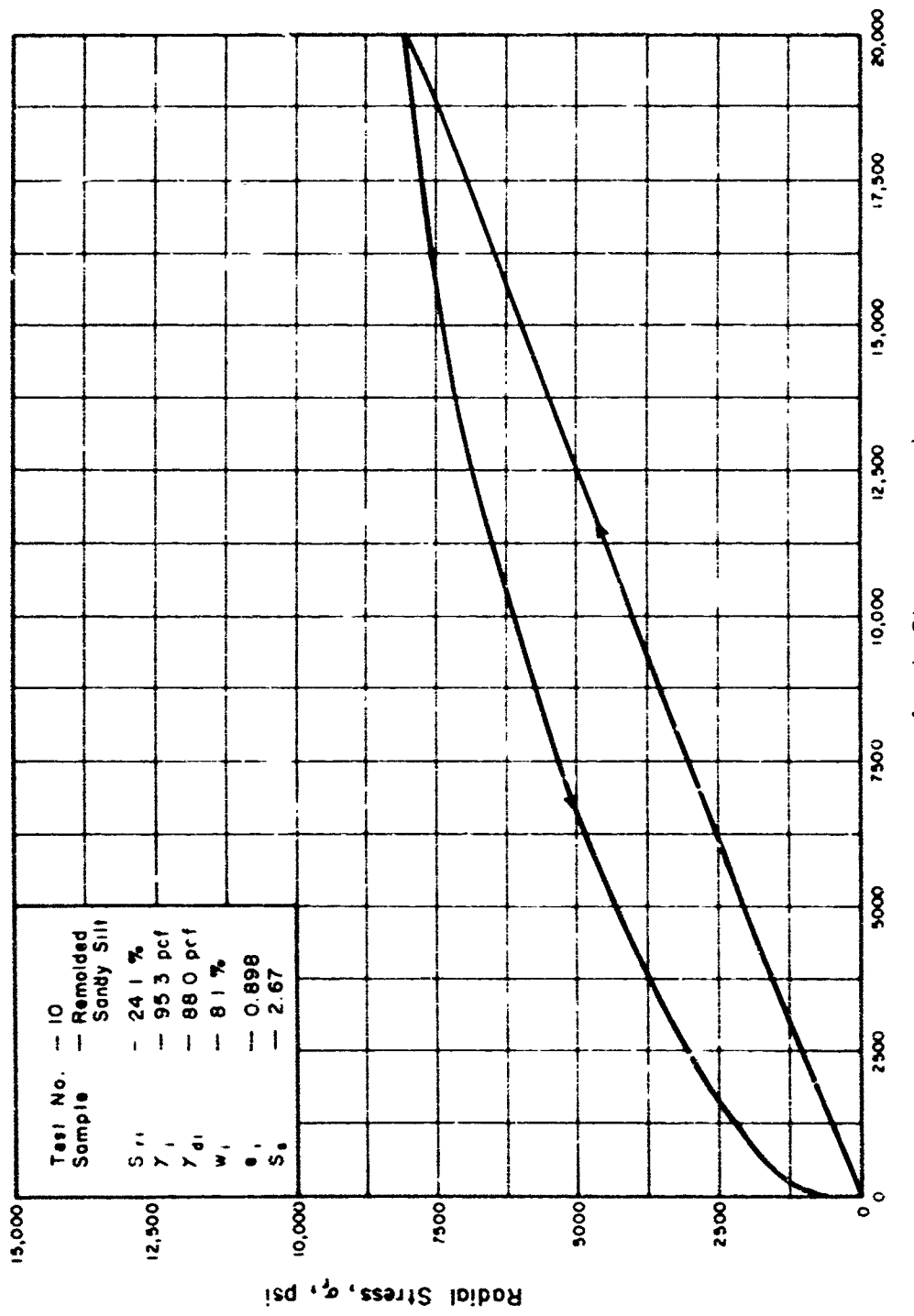


Fig. D10 Relation between radial and axial stress, test 10

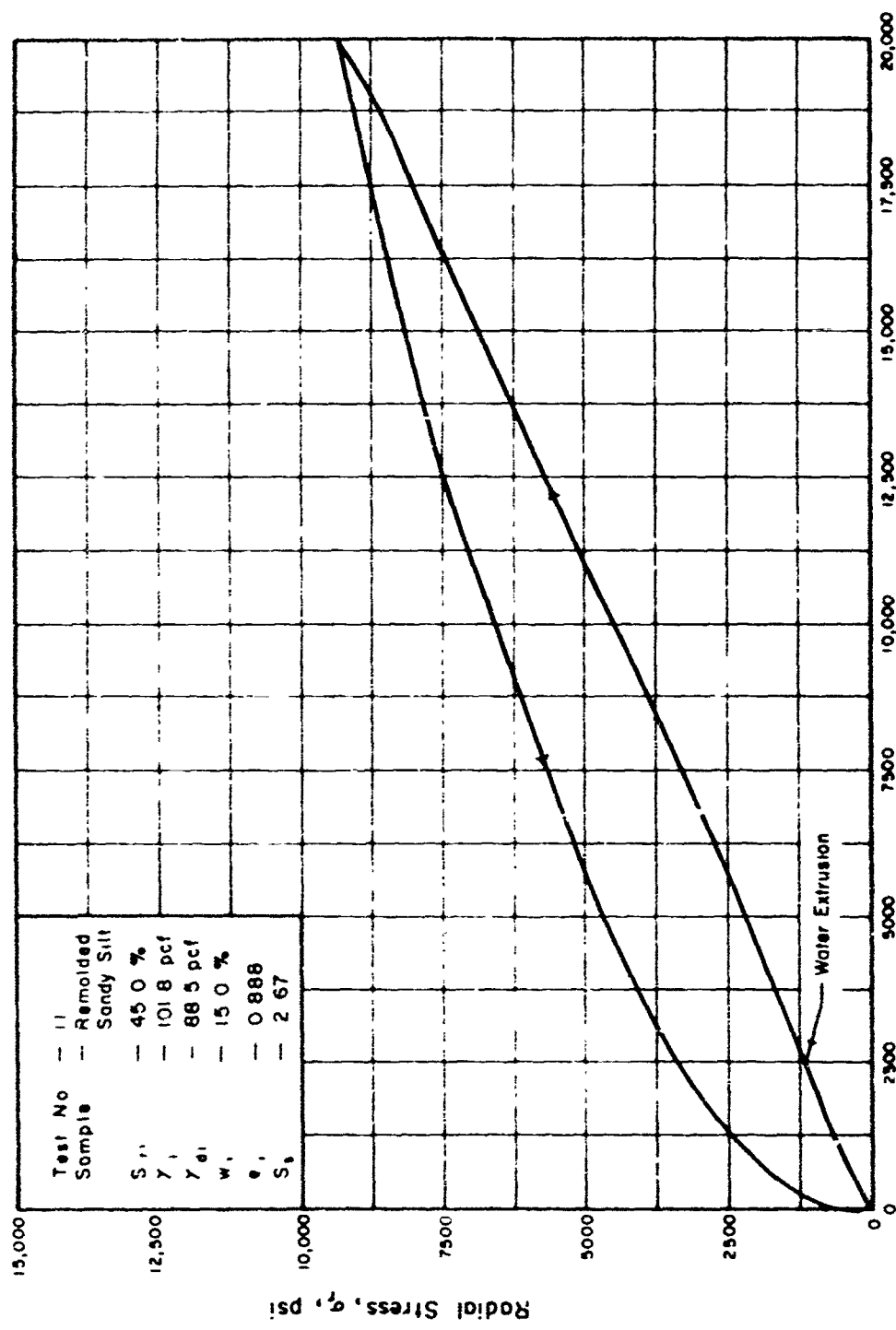


Fig. D11. Relation between radial and axial stress, test 11

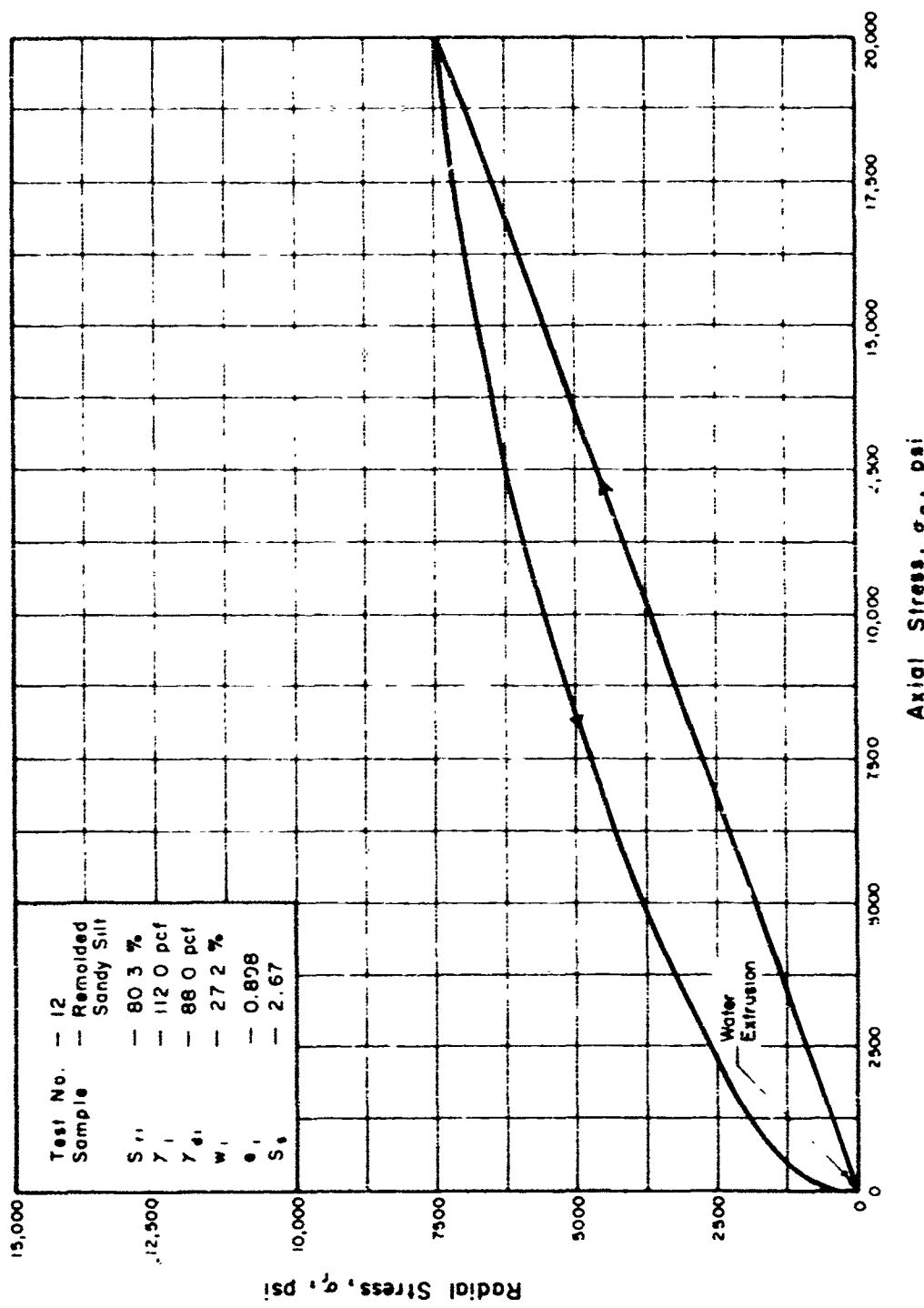


Fig. D12. Relation between radial and axial stress test 12

**APPENDIX E: TABULATED DATA FOR THREE-DIMENSIONAL  
STRESS-STRAIN RELATIONS**

## ONE-DIMENSIONAL STATIC TEST DATA

Test No. 1 Soil Type Undisturbed Soil Location Depth 0-0.5 ft.  
Silty Clay Brown 2-V. Distinct Planes  
- 12.9% S., 38.0% Y, 10.2% Pcf Y, 86.2% S, 2.63 o. 0.902  
- 37% P, 19% Classification Brown Silty Clay w/ sand & trace  
of organic material (CL)

Fig E1

## ONE-DIMENSIONAL STATIC TEST DATA

Test No. 2 Soil Type Undisturbed Soil Location Depth as - 1.1 ft.  
Silty Clay Boring Z-U, Distant Plain 6

w. 19.1 % S., 51.2 % Y., 99.1 pcf Y. 83.3 pcf S. 2.66 e. 0.993  
L. 38 % P. 18 % Classification Brown Silty Clay w/ trace of  
sand (CL)

Fig. E2

### ONE-DIMENSIONAL STATIC TEST DATA

Test No 3 Soil Type Undisturbed Soil Location Depth 1.2 - 1.7 ft  
Silty Clay Boring 2-U, Distant Plain 6  
W. 83 % S., 191 % r, 84.6 pcf  $\gamma_s$ , 17.5 pcf S, 2.69 e, 1.170  
L. 42 % P, 21 % Classification Brown Silty Clay (CL)

$\frac{\sigma_0 + 2\sigma_r}{3}$	$\frac{\epsilon_0}{3}$	$\frac{\sqrt{2}}{3}(\sigma_0 - \sigma_r)$	Radial Stress $\sigma_r$	Degree of Saturation $S_r$	$\frac{\sigma_0 + 2\sigma_r}{3}$	$\frac{\epsilon_0}{3}$	$\frac{\sqrt{2}}{3}(\sigma_0 - \sigma_r)$	Radial Stress $\sigma_r$	Degree of Saturation $S_r$
PSI	in/in	PSI	PSI	%	PSI	in/in	PSI	PSI	%
0	0	0			12100	0.150	3490		
3	0.001	5			12700	0.150	3720		
36	0.005	10			13300	0.151	4000		
92	0.012	6			14000	0.151	4240		
152	0.030	34			12500	0.151	3440		
234	0.044	47			11100	0.151	2740		
311	0.056	63			9500	0.151	1620		
405	0.064	67			8100	0.150	1350		
458	0.071	100			6820	0.150	825		
600	0.081	166			5500	0.149	350		
735	0.088	163			4150	0.148	-127		
1100	0.101	280			2640	0.147	-452		
1430	0.109	405			1800	0.145	-570		
1800	0.115	495			1290	0.144	-560		
2090	0.120	640			980	0.143	-550		
2390	0.123	780			880	0.143	-550		
2740	0.126	875			790	0.143	-520		
3440	0.131	1160			68	0.141	-465		
4130	0.134	1400							
4710	0.137	1610							
5400	0.140	1840							
6050	0.141	2070							
--	0.143	--							
7400	0.145	2530							
8250	0.146	2640							
9100	0.147	2760							
9900	0.148	2880							
10700	0.149	3070							
11400	0.150	3270							

Fig. E3

# ONE-DIMENSIONAL STATIC TEST DATA

Test Nr 4 Soil Type Undisturbed Soil Location Depth 1.7-2.3 ft.  
Silty Clay Boring 24, Distant Plain  
W. 90 % S., 20.1 % Y, 83 L pcf  $\gamma_0$ , 76.2 pcf  $S_1$ , 2.69 e, 1.200  
L. 44 % P, 23 % Classification Brown Silty Clay (c)

$\frac{\sigma_3 + 2\sigma_r}{3}$	$\frac{\epsilon_0}{3}$	$\frac{\sqrt{2}}{3}(\sigma_0 - \sigma_r)$	Radial Stress $\sigma_r$	Degree of Saturation $S_r$	$\frac{\sigma_3 + 2\sigma_r}{3}$	$\frac{\epsilon_0}{3}$	$\frac{\sqrt{2}}{3}(\sigma_0 - \sigma_r)$	Radial Stress $\sigma_r$	Degree of Saturation $S_r$
PSI	in/in	PSI	PSI	%	PSI	in/in	PSI	PSI	%
0	0	0			10200	0.151	4800		
3	0.001	5			10700	0.151	5180		
23	0.003	19			11300	0.152	5470		
47	0.006	38			11850	0.152	5750		
135	0.022	46			10750	0.152	4720		
193	0.039	75			9550	0.152	3840		
277	0.053	87			9400	0.152	2900		
324	0.062	125			7150	0.151	2000		
376	0.070	157			4900	0.150	780		
525	0.080	192			3660	0.149	236		
680	0.087	226			2240	0.148	-193		
970	0.100	372			1580	0.146	-415		
1320	0.109	475			1110	0.146	-405		
1610	0.114	630			-	0.147	-		
1940	0.119	720			-	0.144	-		
2270	0.123	870			620	0.143	-410		
2570	0.126	1010			50	0.141	-390		
3230	0.130	1250							
3820	0.134	1540							
4440	0.137	1810							
5100	0.139	2040							
5630	0.141	2370							
6200	0.143	2670							
6750	0.145	3000							
7350	0.146	3250							
7950	0.148	3580							
8500	0.149	3900							
9020	0.150	4220							
9600	0.150	4500							

Fig. E4

### ONE-DIMENSIONAL STATIC TEST DATA

Test No 5 Soil Type Remolded Silty Clay Soil Location Depth 0-5 ft.  
Bag Sample, Distant Plain 6  
w. 4.8 % S<sub>r</sub>, 13.5 % r, 900 psi T<sub>d</sub>, 85.8 psi S<sub>s</sub>, 2.69 e, 0.960  
L. 34 % P, 16 % Classification Brown Silty Clay (CL)

$\frac{\sigma_0 + 2\sigma_r}{3}$	$\frac{\epsilon_a}{3}$	$\frac{\sqrt{2}}{3}(\sigma_0 - \sigma_r)$	Radial Stress $\sigma_r$	Degree of Saturation $S_r$
psi	in/in	psi	psi	%
0	0	0	0	
3	0.004	5	0	
23	0.012	19	10	
81	0.021	14	71	
137	0.032	44	106	
187	0.041	80	31	
275	0.047	89	212	
317	0.051	130	225	
391	0.056	147	287	
510	0.063	205	365	
663	0.068	238	495	
1000	0.078	353	750	
1334	0.085	470	1001	
673	0.091	585	1260	
980	0.095	722	1470	
2300	0.099	849	700	
2633	0.102	967	1950	
3280	0.108	217	2420	
3913	0.111	1477	2870	
4573	0.114	718	3360	
5213	0.117	1970	3820	
5867	0.119	2220	4300	
6580	0.121	2420	4870	
713	0.123	2750	5170	
7753	0.125	3005	5630	
8360	0.126	3280	6040	
9000	0.127	3540	6500	
9667	0.129	3770	7000	
0,333	0.130	4000	7500	

$\frac{\sigma_0 + 2\sigma_r}{3}$	$\frac{\epsilon_a}{3}$	$\frac{\sqrt{2}}{3}(\sigma_0 - \sigma_r)$	Radial Stress $\sigma_r$	Degree of Saturation $S_r$
047	0.130	4200	3070	
167	0.131	470	8500	
2323	0.132	4630	9070	
3067	0.133	450	9600	
2367	0.133	3835	9350	
0,900	0.133	2890	8850	
3667	0.132	2000	8250	
8333	0.132	175	500	
5667	0.132	235	5500	
4233	0.130	-5	-350	
200	0.27	-474	3050	
820	0.128	-579	2230	
1307	0.28	-524	760	
1000	0.127	-565	400	
93	0.27	-54	1320	
830	0.127	-550	225	
667	0.26	-471	000	

Fig. E5

# ONE-DIMENSIONAL STATIC TEST DATA

Test No. 6 Soil Type Remolded Soil Location Depth C-5 ft.  
Silty Clay Bag Sample Dist. Plain 6  
w<sub>s</sub> 2.7 % S<sub>r</sub> 25.3 % γ<sub>d</sub> 96.8 psf γ<sub>a</sub> 79.2 psf S<sub>v</sub> 2.69 e<sub>v</sub> 1.120  
L<sub>c</sub> 34 % P<sub>c</sub> 16 % Classification Brown silty clay (CC)

$\frac{\sigma_0 + 2\sigma_r}{3}$	$\frac{\epsilon_0}{3}$	$\frac{\sqrt{2}}{3}(\sigma_0 - \sigma_r)$	Radial Stress $\sigma_r$	Degree of Saturation $S_r$ %	$\frac{\sigma_0 + 2\sigma_r}{3}$	$\frac{\epsilon_0}{3}$	$\frac{\sqrt{2}}{3}(\sigma_0 - \sigma_r)$	Radial Stress $\sigma_r$	Degree of Saturation $S_r$ %
psi	in./in.	psi	psi	%	psi	in./in.	psi	psi	%
0	0	—	0		—	0.144	—	—	
3	0.003	5	0		—	0.144	—	—	
31	0.027	14	21		—	0.146	—	—	
71	0.049	21	56		—	0.145	—	—	
143	0.073	37	122		—	0.145	—	—	
212	0.085	63	167		—	0.145	—	—	
302	0.095	69	253		—	0.144	—	—	
348	0.100	107	272		—	0.143	—	—	
393	0.104	146	290		—	0.143	—	—	
558	0.112	173	433		—	0.143	—	—	
646	0.117	250	470		—	0.143	—	—	
1010	0.125	348	760		—	0.143	—	—	
1320	0.130	480	975		—	0.142	—	—	
1680	0.134	582	1260		—	0.142	—	—	
1990	0.136	710	1490		—	0.141	—	—	
2360	0.138	803	1790		—	0.141	—	—	
2760	0.139	878	2130		—	0.139	—	—	
3530	0.140	1035	2800						
4300	0.140	1200	3450						
5400	0.141	1130	4600						
6380	0.141	1168	5520						
7220	0.141	1255	6330						
8200	0.141	1270	7300						
9167	0.142	1292	8250						
10110	0.143	1327	9180						
12267	0.143	1220	11400						
13400	0.143	1130	12600						
—	0.143	—	—						
—	0.143	—	—						

Ex. E6

### ONE-DIMENSIONAL STATIC TEST DATA

Test No 7 Soil Type Remolded Soil Location Depth 0-5 ft  
Silty Clay Bag Prairie, Distant Plane  
 $w = 9.8 \text{ %}$   $s_s = 271 \text{ %}$   $r = 98.5 \text{ psf}$   $\sigma_0 = 85.2 \text{ psf}$   $s_i = 2.69 \text{ %}$   $e = 0.972$   
 $L = 34 \text{ %}$   $P = 16 \text{ %}$  Classification Brown Silty Clay (GL)

$\frac{\sigma_0 + 2\sigma_r}{3}$	$\frac{e_0}{3}$	$\frac{\sqrt{2}}{3}(\sigma_0 - \sigma_r)$	Radial Stress $\sigma_r$	Degree of Saturation $S_i$	$\frac{\sigma_0 + 2\sigma_r}{3}$	$\frac{e_0}{3}$	$\frac{\sqrt{2}}{3}(\sigma_0 - \sigma_r)$	Radial Stress $\sigma_r$	Degree of Saturation $S_i$
psf	in/in	psf	psf	%	psf	in/in	psf	psf	%
0	0	-	0	0	14333	0.128	470	14000	
3	0.002	5	0	0	12300	0.128	141	12200	
34	0.008	-3	56		11200	0.128	283	11800	
101	0.029	0	101		12500	0.127	-353	8750	
149	0.051	38	119		4900	0.127	-634	5350	
22	0.064	56	182		3000	0.126	-704	3500	
299	0.073	76	248		2007	0.125	-710	2510	
354	0.081	106	280		1453	0.124	-671	1930	
450	0.086	107	372		1147	0.124	-667	1620	
608	0.093	135	512		1020	0.123	-648	1480	
725	0.098	194	587		943	0.123	-630	1390	
1017	0.107	284	895		793	0.122	-560	1190	
1500	0.113	352	1250						
1867	0.116	446	1550						
2280	0.120	508	1920						
2673	0.122	583	2260						
327	0.123	573	180						
4220	0.124	550	3830						
5267	0.125	517	4900						
6387	0.126	432	6080						
7700	0.126	212	7550						
8333	0.127	470	8000						
9300	0.127	493	8950						
10133	0.127	610	9700						
11067	0.127	658	10600						
12000	0.128	704	11500						
12867	0.128	800	12300						
13800	0.128	845	13200						
14800	0.128	845	14200						

Fig. E7

### ONE-DIMENSIONAL STATIC TEST DATA

Test No 8 Soil Type Remolded Soil Location Depth 0-6 ft  
Silty Clay Bag Sample, Distinct Plaine  
 $\pi_0$  19.6 % S. 84.2 % Y. 102.0 pcf  $\gamma_s$  85.4 pcf  $S_r$  2.69  $\epsilon_r$  0.970  
L 24 % P. 16 % Classification Brown Silty Clay (c.)

$\frac{\sigma_0 + 2\sigma_i}{3}$	$\frac{\epsilon_0}{3}$	$\sqrt{2}(\sigma_0 - \sigma_i)$	Radial Stress $\sigma_r$	Degree of Saturation $S_r$ %	$\frac{\sigma_0 + 2\sigma_i}{3}$	$\frac{\epsilon_0}{3}$	$\sqrt{2}(\sigma_0 - \sigma_i)$	Radial Stress $\sigma_r$	Degree of Saturation $S_r$ %
psl	in/in	psl	psl	%	psl	in/in	psl	psl	%
0	0	0	0		5000	0.082	0	6000	
3	0.007	5	0		7000	0.083	0	7000	
17	0.062	24	0		7980	0.083	14	7970	
41	0.072	41	12		8920	0.084	56	8880	
82	0.076	48	48		9900	0.084	70	9850	
131	0.077	49	96		11000	0.084	0	11000	
227	0.077	51	101		8000	0.084	0	8000	
317	0.077	58	276		6000	0.083	0	6000	
405	0.077	67	358		4027	0.083	-19	4040	
520	0.078	56	180		3047	0.083	-33	3070	
625	0.078	53	588		2047	0.082	-33	2070	
723	0.078	54	685		1007	0.082	-5	1010	
795	0.078	73	744		567	0.082	-47	600	
900	0.078	70	850		237	0.082	-26	256	
960	0.078	99	890		123	0.082	-16	134	
-	0.078	-	975		81	0.082	-22	97	
1050	0.078	70	1000		24	0.081	-17	36	
1165	0.079	78	1110						
1397	0.079	75	1340						
1507	0.079	66	1460						
1693	0.079	75	1640						
1887	0.080	80	1830						
2137	0.080	80	2080						
2413	0.080	61	2370						
2690	0.080	42	2660						
2947	0.080	38	2920						
3433	0.080	47	3400						
3933	0.081	47	3900						
5000	0.082	0	5000						

Fig. E8

### ONE-DIMENSIONAL STATIC TEST DATA

Test No 9 Soil Type Renamed Soil Location Depth 5-22 ft  
Sandy Silt Boring 5-4, Distant Fluvial  
w. 31 % S., 9.4 % Y, 92.0 pcf  $\gamma_s$ , 89.0 pcf  $S_s$ , 2.667 e, 0.876  
L. 20 % P. 19 % Classification Brown Sandy Silt (ML)

$\frac{\sigma_0 + 2\sigma_r}{3}$	$\frac{\epsilon_0}{3}$	$\frac{\sqrt{2}}{3}(\sigma_0 - \sigma_r)$	Radial Stress $\sigma_r$	Degree of Saturation $S_r$	$\frac{\sigma_0 + 2\sigma_r}{3}$	$\frac{\epsilon_0}{3}$	$\frac{\sqrt{2}}{3}(\sigma_0 - \sigma_r)$	Radial Stress $\sigma_r$	Degree of Saturation $S_r$
psi	in/in	psi	psi	%	psi	in/in	psi	psi	%
0	0	0			10340	.110	4790		
83	.002	.47			10710	.111	5080		
914	.011	6.1			11410	.112	5450		
655	.016	24.3			12100	.113	5600		
197	.022	43.5			11130	.113	4500		
200	.020	70.5			10050	.113	3500		
249	.031	107			8850	.113	2120		
331	.035	119			7550	.113	1740		
380	.038	156			6450	.113	1100		
513	.043	202			5280	.111	515		
634	.047	260			4180	.110	132		
910	.054	417			2720	.109	710		
1220	.061	550			1920	.108	650		
1492	.066	710			1473	.107	7690		
1815	.071	839			1100	.106	6280		
2190	.074	970			945	.105	604		
2420	.078	1110			870	.105	580		
3010	.082	1400			653	.102	460		
3620	.087	1670							
4230	.091	1940							
4850	.094	2280							
5380	.096	2550							
6000	.099	2830							
6680	.101	3100							
7160	.103	3430							
7760	.105	3690							
8330	.106	3950							
8940	.108	4270							
9550	.109	4540							

### ONE-DIMENSIONAL STATIC TEST DATA

Test No 10 Soil Type Remolded sandy silt Soil Location Depth 5-22 ft Boeing 5-4, Distant Plain 6  
w. 81 % S., 241 % r, 25.2 pct r<sub>o</sub>, 28.0 pct S<sub>r</sub>, 2.62 e, 0.898  
L. 20 % P. 19 % Classification Brown Sandy Silt (ML)

$\sigma_0 + 2\sigma_r$	$\frac{\epsilon_0}{3}$	$\frac{\sqrt{2}}{3}(\sigma_0 - \sigma_r)$	Radial Stress $\sigma_r$	Degree of Saturation $S_r$		$\sigma_0 + 2\sigma_r$	$\frac{\epsilon_1}{3}$	$\frac{\sqrt{2}}{3}(\sigma_0 - \sigma_r)$	Radial Stress $\sigma_r$	Degree of Saturation $S_r$
psi	in/in	psi	psi	%		psi	in/in	psi	psi	%
0	0	0				10142	.121	4840		
34	.002	.171				10702	.123	5150		
70	.010	.161				11802	.123	5400		
99	.020	1				12032	.123	5650		
155	.031	.32				11025	.123	4400		
224	.038	.56				9932	.123	3680		
274	.043	.89				8722	.123	2670		
317	.057	1.29				7432	.122	1840		
402	.050	1.39				6352	.122	1160		
497	.077	2.14				5192	.121	575		
633	.061	2.60				3942	.121	47		
927	.070	4.04				2500	.119	358		
1234	.077	5.50				1662	.118	470		
1522	.081	6.91				1102	.116	430		
1826	.086	8.30				842	.115	452		
2123	.089	9.75				517	.114	295		
2440	.092	11.00				402	.113	254		
3030	.097	13.90				224	.105	159		
3620	.100	16.90								
4210	.104	19.70								
4832	.106	22.90								
5300	.109	25.60								
6000	.111	28.80								
6550	.111	31.40								
7180	.115	34.10								
7790	.116	36.90								
8370	.117	39.80								
8920	.119	43.00								
9530	.120	45.60								

Fig. E10

### ONE-DIMENSIONAL STATIC TEST DATA

Test No 11 Soil Type Reclaimed  
Sandy Silt Soil Location Depth 5-27 ft  
Boring 2-14, Distant Plain in  
w. 15.0 % S., 45.0 % Y, 101.8 psf Y<sub>s</sub>, 88.5 psf S<sub>s</sub>, 2.67 e, 0.000  
L. 20 % P, 19 % Classification 24-cm Sandy Silt (ML)

$\sigma_0 + 2\sigma_r$	$\epsilon_0$	$\sqrt{2}(\sigma_0 - \sigma_r)$	Radial Stress $\sigma_r$	Degree of Saturation $S_f$ %	$\sigma_0 + 2\sigma_r$	$\epsilon_0$	$\sqrt{2}(\sigma_0 - \sigma_r)$	Radial Stress $\sigma_r$	Degree of Saturation $S_f$ %
psi	in/in	psi	psi	%	psi	in/in	psi	psi	%
0	0	0			10860	.117	4340		
3	.003	.47			11850	.118	4440		
228	.015	.192			13150	.118	4850		
785	.025	.153			12860	.119	5050		
192	.034	.5			11620	.119	4140		
271	.040	.208			10630	.119	3230		
323	.045	.405			9160	.119	2360		
387	.048	.80			7200	.118	1610		
445	.051	.96			6570	.118	1010		
510	.056	.142			5370	.117	420		
702	.061	.211			4140	.116	.99		
959	.069	.383			2205	.115	.500		
117	.074	.504			1830	.114	.385		
1572	.079	.655			1284	.112	.355		
1890	.083	.780			885	.111	.485		
2200	.086	.920			665	.110	.400		
2400	.089	.990			565	.109	.364		
3050	.094	.380			307	.101	.218		
3710	.098	.1520							
4350	.101	.1870							
4980	.103	.2180							
5650	.105	.2970							
6330	.107	.2580							
6970	.108	.2850							
7650	.110	.3080							
8300	.112	.3320							
8980	.114	.3680							
9600	.115	.3920							
10180	.116	.4110							

Fig E11

# ONE-DIMENSIONAL STATIC TEST DATA

Test No 12 Soil Type Bouldered Sandy Silt Soil Location Depth 5-22 ft.  
Baray 5-6 Trident Plaza  
67.2 % S., 80.3 % Y., 112.0pcf T<sub>0</sub>, 880pcf S<sub>r</sub>, 2.67 e, 0.898  
20 % P, 19 % Classification Brown Sandy Silt (ML)

$\sigma_0 + 2\sigma_r$ 3	$\epsilon_0$ 3	$\sqrt{2}(\sigma_0 - \sigma_r)$	Radial Stress $\sigma_r$	Degree of Saturation $S_r$
PSI	in/in	psi	psi	%
0	0	0		
3	.011	4.7		
7	.019	8.6		
10	.025	13.5		
16	.029	16.6		
27	.031	20		
47	.034	24		
74	.036	40.3		
118	.037	42		
202	.037	46		
219	.040	46.3		
243	.041	48.2		
285	.044	52.3		
362	.046	59.2		
410	.048	67.6		
459	.049	71.2		
542	.051	77.4		
700	.054	88.2		
835	.057	97.0		
940	.059	560		
1112	.062	625		
1210	.064	773		
1650	.069	923		
2010	.071	1150		
2280	.074	1210		
3060	.077	1510		
3640	.080	1800		
4050	.082	2080		
4650	.084	2372		

$\sigma_0 + 2\sigma_r$ 3	$\epsilon_0$ 3	$\sqrt{2}(\sigma_0 - \sigma_r)$	Radial Stress $\sigma_r$	Degree of Saturation $S_r$
5256	.086	21600		
5830	.088	20500		
6400	.090	22600		
6970	.091	35600		
7570	.093	38400		
8150	.094	41500		
8720	.095	44500		
9310	.096	47000		
9910	.097	50400		
10520	.098	53600		
11100	.098	56400		
11100	.100	59200		
10550	.100	49100		
9460	.099	35200		
8360	.099	39400		
7100	.098	20700		
5990	.098	14300		
4830	.097	825		
3680	.097	760		
2240	.096	719		
1850	.095	318		
910	.093	358		
1456	.093	312		
4660	.092	260		
121	.091	263		
250	.087	1760		

Fig. E12

APPENDIX F OCTAHEDRAL NORMAL STRESS VERSUS  
OCTAHEDRAL LINEAR STRAIN

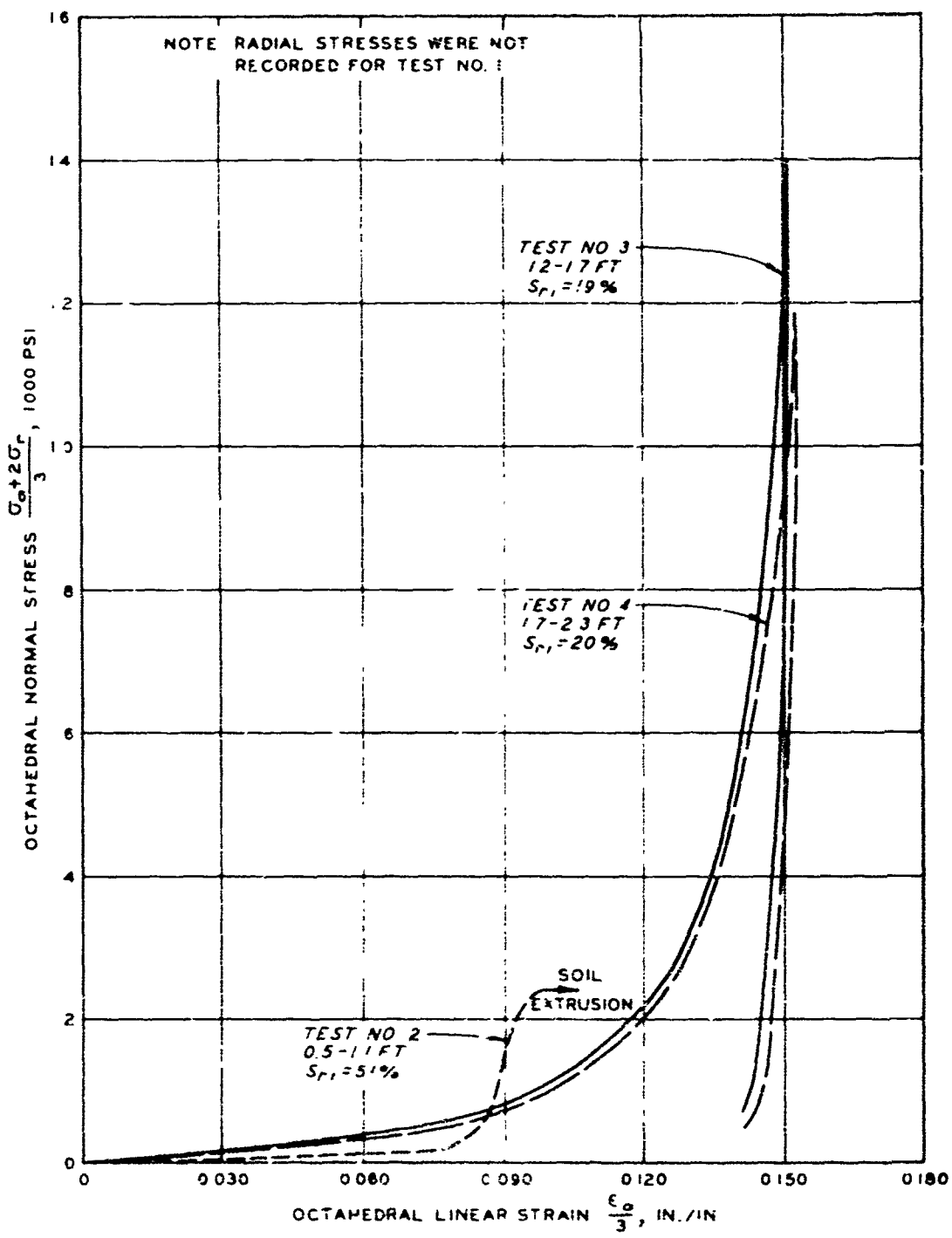


Fig. F1. Octahedral normal stress versus octahedral linear strain  
for the undisturbed samples of silty clay

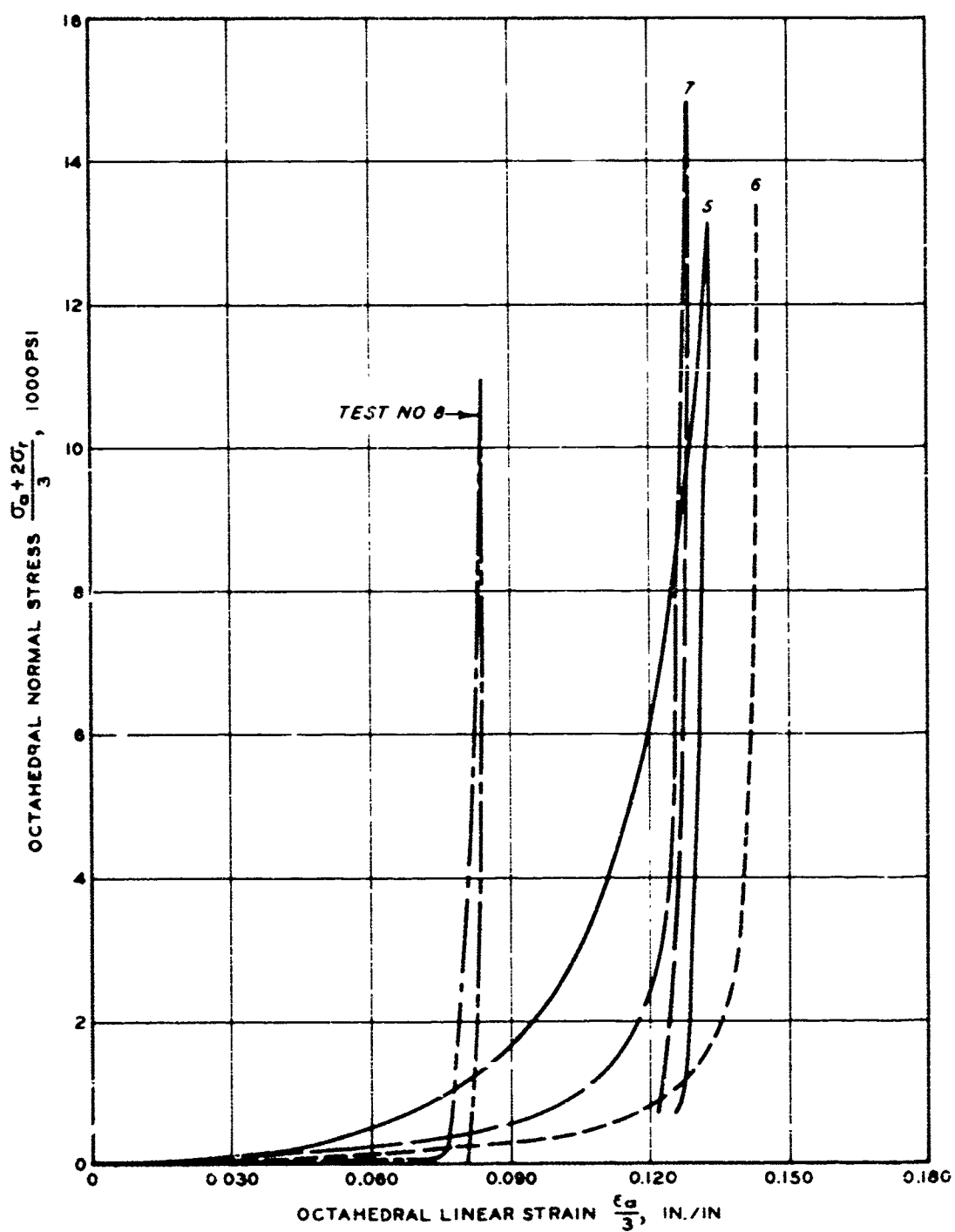


Fig. F2. Octahedral normal stress versus octahedral linear strain  
for the compacted samples of silty clay

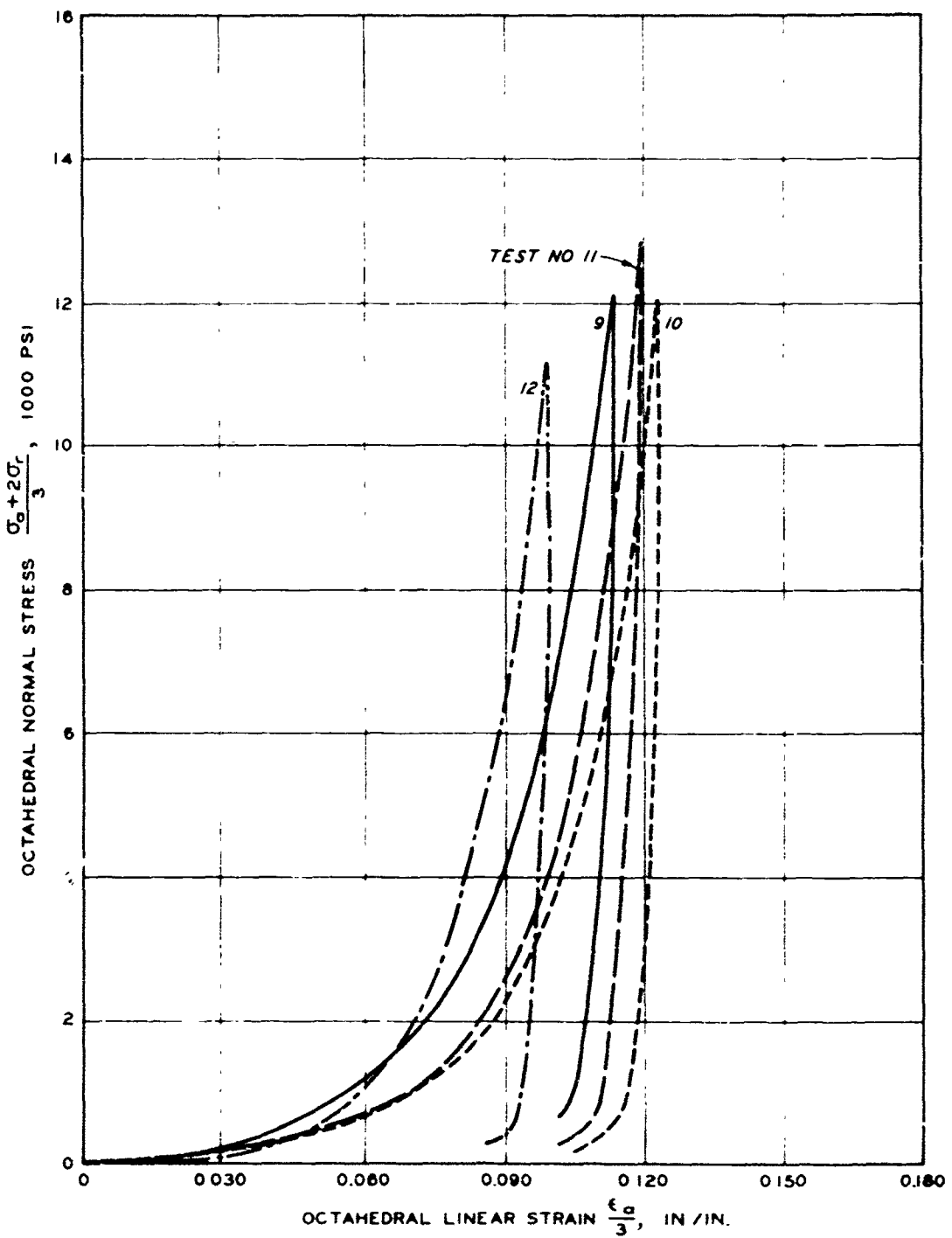


Fig. F3 Octahedral normal stress versus octahedral linear strain  
for the compacted samples of sandy silt

**APPENDIX G: OCTAHEDRAL SHEARING STRESS VERSUS  
OCTAHEDRAL NORMAL STRESS**

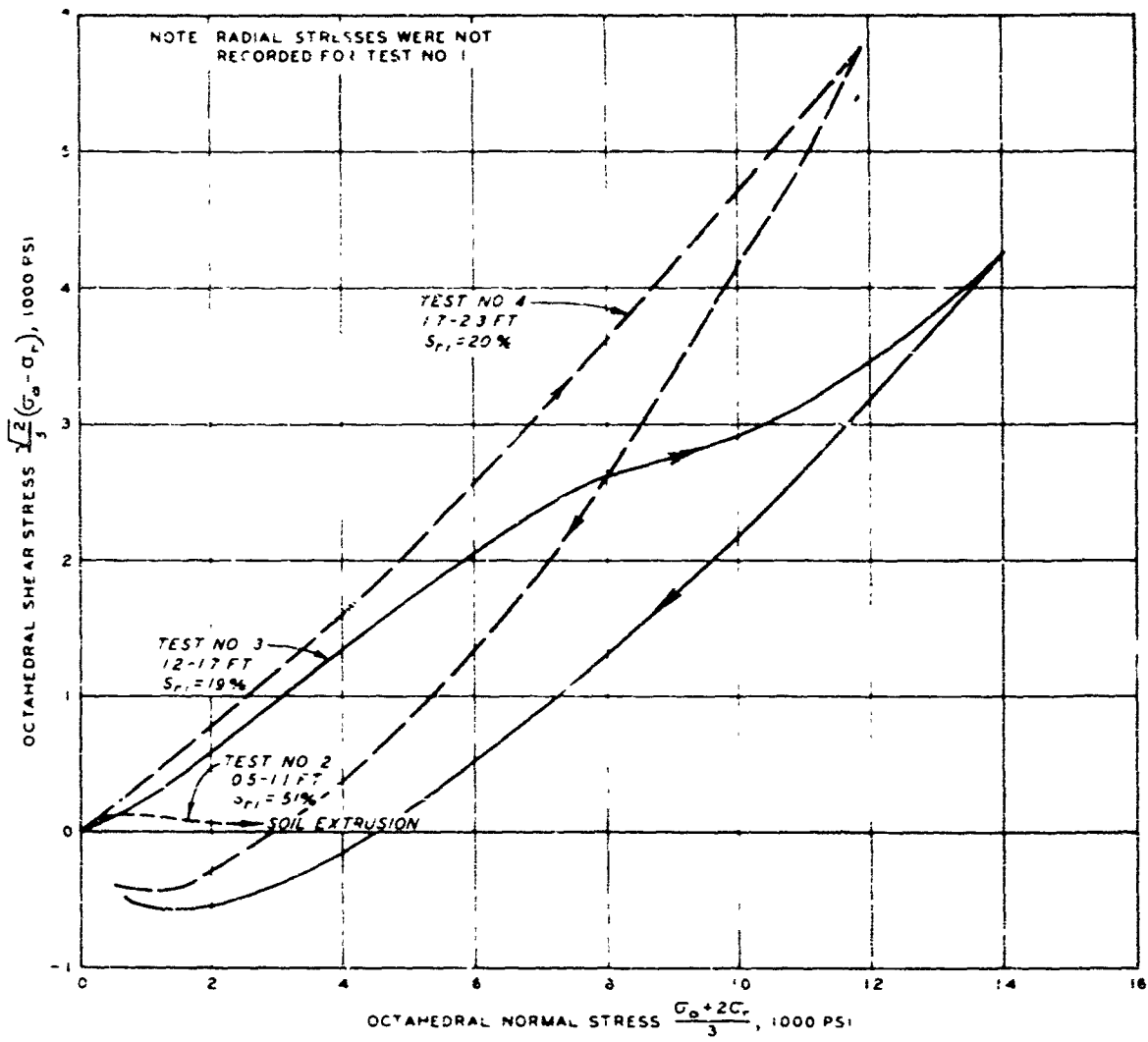


Fig G1 Octahedral shearing stress versus octahedral normal stress for the undisturbed samples of silty clay

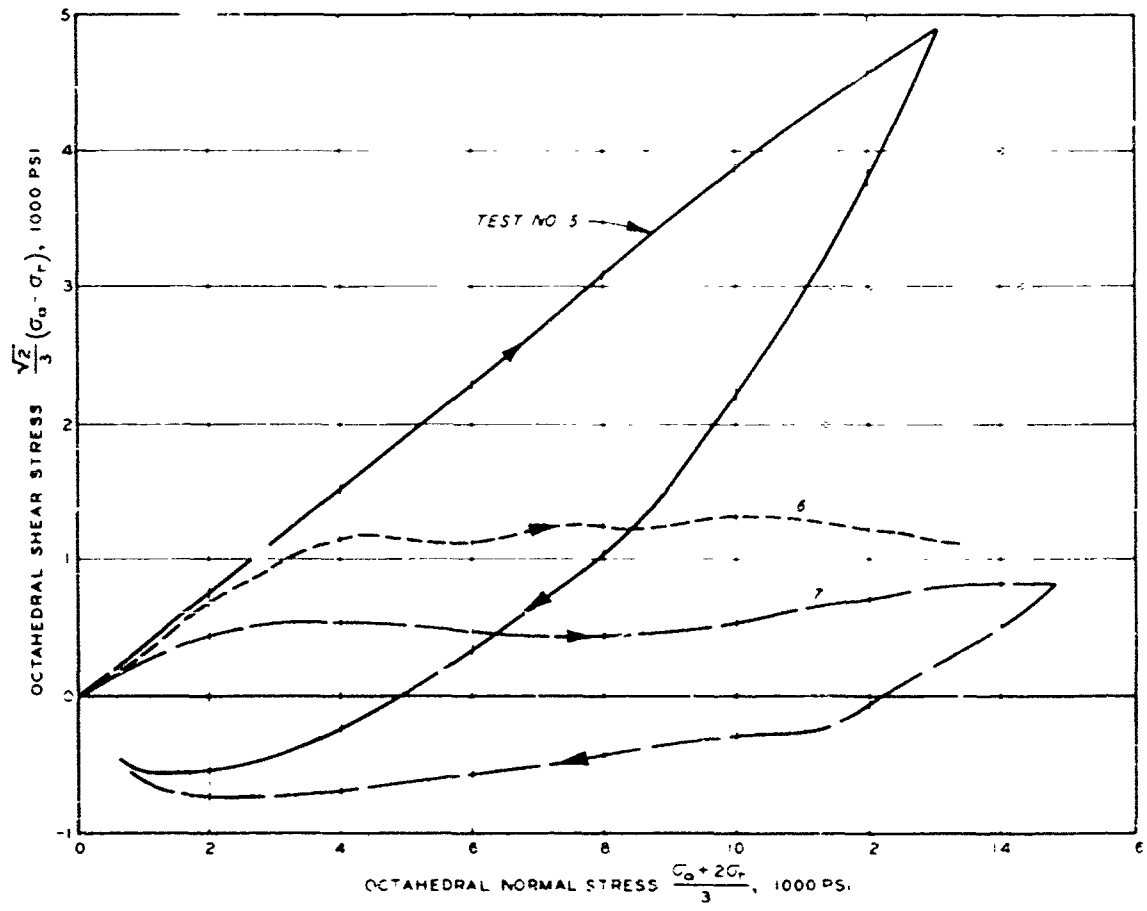


Fig. G2. Octahedral shearing stress versus octahedral normal stress for the compacted samples of silty clay

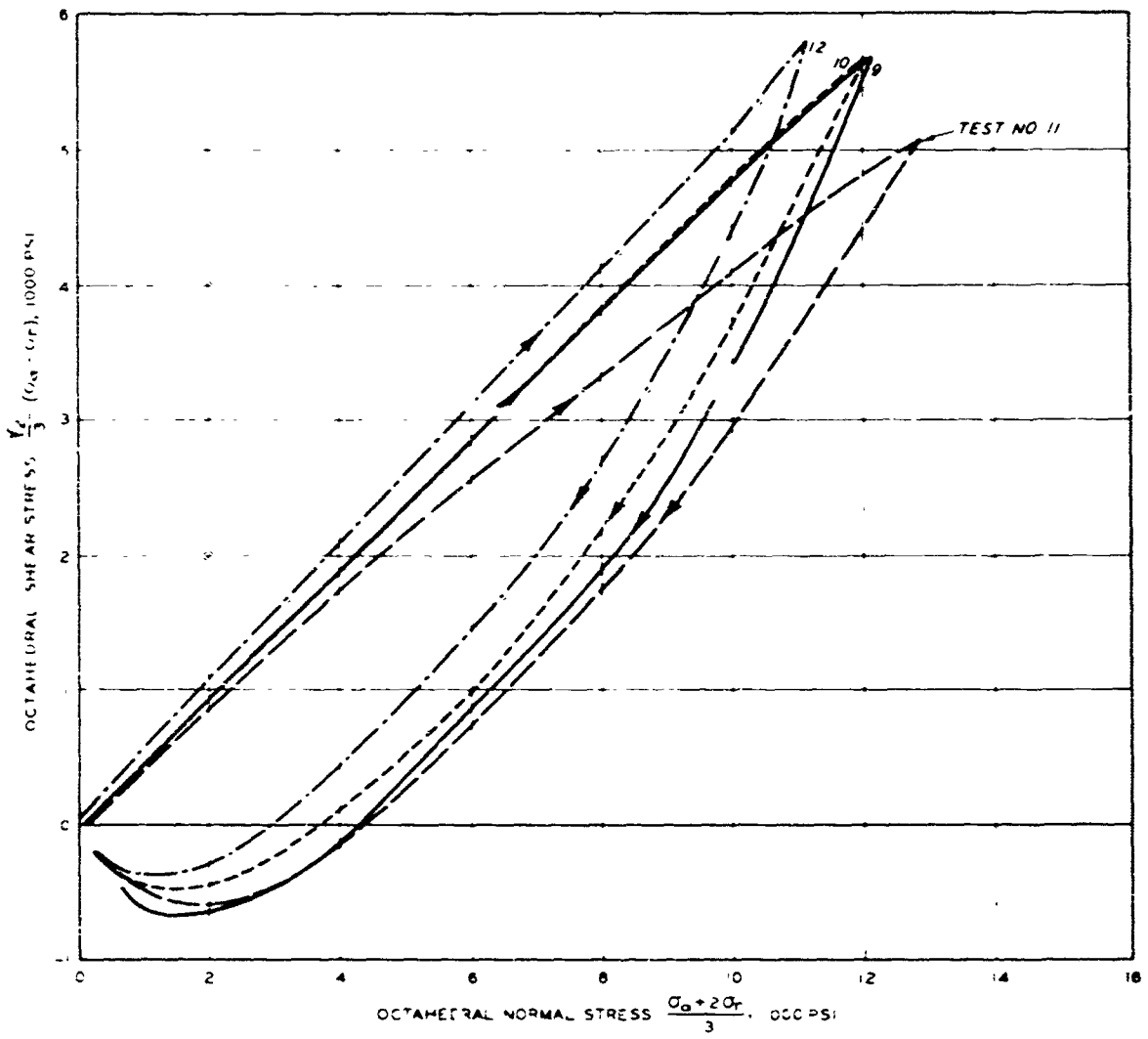


Fig G3. Octahedral shearing stress versus octahedral normal stress for the compacted samples of sandy silt

Unclassified

Security Classification

DOCUMENT CONTROL DATA - R & D

Security classification of title, body of abstract and indexing annotation must be entered when the overall report is classified.	
1 ORIGINATING ACTIVITY (Corporate author) M. T. Dawson, Foundation Engineer Champaign, Illinois	2a REPORT SECURITY CLASSIFICATION Unclassified
2b GROUP	
3 REPORT TITLE EFFECT OF DEGREE OF SATURATION ON COMPRESSIBILITY OF SOILS FROM THE DEFENCE RESEARCH ESTABLISHMENT, SUFFIELD	
4 DESCRIPTIVE NOTES (Type of report or "Inclusive dates") Final report	
5 AUTHOR(S) (First name, middle initial, last name) A. J. Hendron, Jr. M. T. Dawson J. F. Parola	
6 REPORT DATE April 1969	7a TOTAL NO. OF PAGES 98
7b CONTRACT OR GRANT NO	
8 PROJECT NO Purchase Order No WESBPJ-68-67	9b ORIGINATOR'S REPORT NUMBER(S)
10 DISTRIBUTION STATEMENT This document has been approved for public release and sale its distribution is unlimited.	
11 SUPPLEMENTARY NOTES Prepared under contract for U S Army Engineer Waterways Experiment Station Vicksburg, Mississippi	12 SPONSORING MILITARY ACTIVITY Defense Atomic Support Agency Washington, D C
13 ABSTRACT Soil tests were conducted to provide information on the influence of degree of saturation on high-pressure stress-strain relations of undisturbed and remolded soils from the Defence Research Establishment, Suffield, and to provide input data for computer codes concerning the relation between stress and strain invariants at high pressures. As expected, the test results presented herein show that large strains do not develop at high pressures in fine-grained soils such as silt and clay. The test program consisted of 12 one-dimensional tests on 4 specimens each of undisturbed and remolded silty clay, and 4 specimens of remolded sandy silt. In all tests the radial strain was essentially zero. Axial and radial stresses and axial strain were measured. The tests were carried to an axial stress of 20,000 psi unless soil extrusion occurred at a lower stress. The following conclusions were reached. The degree of saturation and the initial void ratio are the most significant variables governing the one-dimensional stress-strain relations of soil at high pressures. For pressures exceeding 3000 psi the compacted specimens and undisturbed specimens of Suffield soil yield the same relation if the initial degree of saturation and initial void ratio are identical before loading. A lower bound to the secant modulus of deformation $M_s$ at a given level of axial stress $\sigma_a$ is given for both compacted and undisturbed samples of fine-grained soil subjected to pressures greater than 3000 psi. The average unloading modulus of Suffield soils subjected to pressures greater than 3000 psi is approximately 10 times the loading secant modulus of deformation $M_s$ . It is probable that the stiffness of the Suffield soils when unsaturated will be greater under dynamic loading than the static values given herein. Previous comparisons of static and dynamic values of constrained moduli of Suffield soils have shown that the dynamic values are twice the static values. This observation is consistent with similar comparisons for NTS Frenchman Flat silt.	

DD FORM 1 NOV 68 1473

REPLACES DD FORM 1473, 1 JAN 64, WHICH IS  
COMPLETE FOR ARMY USE.

Unclassified  
Security Classification

Unclassified

Security Classification

ITEM NUMBER	ITEM DESCRIPTION		ITEM TYPE		ITEM STATUS	
	ITEM ID	ITEM NAME	ITEM CODE	ITEM TYPE	ITEM STATUS	ITEM DATE
1	DEF-001	Defence Research Establishment Suffield	DRS-001	Project	Active	2023-01-01
2	SAT-002	Saturated soils	SAT-002	Experiment	In Progress	2023-01-01
3	SOIL-003	Soil compacting	SOIL-003	Procedure	Completed	2023-01-01
4	STRA-004	Soil strain	STRA-004	Instrumentation	Active	2023-01-01
5	STRE-005	Soil stress	STRE-005	Instrumentation	Active	2023-01-01

Unclassified

Security Classification